

2018

Manipulating push-pull systems to probe biology and photochemistry

Andrea Thooft
Iowa State University

Follow this and additional works at: <https://lib.dr.iastate.edu/etd>

 Part of the [Organic Chemistry Commons](#)

Recommended Citation

Thooft, Andrea, "Manipulating push-pull systems to probe biology and photochemistry" (2018). *Graduate Theses and Dissertations*. 16678.
<https://lib.dr.iastate.edu/etd/16678>

This Dissertation is brought to you for free and open access by the Iowa State University Capstones, Theses and Dissertations at Iowa State University Digital Repository. It has been accepted for inclusion in Graduate Theses and Dissertations by an authorized administrator of Iowa State University Digital Repository. For more information, please contact digirep@iastate.edu.

Manipulating push-pull systems to probe biology and photochemistry

by

Andrea Thooft

A dissertation submitted to the graduate faculty
in partial fulfillment of the requirements for the degree of

DOCTOR OF PHILOSOPHY

Major: Organic Chemistry

Program of Study Committee:
Brett VanVeller, Major Professor
William Jenks
Emily Smith
Levi Stanley
Yan Zhao

The student author, whose presentation of the scholarship herein was approved by the program of study committee, is solely responsible for the content of this dissertation. The Graduate College will ensure this dissertation is globally accessible and will not permit alterations after a degree is conferred.

Iowa State University

Ames, Iowa

2018

Copyright © Andrea Thooft, 2018. All rights reserved.

TABLE OF CONTENTS

	Page
LIST OF ABBREVIATIONS AND DESCRIPTIONS	iv
ACKNOWLEDGEMENTS	viii
ABSTRACT	x
CHAPTER 1: PHOTOPROCESSES IN ORGANIC CHEMISTRY	1
1.1 Organic fluorophores	1
1.2 Properties and uses of NBD	3
1.3 Photochemical reactions	5
1.4 Ortho-nitrobenzyl protecting group	8
1.5 Conclusion	11
1.6 References	11
CHAPTER 2: A SMALL PUSH-PULL FLUOROPHORE FOR TURN-ON FLUORESCENCE	14
2.1 Abstract	14
2.2 Introduction	14
2.3 Results and Discussion	16
2.4 Conclusions	23
2.5 Experimental	24
2.6 References	44
CHAPTER 3: CONTROLLING PHOTO-CLEAVAGE: SYNTHESIS AND PHOTOCHEMISTRY OF THE MALLEABLE EXCITED-STATES OF BENZO-DIAZOLE CHROMOPHORES	46
3.1 Abstract	46
3.2 Introduction	46
3.3 Results and Discussion	52
3.4 Conclusions	59
3.5 Experimental	59
3.6 References	72
CHAPTER 4: TURNING PHOTOREACTIONS ON AND OFF FOR SEQUENCE-INDEPENDENT PHOTOCHEMISTRY	75
4.1 Abstract	75
4.2 Introduction	75
4.3 Results and Discussion	79
4.4 Conclusions	85

4.5 Experimental	86
4.6 References	93
CHAPTER 5: CONCLUSIONS AND FUTURE DIRECTIONS	95

LIST OF ABBREVIATIONS AND DESCRIPTIONS

Abbreviation	Description
Abs	Absorbance
AcCl	Acetyl Chloride
Ac ₂ O	Acetic Anhydride
ACN	Acetonitrile
AcOH	Acetic Acid
ADP	Adenosine Diphosphate
Ar	Aryl
ATP	Adenosine Triphosphate
BD	Benzo(heteroatom)diazole
Boc	<i>tert</i> -butyloxycarbonyl
Boc ₂ O	Di- <i>tert</i> -butyl dicarbonate
Calcd	Calculated
CBD(O)	Cyanobenzoxadiazole
CBD(S)	Cyanobenzothiadiazole
CT	Charge Transfer
DCM	Dichloromethane
DIEA	Diisopropylethylamine
DMA	Dimethylacetamide
DMAP	4-Dimethylaminopyridine
DMF	Dimethylformamide
DMFDMA	N,N-dimethylformamide dimethyl acetal

DMSO	Dimethylsulfoxide
Em	Emission
eq	equivalent
ESI-TOF	Electrospray Ionization Time-of-Flight
EtOAc	Ethyl Acetate
EtOH	Ethanol
GFP	Green Fluorescent Protein
EDG	Electron Donating Group
EWG	Electron Withdrawing Group
h	hour
HPLC	High Performance Liquid Chromatography
HRMS	High-Resolution Mass Spectrometry
h ν	light
Hz	Hertz
IR	Infrared
LG	Leaving Group
Me	Methyl
MeCN	Acetonitrile
MeOH	Methanol
MHz	Megahertz
μm	micrometer
min	minute
mL	milliliter

mm	millimeter
mmol	millimole
N ₂	Nitrogen
NBD	Nitrobenzoxadiazole
NEt ₃	Triethylamine
nm	nanometer
NMP	N-methyl-2-pyrrolidone
NMR	Nuclear Magnetic Resonance
Nu	Nucleophile
PPG	Photocleavable Protecting Group
ppm	parts per million
PT	Proton Transfer
R _f	Retardation factor
rpm	revolutions per minute
SBD	Sulfonamidebenzoxadiazole
SI	Supporting Information
<i>t</i> Bu	<i>tert</i> -butyl
TFA	Trifluoroacetic Acid
TFAA	Trifluoroacetic Anhydride
THF	Tetrahydrofuran
TICT	Twisted Intramolecular Charge Transfer
TLC	Thin-layer Chromatography
TMS	Trimethylsilyl

UPLC

Ultra Performance Liquid Chromatography

UV

Ultraviolet

UV-vis

Ultraviolet-visible

ACKNOWLEDGEMENTS

First I'd like to thank Brett VanVeller for taking me into his research group and teaching me about photophysics and photochemistry. Thank you for your support and encouragement. Thanks also to my committee for their inputs and suggestions during my studies here at Iowa State University.

I'd also like to thank many current and former lab mates who have helped throughout the years. To Manibarsha Goswami and Shreyosree Chatterjee for teaching me synthetic techniques and introducing me to the wonderful world of Indian food and Bollywood music. Thanks to Selin Demirci, Yen Nguyen, Caroline Warner and Kyle Cassaidy for your synthetic help. You all helped to make it possible for me to finish this degree in a timely manner (and made graduate school a much more enjoyable experience).

Thank you to many friends who've helped keep me motivated throughout the years. Lynette Edsall who encouraged me to keep going, even when I wanted to throw in the towel too many times to count. To Andra Castle and Paige Bouc for listening to me vent and helping to make the tears of frustration vanish into laughter and peace. To Janci Bronson who helped keep me sane by allowing me to continue piano lessons (and use the right side of my brain every once in a while). There are numerous others who have helped to keep me going that I probably have missed here as well but thank you to them too.

I'd like to thank my parents for all of their encouragement and support my whole life. It is your encouragement of my exploring and questioning that allowed me to even make it to graduate school. Additionally you've helped inspire me to keep going and know that you'll be proud of me no matter what.

And to my wonderful husband Andrew. None of this would have been possible without you. You helped encourage me to not quit. You showed me what it means to love someone at their best and their worst. This degree should be yours as well as mine because without you, I wouldn't have made it past the first year.

Finally thank you to my beautiful daughter Gwenevere. You have brought so much happiness and joy to my life. You have helped to give me perspective on what really matters, especially on days where it felt like nothing was working and I'd never be able to finish. I hope that I can encourage you to pursue your dreams as much as others have encouraged me. I hope that I can inspire you to reach for the stars and not let anything hold you back. I hope I can be the mom that you deserve.

ABSTRACT

Photochemistry and photophysics are two rapidly expanding areas in science. The first part of this dissertation looks at the synthesis of a new fluorescent probe based on the well-known fluorophore nitrobenzoxadiazole (NBD). We synthesized a new derivative using the nitrile functional group as the electron withdrawing group. Our results showed our fluorophore (CBD) displayed redder emission than the nitro counterpart, and an emission range that was similar to that of the sulfonamide containing derivatives. Additionally CBD displayed extensive solvatochromic properties: high quantum yield and bluer emissions in nonpolar solvents while low quantum yield and redder emissions as the solvent polarity increased.

The second part of this dissertation looks at the extensively used photocleavable protecting group (PPG) ortho-nitrobenzyl. We synthesized a new derivation of the ortho-nitrobenzyl PPG which demonstrated photocleavable properties which could be tuned by adjusting the solvent. Photocleaving reactions were observed in nonpolar solvents while no photocleaving reactions were observed in polar solvents. Work is currently underway to better understand this PPG.

CHAPTER 1: PHOTOPROCESSES IN ORGANIC CHEMISTRY

1.1 Organic Fluorophores

Fluorescent molecules, both naturally occurring fluorophores and those synthesized in the lab, have proven invaluable to the study of various systems such as protein detection¹, substrate/enzyme interactions², analyte detection³, analyzing molecular movements⁴ as well as countless other applications. A fluorescent probe allows the researcher to visualize various chemical and biological processes. The wide variety of commercially available fluorophores allows the researcher to choose a fluorophore to meet his or her specific need based on photophysical properties such as absorption and emission wavelength, quantum yield, tendency to photobleach, etc.⁵

Molecules can undergo many different processes when absorbing light and understanding these processes allows chemists to utilize photochemical and photophysical processes to aid in research. As shown in figure 1.1, electrons can go through multiple pathways upon absorption of a photon of light. Upon excitation from the ground state, S_0 , to the excited state the electron rapidly relaxes to the lowest excited state, notated as S_1 . From here the molecule can nonradiatively decay back to the ground state in a process known as internal conversion. Alternatively, the excited state can undergo fluorescence by emitting a photon of light in a process known as fluorescence.

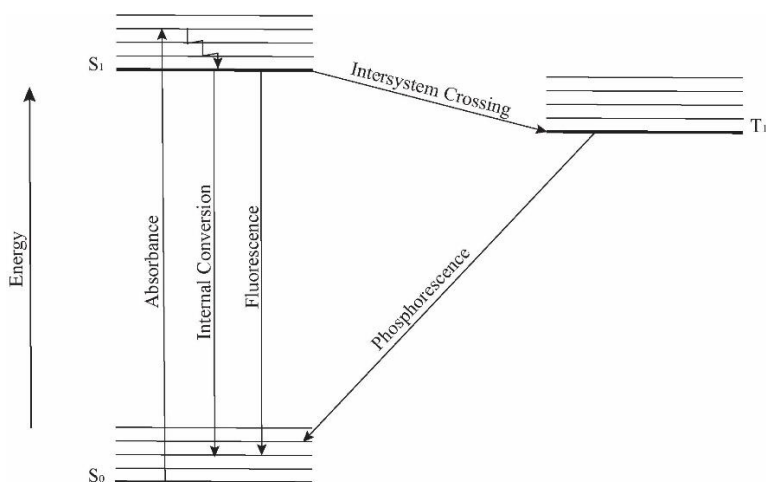


Figure 1.1 Jablonski diagram demonstrating movements of electrons upon photon absorbance.

An excited state can also undergo intersystem crossing from the S_1 state to the T_1 state. Internal conversion requires the electron to undergo a spin flip. In the ground state and the singlet excited state, the electrons are spin paired. However, during intersystem crossing, the electron flips so the electrons are no longer spin paired and have parallel spins. Once in the T_1 state, the electron can either nonradiatively decay back to the ground state, undergoing a spin flip in the process. Alternatively the electron can emit light in a process known as phosphorescence while relaxing to the ground state while simultaneously spin flipping back to a spin paired configuration (Figure 1.2).^{6,7}

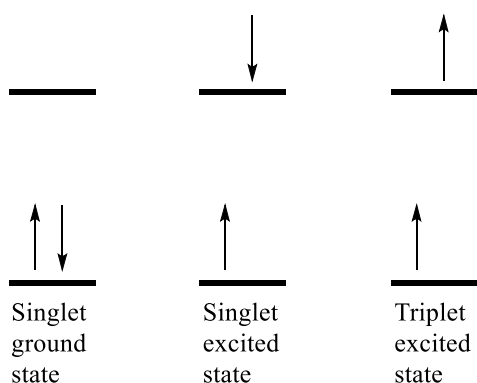


Figure 1.2 Electron diagram demonstrating singlet ground state, singlet excited state and triplet excited state.

The ability of some molecules to undergo fluorescence and phosphorescence has been exploited for studying different systems in chemistry and biology as well as many other sciences. Fluorophores run the range of UV absorbing, to visible light, to near-infrared. Additionally fluorophores can be small molecules that naturally occur in vivo, such as a few amino acids⁸, all the way to large, bulky fluorescent proteins such as GFP⁹. Figure 1.3 shows a variety of natural and synthetic fluorophores and demonstrates the wide range of emission wavelengths that fluorophores can cover: from ultraviolet to near infrared wavelengths.⁸

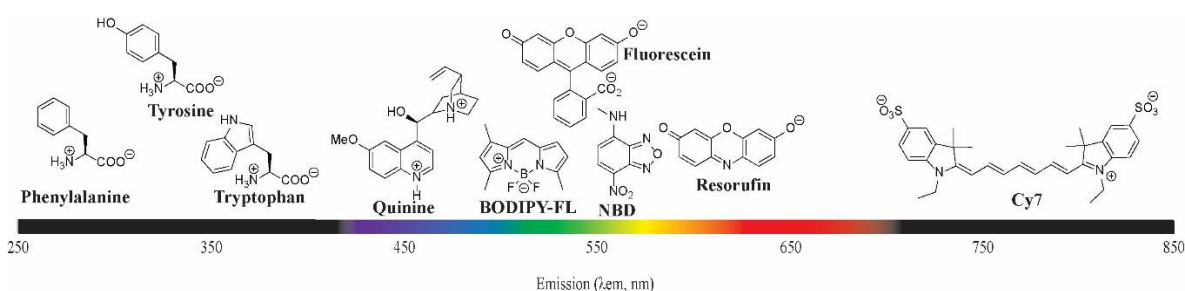


Figure 1.3 Commonly used fluorescent molecules and their emission wavelength.

1.2 Properties and Uses of NBD

One structural feature of many fluorophores is sometimes dubbed the push-pull system. These molecules have electron donating groups and electron withdrawing groups that are in conjugation with each other via an intervening π -system (Figure 1.4).¹⁰ By altering the EDG and EWG on these types of fluorophores, the absorbance wavelength can be tuned to a higher or lower emission wavelength. Examples of these fluorophores include the cyanohydrins and benzo(heteroatom)diazoles.

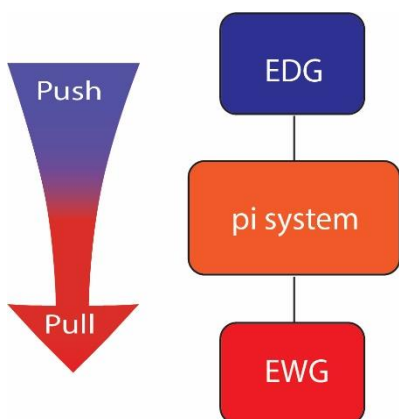
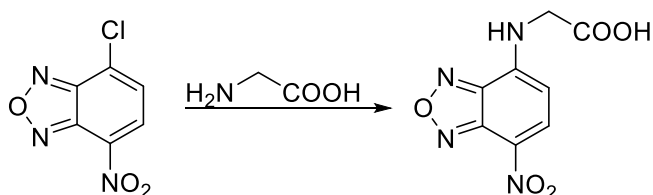


Figure 1.4 Simplified model of push-pull system.

The most widely known benzo(heteroatom)diazole, nitrobenzoxadiazole (NBD), was first discovered in 1968 when a researcher noticed the chloro-precursor reacted with amines from amino acids to form highly fluorescent molecules (Scheme 1.1).¹¹ Not only was the molecule highly fluorescent, it also emits in the green region of the electromagnetic spectrum which was surprising given the molecule's small conjugation length. Additionally, NBD displays highly sensitive solvatochromism behavior. The NBD fluorophore has a high quantum yield in nonpolar solvents while the quantum yield decreases as the solvent becomes more polar to the point where it is almost non-emissive in water. The emission wavelength also undergoes a bathochromic shift as solvent polarity increases. This redshift in emission can be as high as 80 nm when comparing emission of a probe in hexane versus water for some derivatives.



Scheme 1.1 NBD-glycine which was the first reported fluorescence of this fluorophore class.¹¹

The research in our group has looked into better understanding this class of fluorophores and its fluorescent properties. Understanding what regions are responsible for the fluorescent properties would allow researchers to build the optimal fluorophore for their specific research needs. Examples of changes to NBD we'd like to investigate are (i) the effect of the nitrogen atoms in the five membered ring (denoted by Z, Figure 1.5). (ii) What effect do heteroatoms have when placed in the intervening π -system of the six membered ring (denoted by Q, Figure 1.5)? (iii) How does changing the electron withdrawing group (EWG) affect the fluorescence properties (denoted by EWG, Figure 5). While numerous electron donating groups have been investigated, the electron withdrawing groups have been limited to only nitro or and sulfonamide groups.¹²

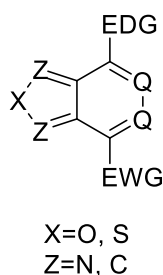


Figure 1.5 NBD derivatives under investigation.

1.3 Photochemical reactions

Molecules are not limited to light emission or nonradiatively relaxing upon excitation with light. Molecules can also undergo photochemical reactions that are initiated by light. This class of reactions is very appealing as it allows the researcher to complete the desired chemistry without introducing potentially toxic reagents that would harm the system and the researcher doesn't risk undesirable chemistry which can be caused by sensitive functional groups.^{13,14} Examples of photochemical reactions include cis-trans isomerization (Figure

1.6A), pericyclic reactions (Figure 1.6B) and Norrish type I and type II reactions (Figure 1.6C and 1.6D respectively).⁶

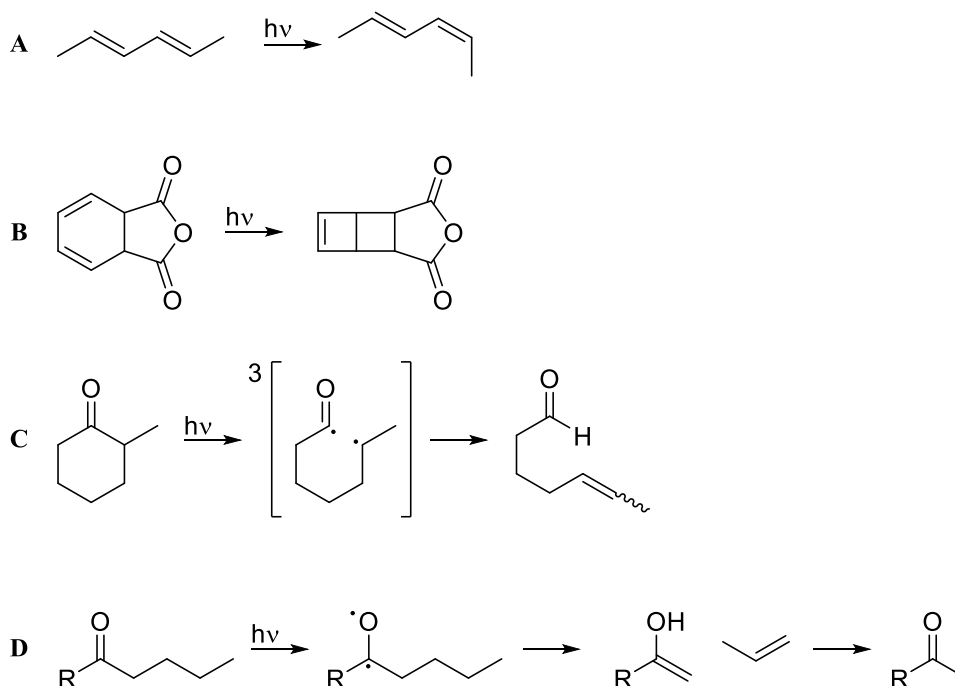


Figure 1.6 Examples of photochemical reactions. (A) cis-trans isomerization. (B) cycloaddition. (C) Norrish type I. (D) Norrish type II.

Another important photochemical reaction that has found applications is the photochemical release of molecular cargo. The cargo could be a small molecules such as ATP to study metabolic flux (Figure 1.7A),¹⁵ or the active form of a drug, specifically intended to target an infected or cancerous cell. These types of reactions can also be used in total synthesis as protecting groups that can be orthogonally activated with light (Figure 1.7B).¹⁶ Finally photochemical reactions can be used to activate a molecule that fluoresces upon release (Figure 1.7C).¹⁷

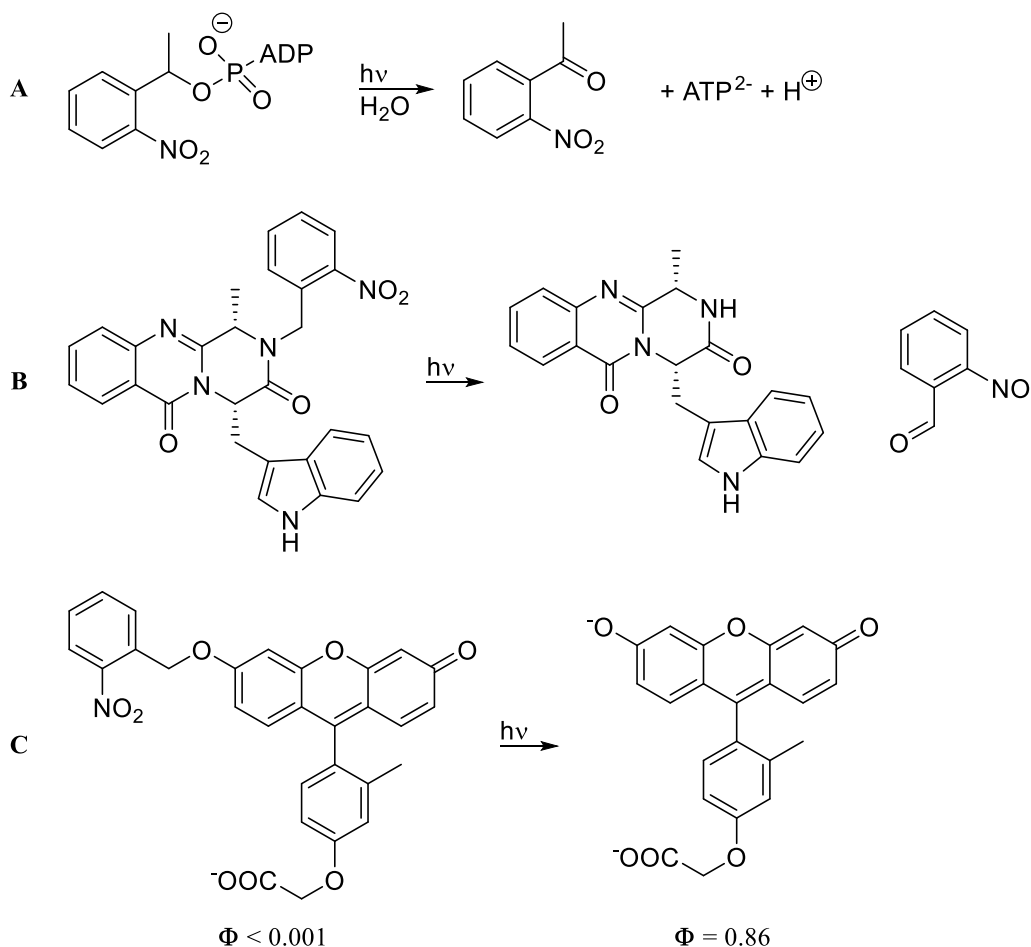


Figure 1.7 Examples of photochemical reactions used in research applications. (A) Photorelease of ATP. (B) Final deprotection in total synthesis. (C) Activation of fluorophore.

As there are numerous PPGs available and many functional groups that can function with PPGs, the use of multiple PPGs in the same system is becoming more common. If a researcher decides to use multiple PPGs, there are multiple factors that need to be taken into consideration.¹⁸ To start the different protecting groups must absorb at different wavelengths for the maximum absorption (Figure 1.8). This difference in maximum absorptions is required due to the researcher desiring only one group to photocleave at a time.

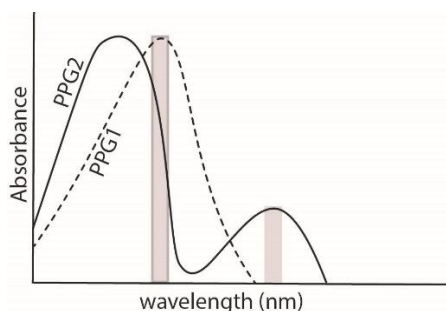


Figure 1.8 Different λ_{max} required when two or more PPGs used in the same system.

When undergoing photocleavage in a system containing multiple PPGs, the researcher is limited to photocleaving from longest wavelength to shortest wavelength. This restriction is necessary due to numerous chromophores absorbing at shorter wavelengths. Consequently more molecules are likely to be reactive at bluer wavelengths as compared to redder wavelengths. Additionally once PPGs are appended to a system of interest, the photoreaction cannot be turned on or off. Subsequently the research is committed to the photochemical reaction pathway once these systems are in place.¹⁹

1.4 Ortho-nitrobenzyl protecting group

One of the most common photocleavable protecting groups is the ortho-nitrobenzyl protecting group.¹³⁻¹⁵ This is due to its small structure, minimizing steric interactions, as well as relatively high quantum yield of photocleavage. The mechanism (Figure 1.9) involves excitation of the nitro group in **1** to form the diradical (**1***) which undergoes rearrangement to form the orthoquinone derivative (**2-Z**) which can isomerize to **2-E**.²⁰⁻²⁴ The orthoquinone can then cyclize (**3**) followed by ring opening to yield the alcohol (**4**) which readily forms the carbonyl to kick off the leaving group to yield the nitroso aldehyde (**5**).²⁵

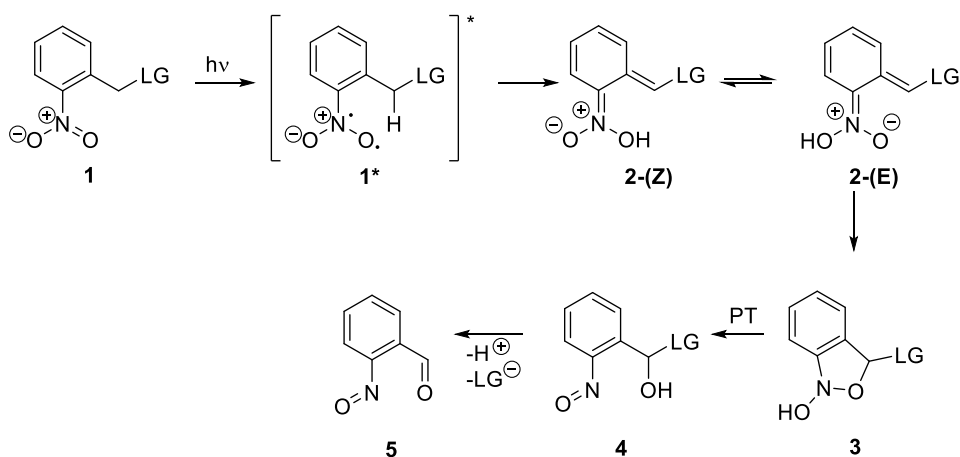


Figure 1.9 o-nitrobenzyl PPG deprotection mechanism.

The simplified ring structure of ortho-nitrobenzyl absorbs light at approximately 300 nm. This absorbance wavelength means when this photocleavable protecting group (PPG) is used with other PPGs in the same system, it will most likely need to be photocleaved last as photocleavage needs to occur from longest to shortest wavelength. Attempts to redshift the absorbance, by creating a push-pull system, have been somewhat successful. Addition of electron donating groups, such as methoxy groups, redshifts the absorbance to approximately 350 nm but the quantum yield of photorelease drops.^{26,27} Ultimately, addition of even more electron donating groups such as dimethylamine further redshifts the absorption to approximately 390 nm, but hydrogen abstraction no longer occurs resulting in no release of the leaving group (Figure 1.10A). The lack of hydrogen abstraction with **8** is due to the excited state of **8** adopting a charge-transfer (CT) state which cannot undergo the hydrogen abstraction necessary for photocleavage (Figure 1.10B).²⁸

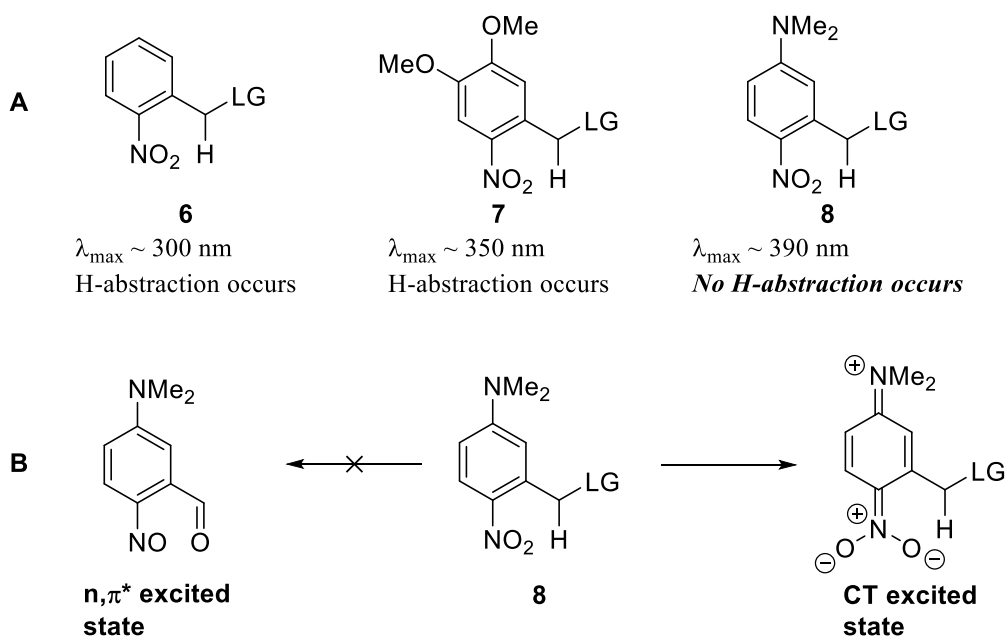


Figure 1.10 (A) Absorption wavelengths of various nitro PPGs and their ability to undergo hydrogen abstraction. (B) Charge transfer excited state of dimethylamine o-nitrobenzyl hydrogen abstraction.

Research in our group is focused on synthesis of a new photocleavable protecting group based on the ortho-nitrobenzyl group with a red shifted absorbance which would allow it to photocleave in the visible region of the electromagnetic spectrum. In order to achieve this goal, we investigated synthesis of a ortho-nitrobenzyl group that contained the core ring structure of benzo(heteroatom)diazoles in order to tune the absorption wavelength of this new photocleavable protecting group (Figure 1.12). In chapters 3 and 4, we also discuss how the nature of the excited state of **10** can be manipulated to turn the photo reaction on or off.

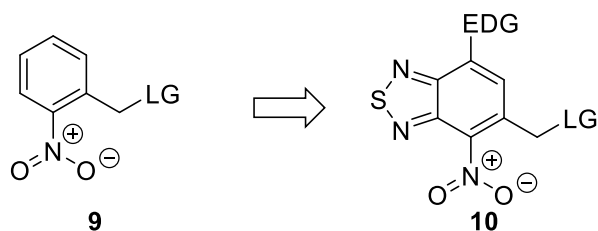


Figure 1.12 Proposed structure of photocleavable protecting group with absorbance in the visible region of the electromagnetic spectrum.

1.5 Conclusion

Photophysical and photochemical processes have greatly expanded the knowledge and capabilities of organic chemistry. These expanded capabilities allowing chemists to visualize biological processes in action or pin-point release of a specific molecule. The ability to better understand the structure-property relationship of fluorophores will further allow chemists to design fluorescent materials to meet their specific research needs. Finally the ability to control and modulate photocleavable protecting groups will expand the systems into which these PPGs can be applied.

1.6 References

1. Giepmans, B. N. G.; Adams, S. R.; Ellisman, M. H.; Tsien, R. Y. *Science* **2006**, *312*, 217-224.
2. Reymond, J.-L.; Wahler, D. *ChemBioChem* **2002**, *3*, 701-708.
3. Lee, M. H.; Kim, J. S.; Sessler, J. L. *Chem. Soc. Rev.* **2015**, *44*, 4185-4191.
4. Ha, T.; Tinnefeld, P. *Annu. Rev. Phys. Chem.* **2012**, *63*, 595-617.
5. Haugland, R. P.; Spence, M. T. Z.; Johnson, I. D.; Basey, A. *The Handbook: A Guide to Fluorescent Probes and Labeling Technologies*. 10th ed.; Molecular Probes: Eugene, OR, 2005.
6. Anslyn, E. V.; Dougherty, D. A. *Modern Physical Organic Chemistry*. University Science Books: Sausalito, CA, 2006.

7. Turro, N. J. *Modern Molecular Photochemistry*. University Science Books: Sausalito, CA, 1991.
8. Lavis, L. D.; Raines, R. T. *ACS Chem. Biol.* **2008**, *3*, 142-155.
9. Sample, V.; Newman, R. H.; Zhang, J. *Chem. Soc. Rev.* **2009**, *38*, 2852-2864.
10. Meier, H. *Angew. Chem. Int. Ed.* **2005**, *44*, 2482-2506.
11. Ghosh, P. B.; Whitehouse, M. W. *Biochem. J.* **1968**, *108*, 155-156.
12. Thoof, A. M.; Cassaidy, K.; VanVeller, B. *J. Org. Chem.* **2017**, *82*, 8842-8847.
13. *Dynamic Studies in Biology*; Goeldner, M.; Givens, R. Eds.; Wiley-VCH, 2005.
14. Klan, P.; Solomek, T.; Bochet, C. G.; Blanc, A.; Givens, R.; Rubina, M.; Popik, V.; Kostikov, A.; Wirz, J. *Chem. Rev.* **2013**, *113*, 119-191.
15. Walker, J. W.; Reid, G. P.; McCray, J. A.; Trentham, D. R. *J. Am. Chem. Soc.* **1998**, *110*, 7170-7177.
16. Hoffmann, N. *Chem. Rev.* **2008**, *108*, 1052-1103.
17. Puliti, D.; Warther, D.; Orange, C.; Specht, A.; Goeldner, M. *Bioorg. Med. Chem.* **2011**, *19*, 1023-1029.
18. Hansen, M. J.; Velema, W. A.; Lerch, M. M.; Szymanski, W.; Feringa, B. L. *Chem. Soc. Rev.* **2015**, *44*, 3358-3377.
19. San Miguel, V.; Bochet, C. G.; del Campo, A. *J. Am. Chem. Soc.* **2011**, *133*, 5380-5388.
20. Schmierer, T.; Laimgruber, S.; Haiser, K.; Kiewisch, K.; Neugebauer, J.; Gilch, P. *Phys. Chem. Chem. Phys.* **2010**, *12*, 15653-15664.
21. Schmierer, T.; Bley, F.; Schaper, K.; Gilch, P. *J. Photoch. Photobiol. A* **2011**, *217*, 363-368.
22. Fröbel, S.; Gilch, P. *J. Photochem. Photobiol. A* **2015**, *318*, 150-159.
23. Schmierer, T.; Ryseck, G.; Villnow, T.; Regner, N.; Gilch, P. *Photochem. Photobiol. Sci.* **2012**, *11*, 1313-1321.
24. Il'ichev, Y. V.; Wirz, J. *J. Phys. Chem. A* **2000**, *104*, 7856-7870.
25. Il'ichev, Y. V.; Schworer, M. A.; Wirz, J. *J. Am. Chem. Soc.* **2004**, *12*, 1097-1113.

26. Charier, S.; Ruel, O.; Baudin, J. B.; Alcor, D.; Allemand, J. F.; Meglio, A.; Jullien, L.; Valeur, B. *Chem. Eur. J.* **2006**, *12*, 1097-1113.
27. Görner, H. *Photochem. Photobiol. Sci.* **2005**, *4*, 822-828.
28. Bochet, C. G. *Tet. Lett.* **2000**, *41*, 6341-6346.

CHAPTER 2: A SMALL PUSH-PULL FLUOROPHORE FOR TURN-ON FLUORESCENCE

Department of Chemistry, Iowa State University, Ames, Iowa 50011, United States

Paper published in *Journal of Organic Chemistry*¹

Reproduced with permission from *Journal of Organic Chemistry*.

©Copyright 2017 American Chemical Society

2.1 Abstract

A new class of push-pull dyes is reported based on the structures of benzoxa- and benzothiadiazole heterocycles. This new class of dyes displays red-shifted wavelengths of emission and greater sensitivity to polarity and hydrogen bonding solvents relative to previously known derivatives.

2.2 Introduction

Environmentally sensitive fluorescent dyes are essential tools for reporting differences in polarity and solvation.^{2,3} In a biological context, dyes with variable fluorescence output find application in the investigation of protein interactions⁴ and lipid membrane dynamics⁵ among many others.⁶⁻¹⁰ The accurate discernment of changes in local environment is only possible if the fluorescent probe displays large differences in luminescent output in response to small differences in its surroundings. The benzo(heteroatom)diazole (BD, heteroatom = O, S) heterocycle¹¹ is notable in this regard for several reasons (Figure 2.1). (i) Substitution of BD with appropriate electron-donating (EDGs) and electron-withdrawing groups (EWGs) creates a push-pull dye that can emit visible light (>400 nm), which is beneficial to avoid interference from biological autofluorescence. (ii) The absorption and emission of visible wavelengths is also noteworthy,

considering the small size of BD relative to other classical dyes such as BODIPY and fluorescein (Figure 2.1). Indeed, smaller sized probes hold greater promise to not bias a system away from native biology. (iii) BD chromophores display dramatic changes in emission intensity in response to environment: high emission in nonpolar environments and almost completely quenched emission in polar media. This behavior makes BD dyes ideal for applications in which changes in solvation can report on macromolecular binding.¹²

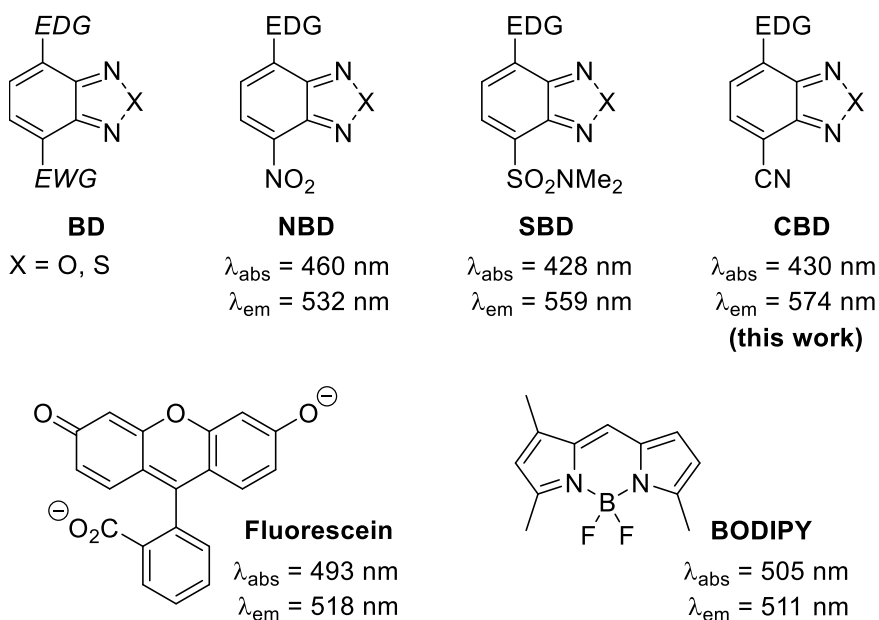


Figure 2.1. Comparison of dye scaffolds and properties. λ_{abs} and λ_{em} values based on reported and measured absorbance and fluorescence in methanol: X = O, EDG = NH_2 ,¹³ Fluorescein,¹⁸ BODIPY.¹⁹

Numerous studies have explored variability in the identity of the EDG of BD to tune emission wavelength and quantum yield. A broad trend emerges that oxygen and aromatic substituted amines (OR, NHAr) as EDGs produce quenched excited states, and only alkyl-substituted amines (NR_2) return high emission intensity.¹³ Alternatively, nitro and sulfonamide are the only two groups that have been studied extensively as EWGs.¹³⁻¹⁵ The objective of this work was to evaluate and characterize the fluorescent properties of a new

class of BD chromophores with a cyano group as the EWG (CBD). Cyano groups are ubiquitous as EWGs in numerous classes of push–pull dye scaffolds,¹⁶ yet the photophysical characteristics of cyano derivatives have not been reported for BD. Moreover, Uchiyama and co-workers posited that hydrogen bonding to the sulfonamide group in SBD played a prominent role in the environmental behavior of SBD in protic solvents.¹⁷ We hypothesized that the greater basicity of the cyano group in CBD, in contrast to the less basic nitro (NBD) and sulfonamide (SBD) groups, would confer even greater sensitivity and response of CBD emission to changes in polarity and solvation.

2.3 Results and Discussion

Our initial evaluation of the cyano group as a competent EWG in BD began with a classic benzoxadiazole NBD scaffold (**1**, Figure 2.2). We were able to rapidly modify **1** to provide **3** via reduction of the nitro group,²⁰ followed by Pd-mediated cross coupling to install the CN acceptor^{21a} in an overall yield of 52% across two steps. Figure 2.2 and Table 2.1 display the absorbance and emission spectra, as well as the quantum yields of **3** in different solvents. The data in Figure 2.2 and Table 2.1 reveal that installation of the cyano group produced fluorescence in the visible region of the spectrum as anticipated. Moreover, the wavelength of emission was highly sensitive to the polarity of the solvent, while the wavelength of absorbance remained relatively unchanged across the solvent series. This solvatochromism behavior²² is common for BD-based chromophores. Another observation from Figure 2.2 is that the quantum yield of fluorescence drops markedly with increasing solvent polarity. This again is a common trait of BD-based chromophores, which have been shown to undergo rapid internal conversion with increasing solvent polarity.¹⁴

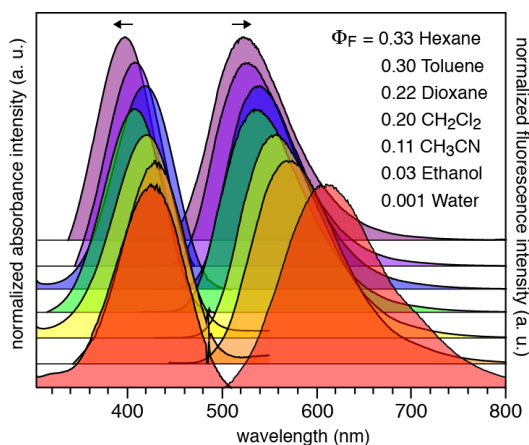
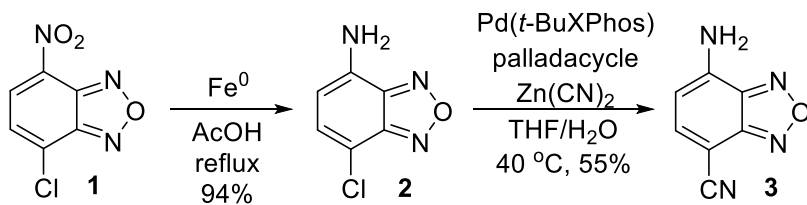


Figure 2.2. Synthesis of cyano-containing benzoxadiazole **3**. Absorbance and emission spectra for **3** showing the solvent polarity and quantum yield effects in various solvents.

Table 2.1. Spectral Properties of 3 in Different Solvents. ^aRelative solvent polarity scale.²³ ^bQuantum yields determined relative to coumarin 153 in ethanol. ^cQuantum yields determined relative to Ru(bipy)₃Cl₂ in water.

Solvent	Polarity value ^a	abs, λ_{\max} (nm)	Em, λ_{\max} (nm)	log ϵ	Φ_F
Hexane	0.009	397	522	3.79	0.329 ^b
Toluene	0.099	409	529	3.79	0.304 ^b
Dioxane	0.164	418	540	3.86	0.218 ^b
CH ₂ Cl ₂	0.309	407	535	3.82	0.195 ^b
CH ₃ CN	0.460	421	557	3.88	0.105 ^b
Ethanol	0.654	430	575	3.91	0.059 ^c
water	1	430	612	3.81	0.002 ^c

To compare the range of emission wavelengths exhibited by **3** with previous NBD and SBD fluorophores, we synthesized **4** and **5** and measured their emission in a series of solvents (Figure 2.3).¹³ The emission wavelengths of **3** span a range of wavelengths twice as large as for **4**, suggesting that **3** is more responsive to changes in polarity than **4**.

Alternatively, the range of wavelengths exhibited by **5** suggests that **3** and **5** are comparable

with respect to sensitivity to overall solvent polarity, although the fluorescence wavelengths of **3** are generally ~10 nm red-shifted relative to **5** (Figure 2.3).

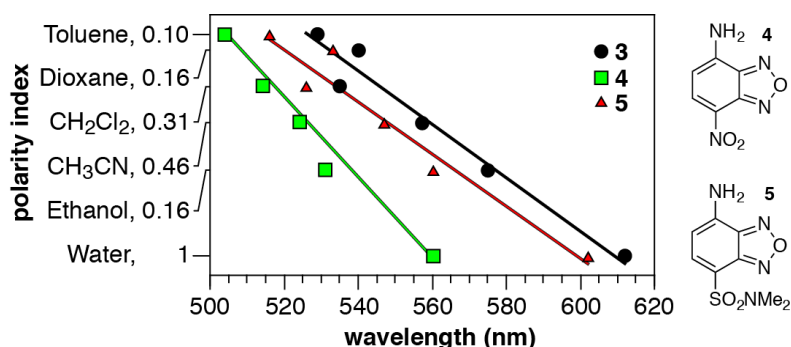
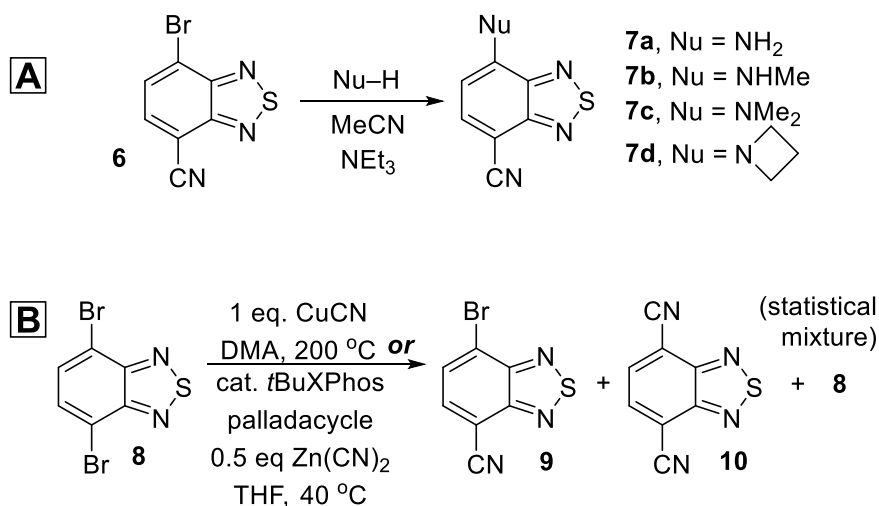


Figure 2.3. Comparison of polarity²³ and wavelength of emission for cyano-containing benzoxadiazole **3** perviously known nitro (**4**)- and sulfonamide (**5**)-containing molecules. **4** was not soluble in hexane for analysis.

We next sought to evaluate how the greater Lewis basicity of the cyano group might confer greater sensitivity of the wavelength of emission to polar protic solvents. We focused on benzothiadiazole ($X = S$) as the core structure because such BDs have been shown to exhibit far greater photostability than congeners where $X = O$ or Se with minimal effect on other photophysical properties such as wavelength or quantum yield.¹⁵ To facilitate this goal, we sought to identify a common CBD ($X = S$) precursor such that EDGs might be easily introduced via elaboration of **6** through nucleophilic aromatic substitution (Scheme 2.1A).

Scheme 2.1. (A) Proposed Synthesis of 7a-d to Explore Different Electron-Donating Groups. (B) Method to Access 6 Directly from Commercially Available 8.



Our initial strategy was to access **6** in a single step from commercially available 4,7-dibromobenzothiadiazole (**8**) via metal-catalyzed cyanation (Table 2.2) using the catalyst systems indicated in Scheme 1B. Initial results of the palladium system^{21a} were not promising because the dicyanated product **9** dominated (Table 2.2). It is likely that **6** is more reactive toward oxidative addition by palladium than the starting compound **8**, making this reaction unattractive for further exploration. Alternatively, the copper-catalyzed conditions^{21b} were not selective and produced statistical mixtures of products (Scheme 1B and Table 2). However, this approach was stymied by difficulties in separating mono- and dicyanated products (**6** and **9**) from unreacted starting material (**8**) on scale. Finally, compound **6** had been reported and was available in five steps from commercially available starting material.²⁴ From **6**, the synthesis of **7a–d** was straightforward following the reaction in Scheme 2.1A.

Table 2.2. Results of Metal-Catalyzed Synthesis of 6 from 8. ^aMicrowave reactor in sealed vials, and temperature monitored using an external IR sensor.

Metal catalyst	Solvent	Temp (°C)	Time	Unreacted 8 (%)	Yield 6 (%)	Yield 9 (%)
Pd	Toluene	40	12 h	92	2	6
Pd	1:1 toluene:water	40	12 h	85	2	13
Pd	THF	40	12 h	94	2	4
Pd	1:1 THF:water	40	12 h	88	3	9
Cu	DMF	200 ^a	5 min	31	47	22
Cu	DMF	200 ^a	10 min	32	43	25
Cu	DMA	200 ^a	5 min	30	54	16
Cu	DMA	200 ^a	10 min	30	49	21
Cu	pyridine	200 ^a	15 min	34	44	22
Cu	NMP	200 ^a	15 min	68	28	4

We tested the photostability of **3** versus **7a** by irradiating both molecules at 420 nm under ambient conditions (Figure 2.4). It was found that the thiadiazole of **7a** did indeed impart greater photostability compared to the oxadiazole in **3** (Figure 4). Consistent with previous observations,¹⁵ the absorption spectrum of **7a** was relatively unchanged over the time of photoirradiation, while **3** photodecomposed rapidly.

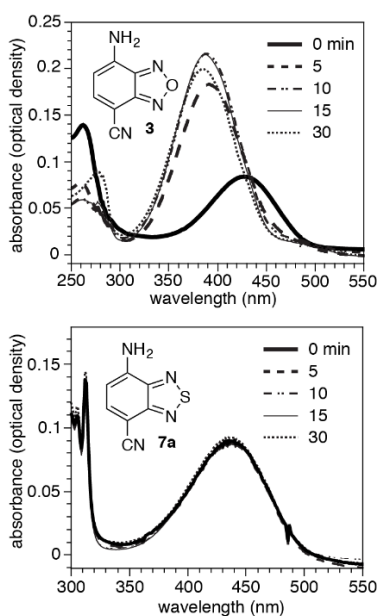


Figure 2.4. Changes in the absorption spectra of **3** and **7a** in aerated tetrahydrofuran upon photoirradiation ($\lambda = 420$ nm) at 25 °C.

To test our hypothesis that the greater basicity of the cyano group would confer greater sensitivity to changes in solvation, we evaluated the response of CBD derivatives **7a–d** to different percentages of dioxane in water (Table 2.3). All derivatives displayed a linear red-shift in emission wavelength with increasing water content. However, the quantum yield of all derivatives dropped substantially in the presence of only a small percentage of water. In general, substitution at the nitrogen EDG produced only small changes in the wavelength of absorption and emission or quantum yield across the derivatives. Of particular note is the behavior of **7d**. Recently, it was demonstrated, that when azetidine was employed as the EDG in a number of push–pull dye systems, the azetidine engendered a substantial increase in quantum yield.²⁵ It was hypothesized that the azetidine reduces the propensity of fluorescence quenching through twisted intramolecular charge transfer (TICT). Unfortunately, this design strategy does not appear to improve the emission intensity of CBD (**7d**, Table 2.3). Previous studies have proposed that the TICT pathway is not the dominant mode of deactivating the emissive excited state for BD fluorophores,²⁷ and our characterization of **7d** (Table 2.3) appears to support this assertion as well. Finally, the emission of **7d** in 0% dioxane does not follow the trend of red-shifting emission wavelength with respect to water content. We do not have a satisfying explanation for this observation at the moment.

Table 2.3. Spectral Properties of CBD Molecules. ^a Φ_F determined relative to Coumarin 153 in EtOH. ^b Φ_F determined relative to Ru(bipy)₃Cl₂ in H₂O; average of two experiments. ^c Φ_F calculated using the refractive index of 100% dioxane.

	dioxane in water (% v/v)	abs λ_{\max} (nm)	em λ_{\max} (nm)	log ϵ	Φ_F
3	0	430	612	3.81	0.002 ^b
	25	432	601	3.75	0.007 ^b
	50	432	583	3.81	0.020 ^b
	75	432	574	3.82	0.054 ^{a,c}
	90	429	567	3.86	0.058 ^{a,c}
	95	423	559	3.92	0.073 ^{a,c}
	100	418	540	3.86	0.218 ^a
7a	0	430	617	3.42	0.002 ^b
	25	434	606	3.45	0.009 ^b
	50	432	596	3.54	0.024 ^b
	75	432	583	3.49	0.066 ^{a,c}
	90	434	573	3.52	0.066 ^{a,c}
	95	430	564	3.58	0.100 ^{a,c}
	100	427	546	3.57	0.363 ^a
7b	0	441	612	3.48	0.005 ^b
	25	447	604	3.52	0.018 ^b
	50	444	594	3.56	0.051 ^b
	75	441	582	3.62	0.132 ^{a,c}
	90	440	569	3.49	0.166 ^{a,c}
	95	438	562	3.56	0.207 ^{a,c}
	100	437	546	3.58	0.407 ^a
7c	0	459	630	3.58	0.005 ^b
	25	460	616	3.49	0.021 ^b
	50	456	603	3.58	0.041 ^b
	75	454	590	3.56	0.113 ^{a,c}
	90	453	575	3.49	0.140 ^{a,c}
	95	448	569	3.55	0.198 ^{a,c}
	100	447	556	3.62	0.410 ^a
7d	0	460	570	3.74	0.006 ^b
	25	462	625	3.87	0.014 ^b
	50	462	616	3.94	0.043 ^b
	75	462	600	3.91	0.149 ^{a,c}
	90	454	585	3.82	0.176 ^{a,c}
	95	458	578	3.92	0.187 ^{a,c}
	100	451	564	3.95	0.389 ^a

We next sought to compare the behavior of NBD (**10**) and SBD (**11**) dyes with the highest reported emission intensity with that of CBD (**7c**) from our series (Figure 2.5).¹⁵ The data in Figure 2.5A show that **7c** had a lower quantum yield compared to **10** or **11** across all combinations of dioxane in water. This observation suggests that the cyano group may contribute to more rapid deactivation of the excited state. However, the dramatic drop in emission intensity in the presence of only 5% water in dioxane suggests the quenching

mechanism is more than simple hydrogen bonding to the cyano group in the excited state and likely involves a more complex process. The dramatic drop in the emission intensity of **7c** also leads to a far greater change in emission intensity in the presence of small quantities of water (Figure 2.5B). Thus, we surmise that CBDs might find applications in biological imaging of lipid bilayers and other structures with low water content. This new class of BD chromophores is stable to a range of pH (see Supporting Information (SI) for details) and probes based on this design principle are currently under investigation in our laboratory.

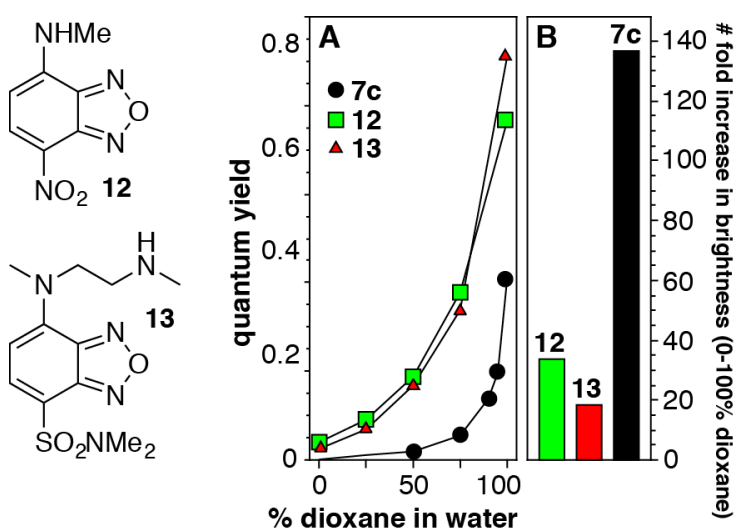


Figure 2.5. (A) Fluorescence quantum yield of BD derivatives in response to changes in hydrogen bonding and polarity. (B) Overall (turn-on) change in emission intensity of BD derivatives.

2.4 Conclusion

We report the first characterization of a new class of environmentally sensitive fluorophores. This new class of dyes, based on benzoxa- and benzothiadiazole, introduces cyano as the electron-withdrawing group within this class of push-pull dyes. The cyano group produces red-shifted wavelengths of emission compared with previously reported dyes that employ nitro or sulfonamide as the electron withdrawing group (the “pull”). The results of this study support our hypothesis that the cyano group increased the environmental

sensitivity of BD fluorophores to water. However, this sensitivity appears to be more complex than simple hydrogen bonding between the cyano group and water. Experiments to ascertain the excited state deactivation pathways are currently underway in our lab. We propose that the dramatic changes in emission intensity in response to small changes in aqueous solvation provided by CBD could provide greater discernment between small changes in polarity around membranes.

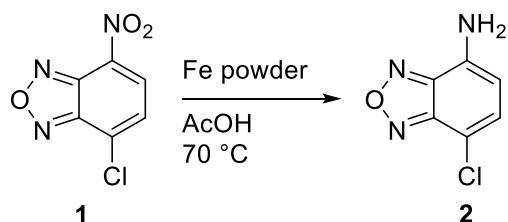
2.5 Experimental

Unless otherwise specified, all commercial products and reagents were used as purchased, without further purification. The synthesis of **7a–d** was based on a previous literature procedure.¹⁷ Microwave reactions were performed in a Biotage initiator using the default power settings for each solvent. Microwave reactions were carried out in sealed vials, and the temperature of the reaction was monitored by an external IR sensor. Analytical thin-layer chromatography (TLC) and flash chromatography of all reactions was performed on silica gel (40 μm) purchased from Grace Davison. All solvents used for photophysical experiments were reagent grade. NMR spectroscopy: ^1H and ^{13}C NMR spectra for all compounds were acquired in deuterated solvents (as indicated) on a Bruker spectrometer at the field strengths reported in the text. The chemical shift data are reported in units of δ (ppm) relative to residual solvent. Absorption and emission spectroscopy: Fluorescence spectra were measured on an Agilent Technologies Cary Eclipse fluorescence spectrophotometer using right-angle detection. Ultraviolet–visible absorption spectra were measured with an Agilent Technologies Cary 8454 UV–vis diode array system and corrected for background signal with a cuvette containing the same solvent used for analysis. Fluorescent quantum yields were determined relative to the fluorescence standard reported in

the text and are corrected for solvent refractive index and absorption differences at the excitation wavelength. The photostability studies were carried out using a Rayonet photoreactor containing 16 side-on fluorescent lamps and an air-cooling fan. CBD(O) and CBD(S) were dissolved in THF at a concentration that produced an optical density (absorbance) of 0.1. The samples were vigorously stirred while undergoing photoirradiation $\lambda = 420$ nm. At 5 min intervals, the sample was removed and analyzed by UV-vis spectroscopy. This process was repeated until the sample had been photoirradiated for 30 min. HPLC spectra were taken on a Waters 2545 Binary Gradient Module with Water 2998 photodiode array detector and XBridge 4.6×250 mm, C18 $5 \mu\text{m}$ column. UPLC spectra were taken on a Waters ACQUITY.

2.5.1 Synthetic Procedures

Scheme 2.2

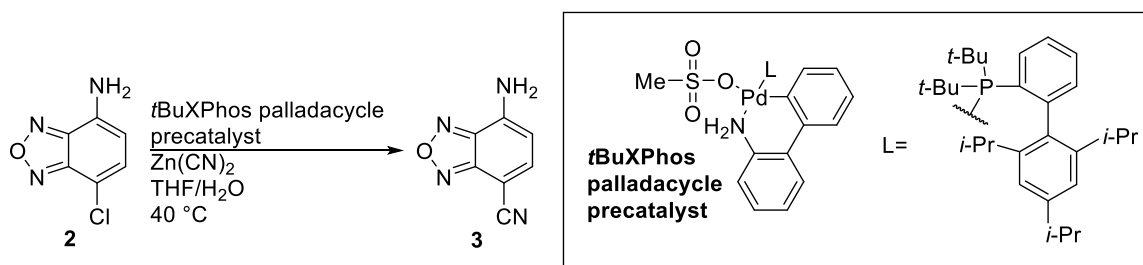


Synthesis of 7-Chloro-2,1,3-benzoxadiazol-4-amine (2). On the basis of a previously reported procedure,²⁸ acetic acid (9 mL) was heated to 70 °C, after which it was degassed and put under N₂. 1 (0.22 g, 1 mmol, 1 eq) and Fe powder (0.18 g, 3 mmol, 3 eq) were added. The mixture was stirred at 70 °C for 30 min. The reaction was cooled to room temperature and concentrated under reduced pressure. The residue was dissolved in ethyl acetate and washed with NaHCO₃ (3×). The aqueous layers were combined and extracted with EtOAc (2×). The organic layers were combined and dried over Na₂SO₄. The solution was concentrated under reduced pressure. The product was purified by silica gel

chromatography (5:1 hexanes:EtOAc) to give **2** as a dark orange powder (0.175 g, 94%).

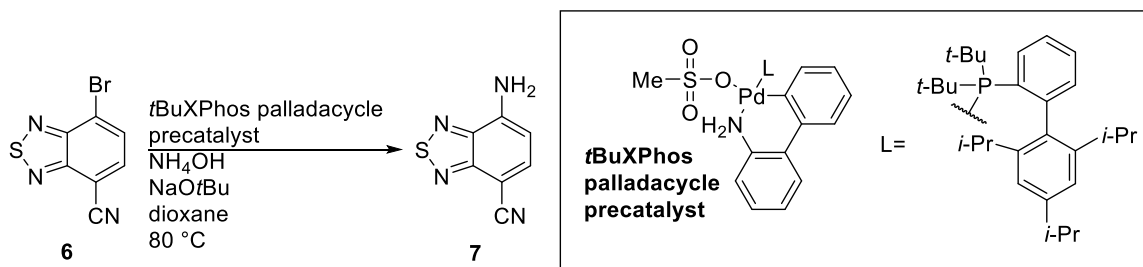
Spectra of product match those previously reported (Scheme 2.2).²⁹

Scheme 2.3



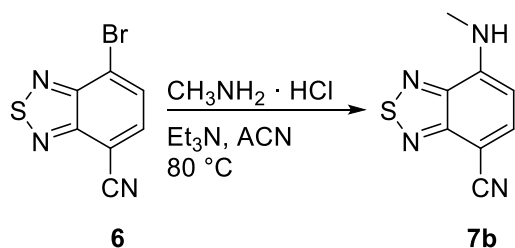
Synthesis of 7-Cyano-2,1,3-benzoxadiazol-4-amine (3). On the basis of the procedure of Cohen et al.,²¹ **2** (0.054 g, 0.3 mmol, 1 eq), Zn(CN)₂ (0.035 g, 0.29 mmol, 1 eq), and *t*BuXPhos palladacycle precatalyst (0.024g, 0.029 mmol, 0.10 eq) were added to a vial and capped with an airtight septum. The vial was put under N₂. In a separate vial, 0.15 mL of THF and 0.75 mL of H₂O were degassed and put under N₂. The THF/water mix was added to **2**. The solution was added to a heat block preheated to 40 °C, and the reaction was stirred rapidly (900 rpm) for 22 h. The reaction was partitioned between EtOAc and satd. NaHCO₃, and the mixture was stirred for 5 min. The layers were separated, and the aqueous layers were extracted with EtOAc (3×). The organic layers were combined, dried over Na₂SO₄, and concentrated under reduced pressure. The product was purified by silica gel chromatography (5:2 hexanes:EtOAc, R_f = 0.23) to give **3** as an orange powder (0.028 g, 55%). ¹H NMR (DMSO, 600 MHz) δ 8.03 (s, 2H), 7.96 (d, J = 8 Hz, 1H), 6.36 (d, J = 8 Hz, 1H). ¹³C NMR (DMSO, 600 MHz) δ 149.1, 144.4, 143.7, 143.2, 116.7, 103.7, 79.1. HRMS (ESI-TOF) m/z: [M + H]⁺ Calcd. for C₇H₄N₄OH 161.0458, found 161.0455 (Scheme 2.3).

Scheme 2.4



Synthesis of 7-Cyano-2,1,3-benzothiadiazol-4-amine (7a). $\mathbf{6}^{24}$ (0.041 g, 0.17 mmol, 1 eq), NaOtBu (0.026 g, 0.27 mmol, 1.6 eq), and *t*BuXPhos palladacycle precatalyst (0.010 g, 0.01 mmol, 0.06 eq) were put under N_2 . In a separate vial, 0.8 mL of dioxane and NH_4OH (0.03 mL, 0.2 mmol, 1.2 eq) were degassed and put under N_2 . The NH_4OH /dioxane solution was added to **6**, and the solution was stirred at $80\text{ }^\circ\text{C}$ for 21 h. The reaction was cooled to room temperature and concentrated under reduced pressure. The product was purified by silica gel chromatography (10:3 hexanes:EtOAc, $R_f = 0.19$) to give **7a** as an orange powder (0.014 g, 45%). ^1H NMR (DMSO, 600 MHz) δ 7.97 (d, $J = 8$ Hz, 1H), 7.53 (s, 2H), 6.59 (d, $J = 8$ Hz, 1H). ^{13}C NMR (DMSO, 600 MHz) δ 154.4, 146.4, 139.7, 117.9, 104.2, 86.4. HRMS (ESI-TOF) m/z : $[\text{M} + \text{H}]^+$ Calcd for $\text{C}_7\text{H}_4\text{N}_4\text{SH}$ 177.0229, found 177.0226 (Scheme 2.4).

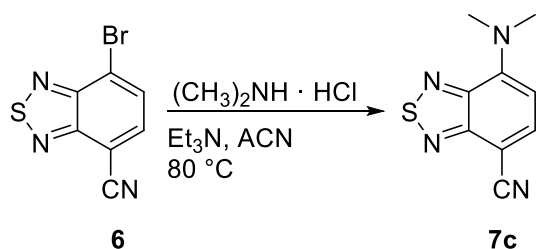
Scheme 2.5



Synthesis of 7-Cyano-2,1,3-benzothiadiazole-4-methylamine (7b). $\mathbf{6}^{24}$ (0.043 g, 0.18 mmol, 1 eq) and methylamine hydrochloride (0.039 g, 0.58 mmol, 3.2 eq) were dissolved in 0.85 mL of acetonitrile. Triethylamine (0.12 mL, 0.85 mmol, 5 eq) was added,

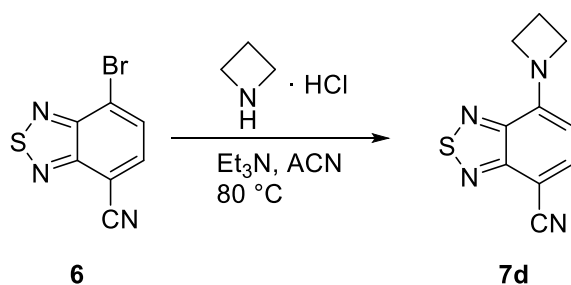
and the solution was stirred for 19 h at 80 °C. The reaction was cooled to room temperature and concentrated under reduced pressure. The product was purified by silica gel chromatography (5:1 hexanes:EtOAc, $R_f = 0.19$) to give **7b** as an orange powder (0.019g, 57%). ^1H NMR (DMSO, 600 MHz) δ 8.07 (d, $J = 8$ Hz, 1H), 8.05 (s, 1H), 6.42 (d, $J = 8$ Hz, 1H), 2.97 (d, $J = 5$ Hz, 3H). ^{13}C NMR (DMSO, 600 MHz) δ 153.9, 145.8, 140.0, 132.4, 117.9, 100.3, 86.5, 29.5. HRMS (ESI-TOF) m/z : $[\text{M} + \text{H}]^+$ Calcd for $\text{C}_8\text{H}_6\text{N}_4\text{SH}$ 191.0386, found 191.0384 (Scheme 2.5).

Scheme 2.6



Synthesis of 7-Cyano-2,1,3-benzothiadiazole-4-dimethylamine (7c). **6**²⁴ (0.041 g, 0.17 mmol, 1 eq) and dimethylamine hydrochloride (0.046 g, 0.56 mmol, 3.3 eq) were dissolved in 0.85 mL of acetonitrile. Triethylamine (0.12 mL, 0.85 mmol, 5 eq) was added, and the solution was stirred for 19 h at 80 °C. The reaction was cooled to room temperature and concentrated under reduced pressure. The product was purified by silica gel chromatography (5:1 hexanes:EtOAc, $R_f = 0.17$) to give **7c** as an orange powder (0.029 g, 84%). ^1H NMR (DMSO, 600 MHz) δ 7.99 (d, $J = 8$ Hz, 1H), 6.49 (d, $J = 8$ Hz, 1H), 3.48 (s, 6H). ^{13}C NMR (DMSO, 600 MHz) δ 155.4, 146.5, 146.1, 138.4, 117.8, 105.0, 87.5, 42.4. HRMS (ESI-TOF) m/z : $[\text{M} + \text{H}]^+$ Calcd for $\text{C}_9\text{H}_8\text{N}_4\text{SH}$ 205.0542, found 205.0541 (Scheme 2.6).

Scheme 2.7



Synthesis of 7-Cyano-2,1,3-benzothiadiazole-4-azetidamine (7d). 6^{24} (0.042 g, 0.17 mmol, 1 eq) and azetidine hydrochloride (0.055 g, 0.59 mmol, 3.5 eq) were dissolved in 0.85 mL of acetonitrile. Triethylamine (0.12 mL, 0.85 mmol, 5 eq) was added, and the solution was stirred for 22 h at 80 °C. The reaction was cooled to room temperature and concentrated under reduced pressure. The product was purified by silica gel chromatography (5:1 hexanes:EtOAc, $R_f = 0.16$) to give **7d** as an orange powder (0.025 g, 68%). $^1\text{H NMR}$ (CDCl_3 , 600 MHz) δ 7.75 (d, $J = 8$ Hz, 1H), 5.99 (d, $J = 8$ Hz, 1H), 4.53 (br s, 4H) 2.58 (quin, $J = 8$ Hz, 2H). $^{13}\text{C NMR}$ (DMSO, 600 MHz) δ 155.0, 145.4, 145.2, 138.6, 118.0, 101.6, 86.2, 46.6, 16.7. HRMS (ESI-TOF) m/z : $[\text{M} + \text{H}]^+$ Calcd for $\text{C}_{10}\text{H}_8\text{N}_4\text{SH}$ 217.0542, found 217.0540 (Scheme 2.7).

General Procedure for Synthesis of 6 via t-BuXPhos Palladacycle. A vial of solvent (0.85 mL) was degassed and added to 4,7-dibromobenzothiadiazole (0.17 mmol), precatalyst (0.009 mmol), and zinc cyanide (0.09 mmol) in a separate flask under nitrogen. The reaction was heated at 40 °C overnight before being partitioned between EtOAc and satd NaHCO_3 . The aqueous layer was extracted with EtOAc (3 \times) concentrated under reduced pressure and analyzed by NMR.

General Procedure for Synthesis of 6 via CuCN. 4,7- Dibromobenzothiadiazole (0.17 mmol) was suspended in the indicated solvent (0.57 mL). The mixture was stirred in

the microwave at the stated time and temperature using default power presets associated with the solvent. After cooling to room temperature, the solution was concentrated under reduced pressure and analyzed by NMR.

2.5.2 NMR Spectra

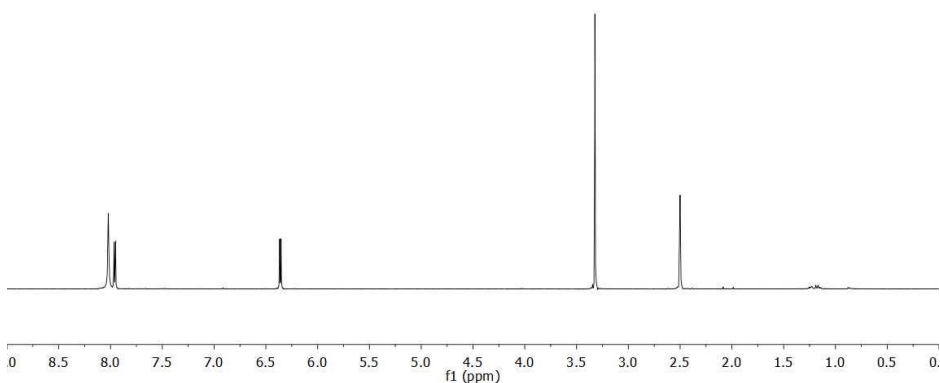


Figure 2.6: ^1H NMR spectra of **3** in DMSO (600 MHz).

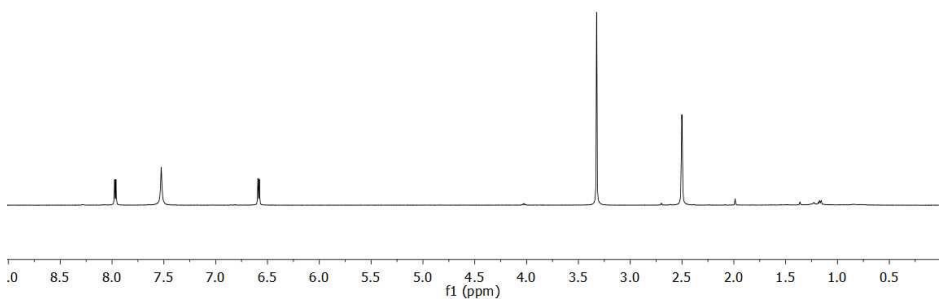


Figure 2.8: ^1H NMR spectra of **7a** in DMSO (600 MHz).

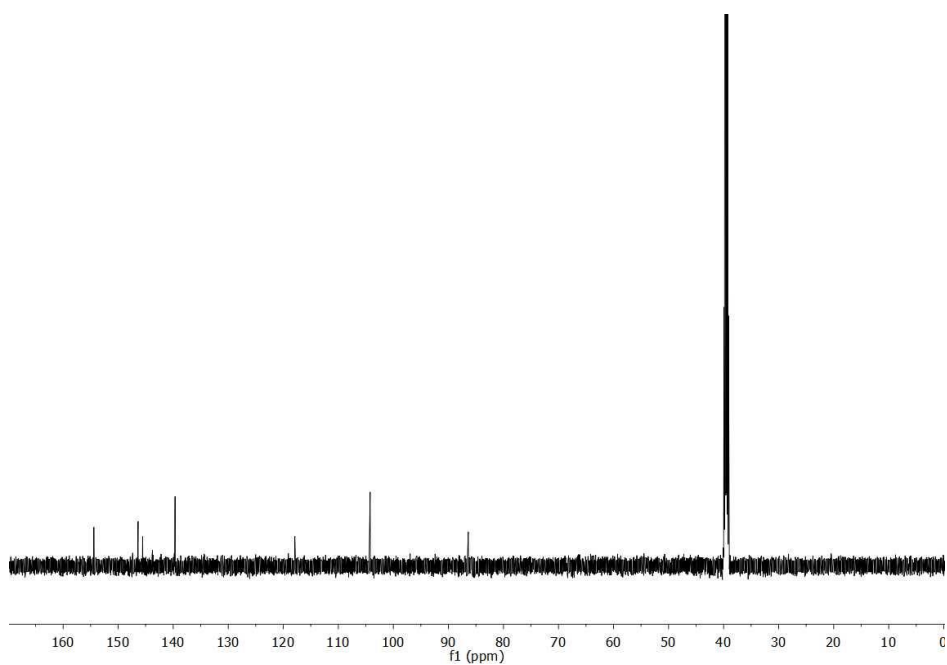


Figure 2.9: ^{13}C NMR spectra of **7a** in DMSO (150 MHz).

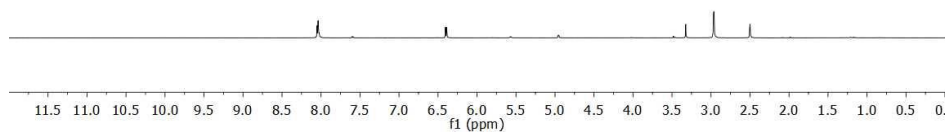


Figure 2.10: ^1H NMR spectra of **7b** in DMSO (600 MHz).

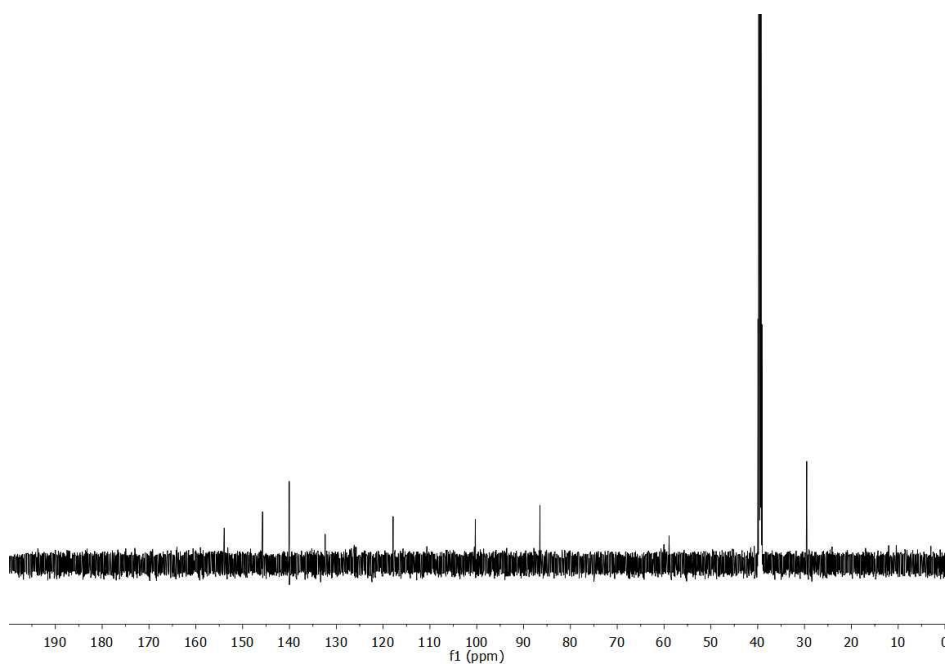


Figure 2.11: ^{13}C NMR spectra of **7b** in DMSO (150 MHz).

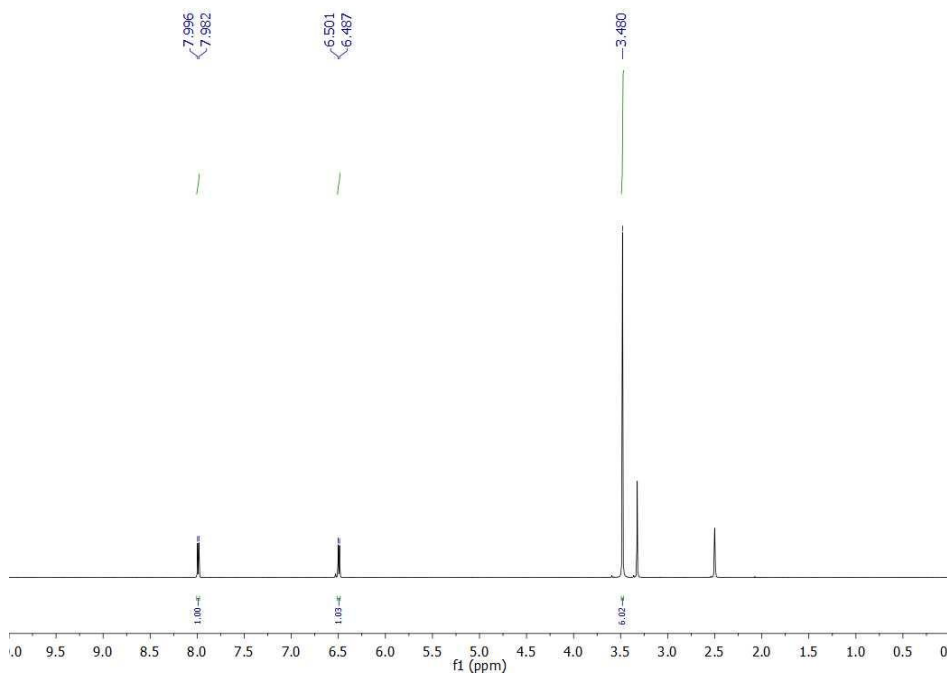


Figure 2.12: ^1H NMR spectra of **7c** in DMSO (600 MHz).

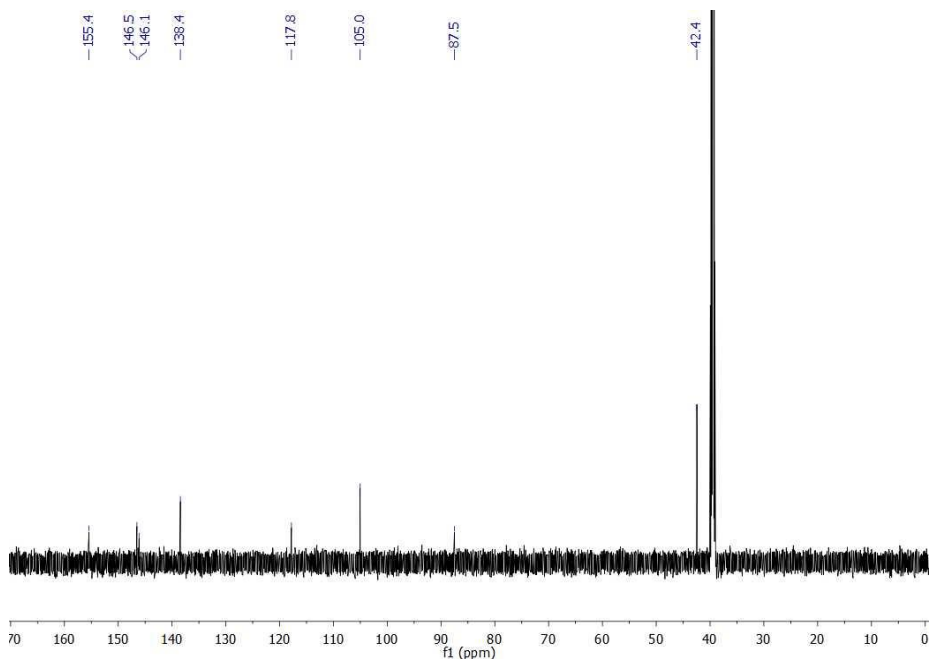


Figure 2.13: ^{13}C NMR spectra of **7c** in DMSO (150 MHz).

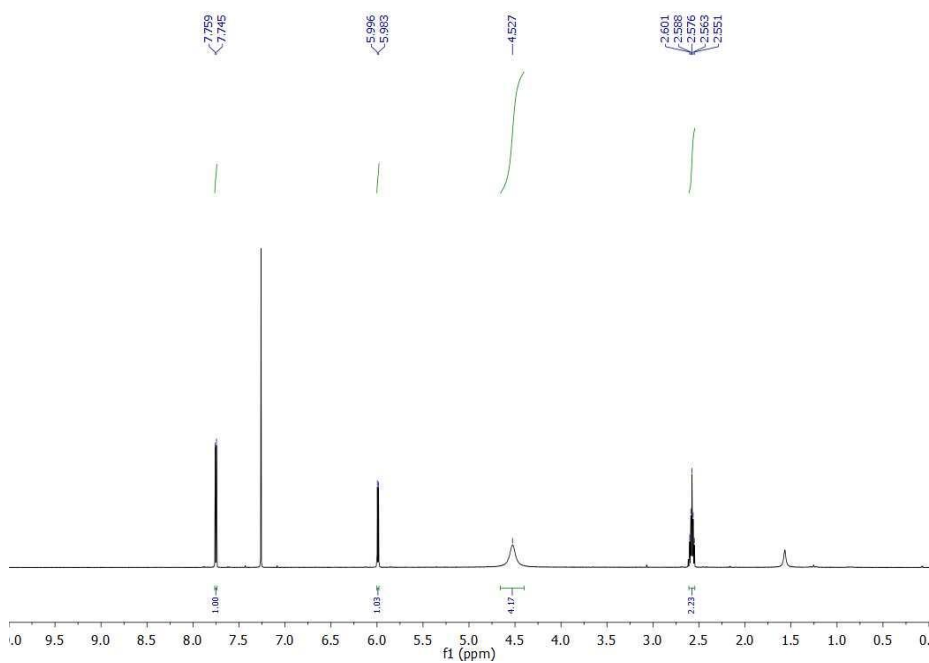


Figure 2.14: ^1H NMR spectra of **7d** in CDCl_3 (600 MHz).

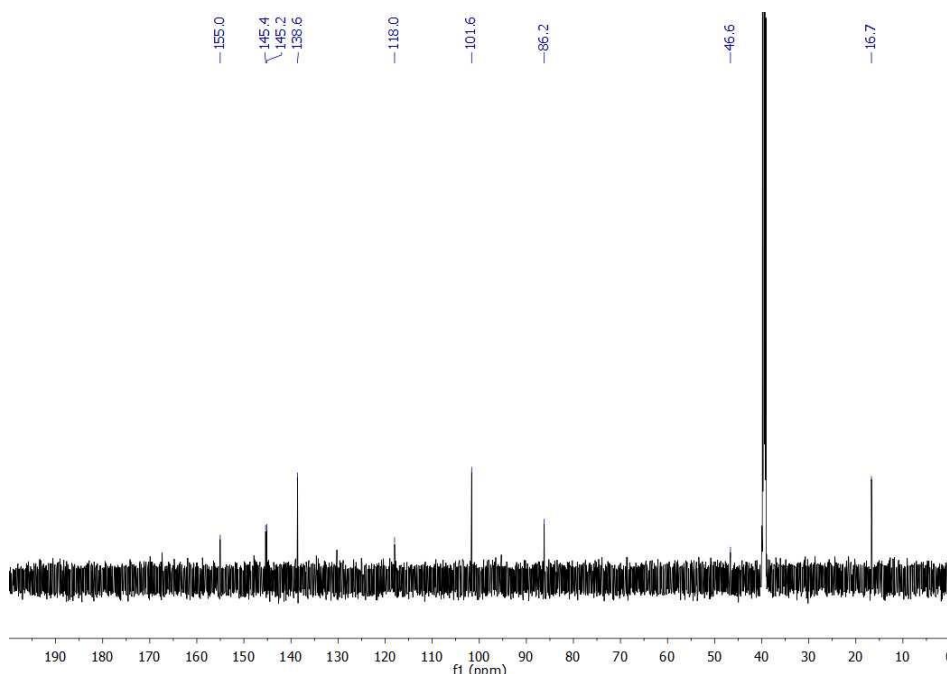


Figure 2.15: ¹³C NMR spectra of **7d** in DMSO (150 MHz).

2.5.3 UV-Vis and Fluorescence Data

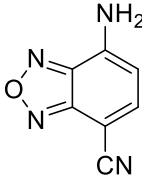
Experimental details for data in tables below:

Following the procedure of Brouwer, A. M. *Pure and Appl. Chem.* **2011**, 83, 2213-2228. All samples for photophysics were diluted until OD was between 0.08-0.1. All quantum yields were calculated using the equation below:

$$\Phi = \frac{F^i F_s n_i^2}{F^s f_i n_s^2} \Phi_f^s$$

Where F_i and F_s are the fluorescence integrations of the sample and standard, respectively; f_s and f_i are the absorption factors of the standard and sample respectively; and n_i and n_s are the refractive indices of the sample solvent and standard solvent respectively.

Table 2.4: Summary of photophysical data for **3**.

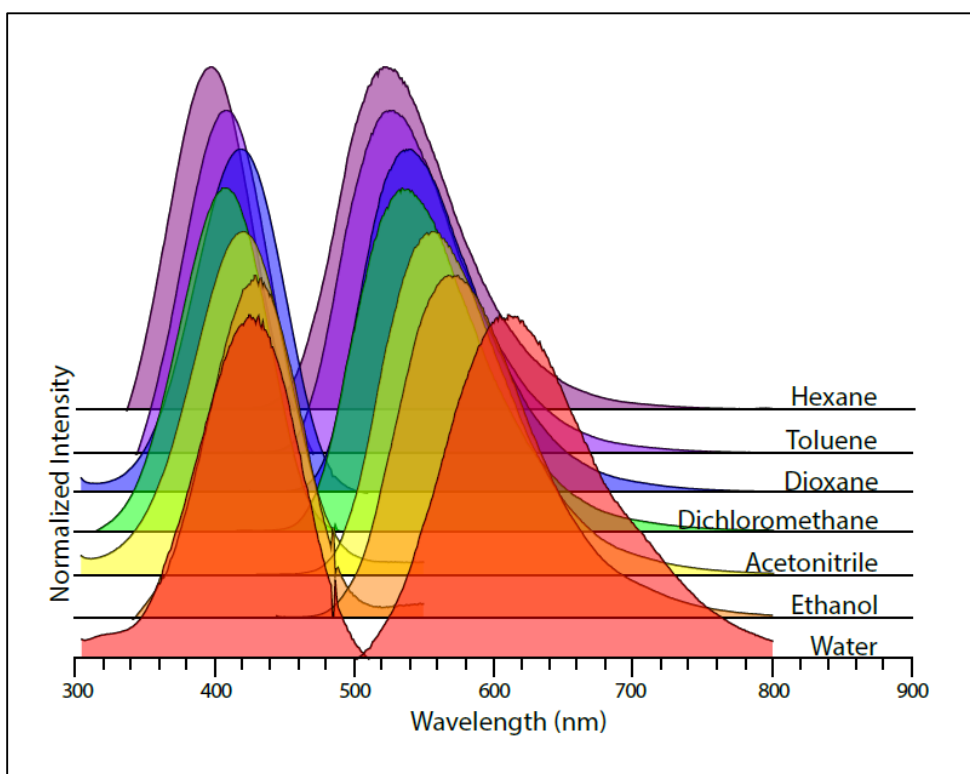
	solvent	Polarity value ^e	Abs λ_{\max} (nm)	Em λ_{\max} (nm)	log ϵ	Φ_F^f
	Hexane	0.009	397	522	3.79	0.329 ^f
	Toluene	0.099	409	529	3.79	0.304 ^f
	Dioxane	0.164	418	540	3.86	0.218 ^f
	Dichloromethane	0.309	407	535	3.82	0.195 ^f
	Acetonitrile	0.460	421	557	3.88	0.105 ^f
	Ethanol	0.654	430	575	3.91	0.027 ^g
	Water	1	430	612	3.81	0.001 ^g

^e Values based on a relative solvent polarity scale reported in Empirical Parameters of Solvent Polarity. In

Solvents and Solvent Effects in Organic Chemistry, Fourth Edition; Reichardt, C., Welton, T., Eds.; Wiley-

VCH: Weinheim, 2011; pp 425-508. Quantum yields determined relative to ^fcoumarin 153 in ethanol and

^gRu(bipy)₃Cl₂ in water.

**Figure 2.16:** UV-Vis absorbance (left) and fluorescence emission (right) spectra of **3**.**Table 2.5:** Summary of photophysical data for **4**.

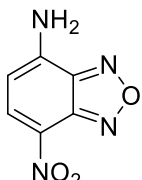
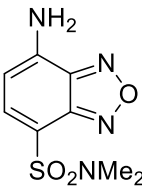
	solvent	Polarity value ^e	Abs λ_{\max} (nm)	Em λ_{\max} (nm)
	Hexane	0.009	Insoluble	Insoluble
	Toluene	0.099	427	504
	Dioxane	0.164	438	518
	Dichloromethane	0.309	430	514
	Acetonitrile	0.460	446	524
	Ethanol	0.654	455	531
	Water	1	467	560

Table 2.6: Summary of photophysical data for **5**.

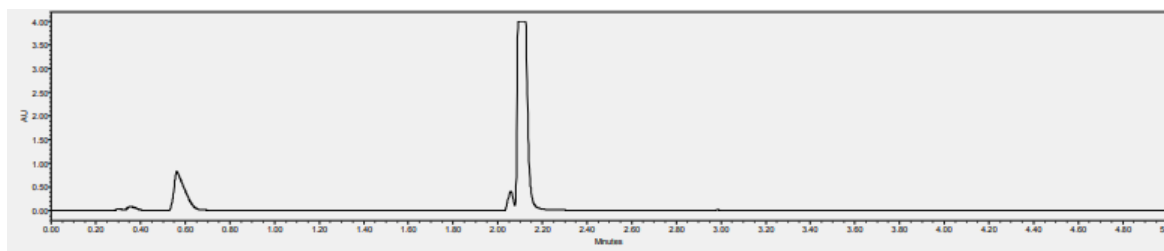
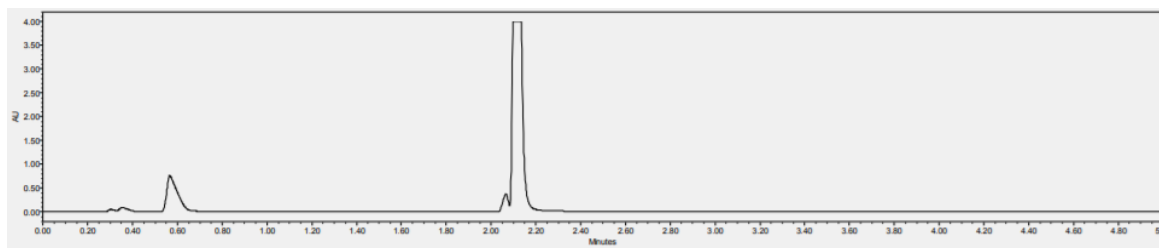
	solvent	Polarity value ^e	Abs λ_{\max} (nm)	Em λ_{\max} (nm)
	Hexane	0.009	392	501
	Toluene	0.099	404	516
	Dioxane	0.164	414	533
	Dichloromethane	0.309	405	526
	Acetonitrile	0.460	414	547
	Ethanol	0.654	426	560
	Water	1	424	602

2.5.4 pH Stability Studies

1 mg of **3** and **7a** was dissolved in 1 mL of 0.5 M HCl, 0.5 M NaOH, and 0.1 M phosphate buffer (pH 7.4). A sample was taken at time = 0 h and time = 12 h and evaluated by UPLC at 254 nm. Degradation of the probes does occur in 0.5 M NaOH over 12 h. The solvent program used was:

Time (min)	% water	% acetonitrile
0	95	5
3	5	95
3.01	0	100
3.5	0	100
3.51	95	5
4	95	5

The peak at 0.60 min is solvent front.

**Figure 2.17:** UPLC trace, **3** in 0.5 M HCl, t = 0 h.**Figure 2.18:** UPLC trace, **3** in 0.5 M HCl, t = 12 h.

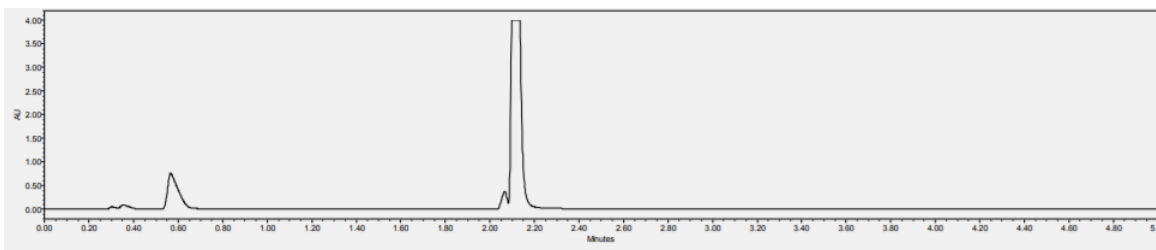


Figure 2.19: UPLC trace, **3** in 0.5 M NaOH, t = 0 h.

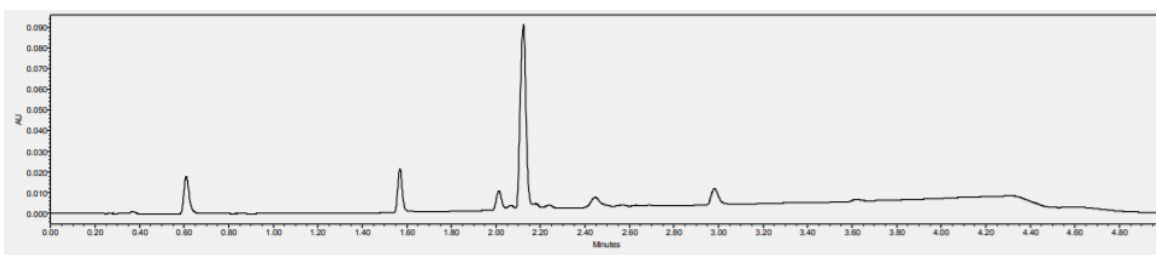


Figure 2.20: UPLC trace, **3** in 0.5 M NaOH, t = 12 h.

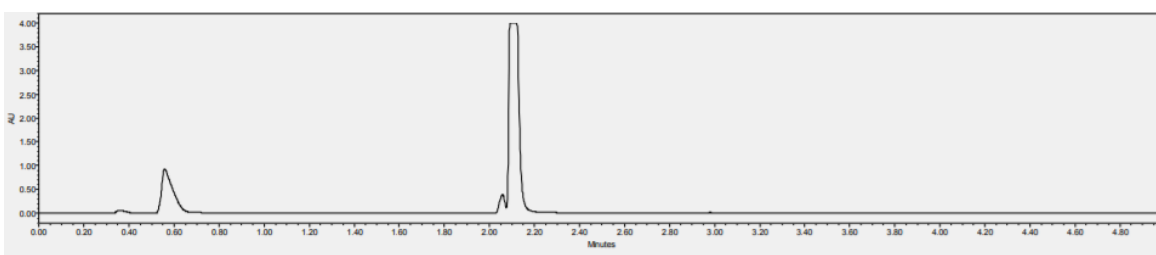


Figure 2.21: UPLC trace, **3** in 0.1 M phosphate buffer (pH 7.4), t = 0 h.

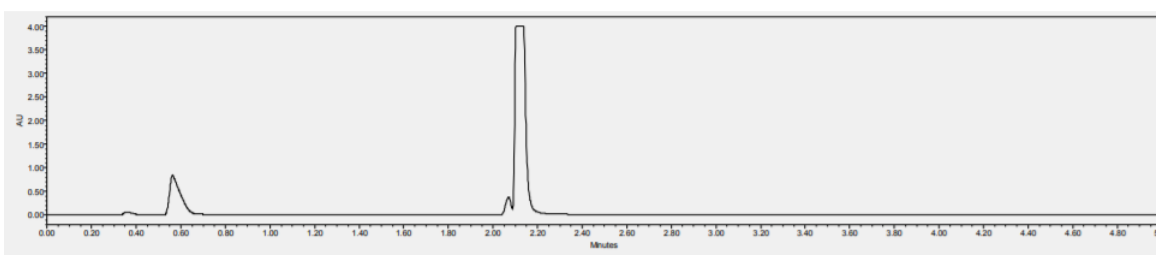


Figure 2.22: UPLC trace, **3** in 0.1 M phosphate buffer (pH 7.4), t = 12 h.

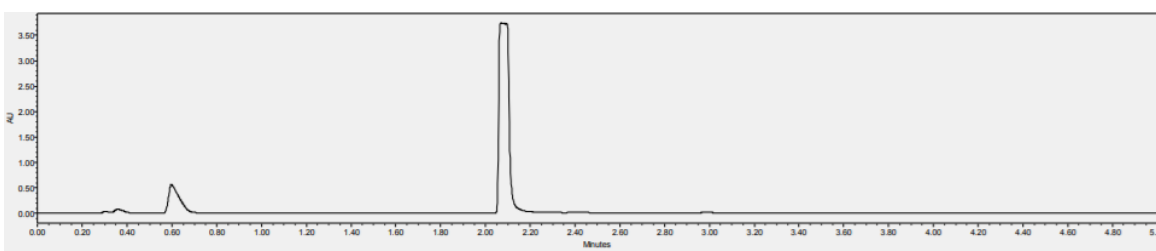


Figure 2.23: UPLC trace, **7a** in 0.5 M HCl, t = 0 h.

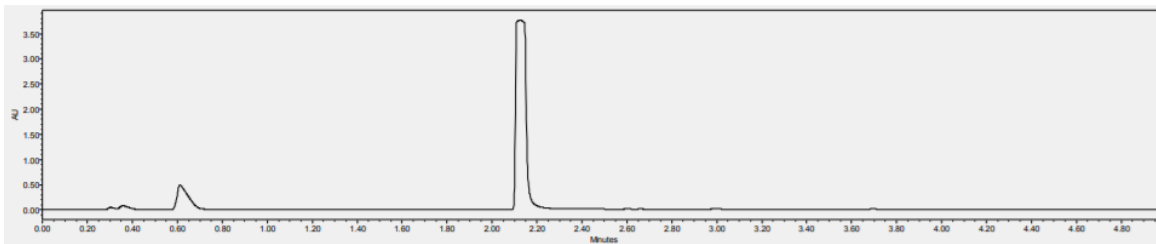


Figure 2.24: UPLC trace, **7a** in 0.5 M HCl, t = 12 h.

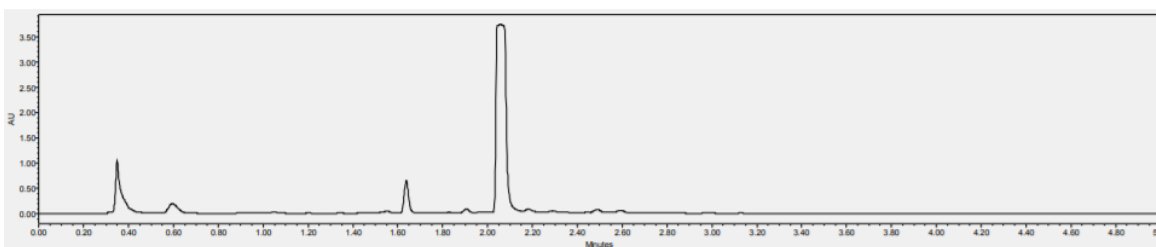


Figure 2.25: UPLC trace, **7a** in 0.5 M NaOH, t = 0 h.

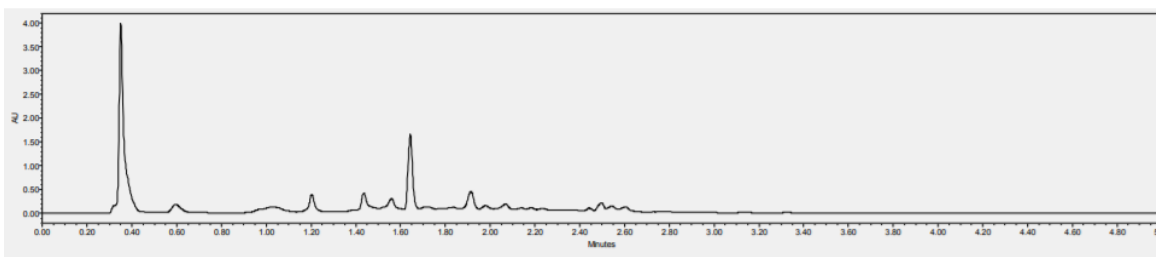


Figure 2.26: UPLC trace, **7a** in 0.5 M NaOH, t = 12 h.

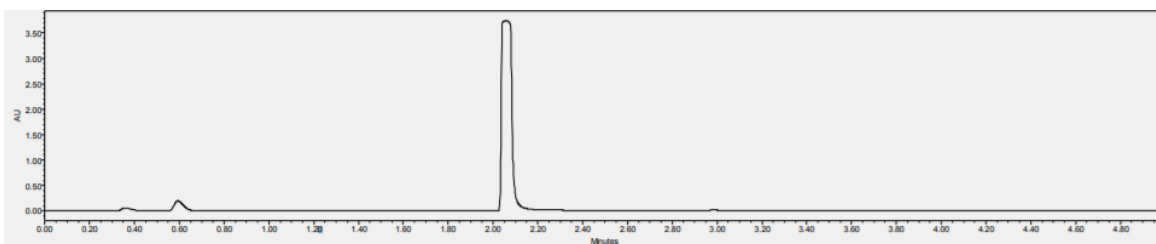


Figure 2.27: UPLC trace, **7a** in 0.1 M phosphate buffer (pH 7.4), t = 0 h.

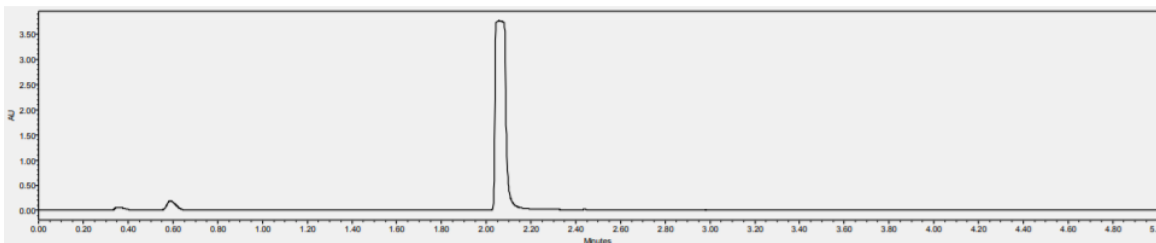


Figure 2.28: UPLC trace, **7a** in 0.1 M phosphate buffer (pH 7.4), t = 12 h.

2.5.5 HPLC Chromatograms

All spectra were taken using a reverse phase C18 column with solvent A:H₂O and solvent B: acetonitrile.

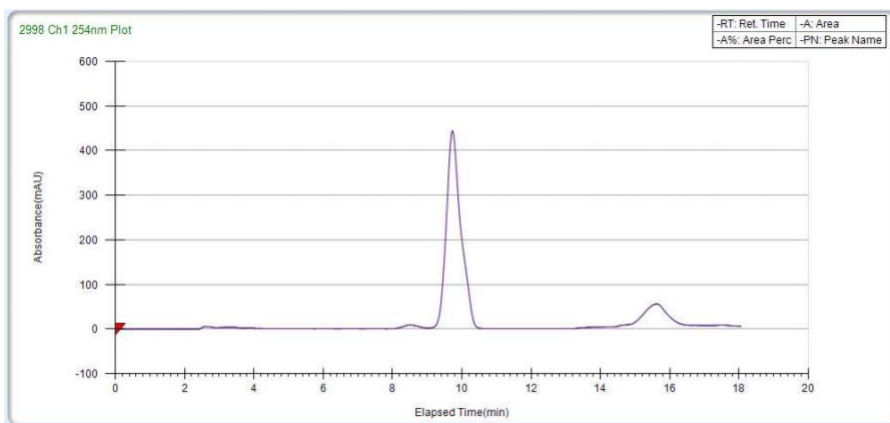


Figure 2.29: HPLC trace, **3**, 254 nm. Method:

Time (min)	% A	% B
0	55	45
10	55	45
10.1	5	95
14	5	95
18	55	45

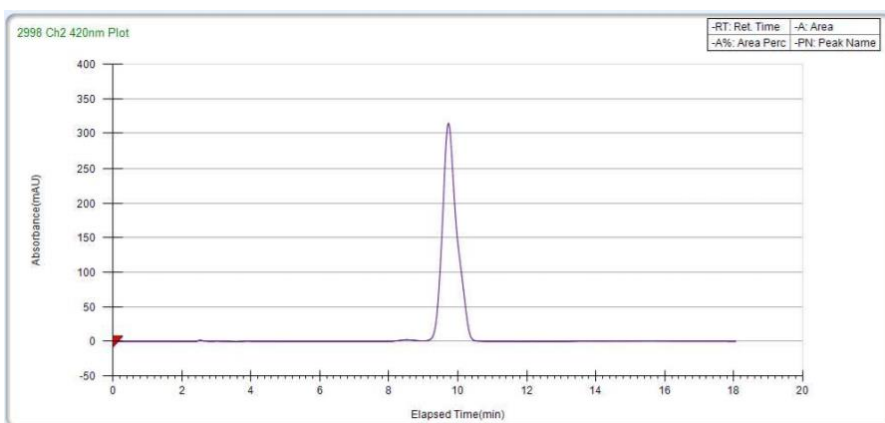


Figure 2.30: HPLC trace, **3**, 420 nm. Method:

Time (min)	% A	% B
0	55	45
10	55	45
10.1	5	95
14	5	95
18	55	45

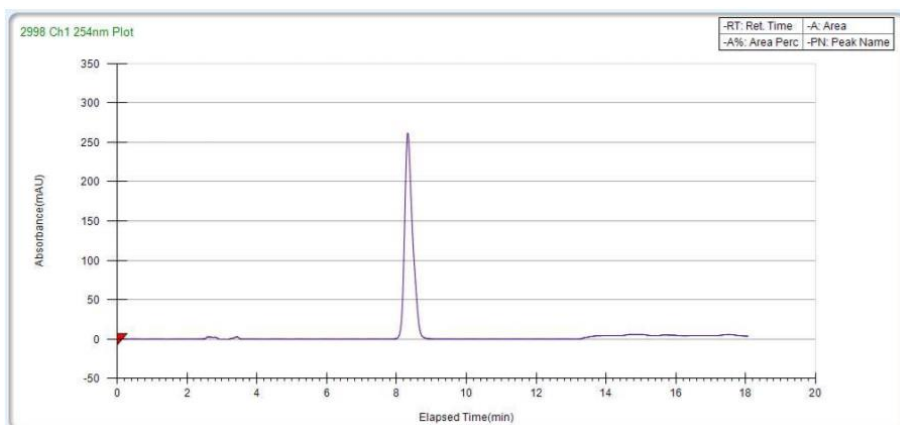


Figure 2.31: HPLC trace, **7a**, 254 nm. Method:

Time (min)	% A	% B
0	55	45
10	55	45
10.1	5	95
14	5	95
18	55	45

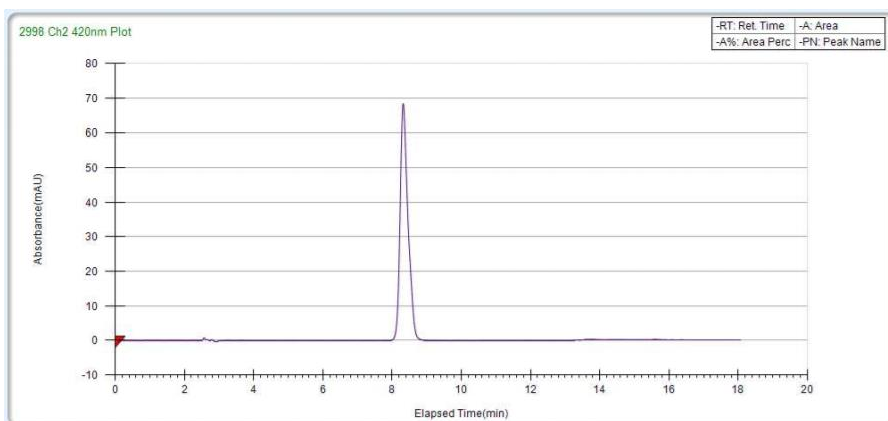


Figure 2.32: HPLC trace, **7a**, 420 nm. Method:

Time (min)	% A	% B
0	55	45
10	55	45
10.1	5	95
14	5	95
18	55	45

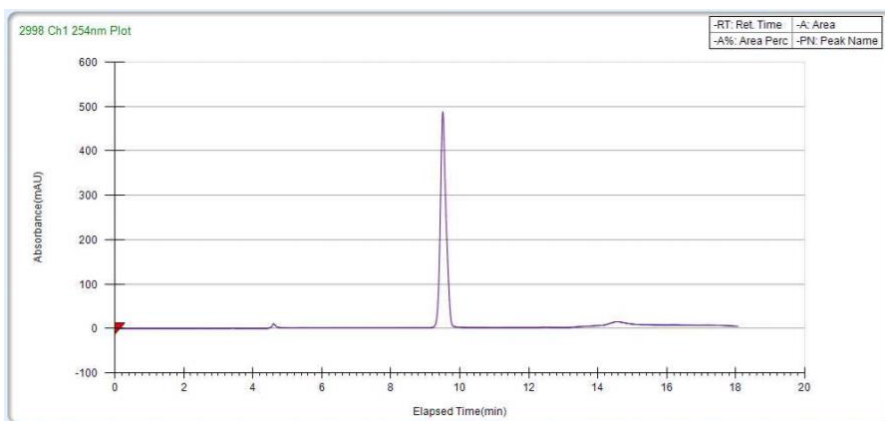


Figure 2.33: HPLC trace, **7b**, 254 nm. Method:

Time (min)	% A	% B
0	95	5
1	40	60
10	35	65
10.1	5	95
14	5	95
18	95	5

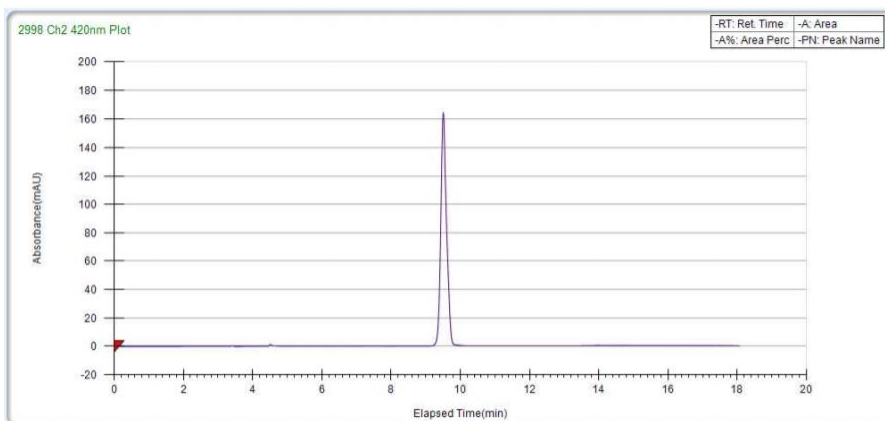


Figure 2.34: HPLC trace, **7b**, 420 nm. Method:

Time (min)	% A	% B
0	95	5
1	40	60
10	35	65
10.1	5	95
14	5	95
18	95	5

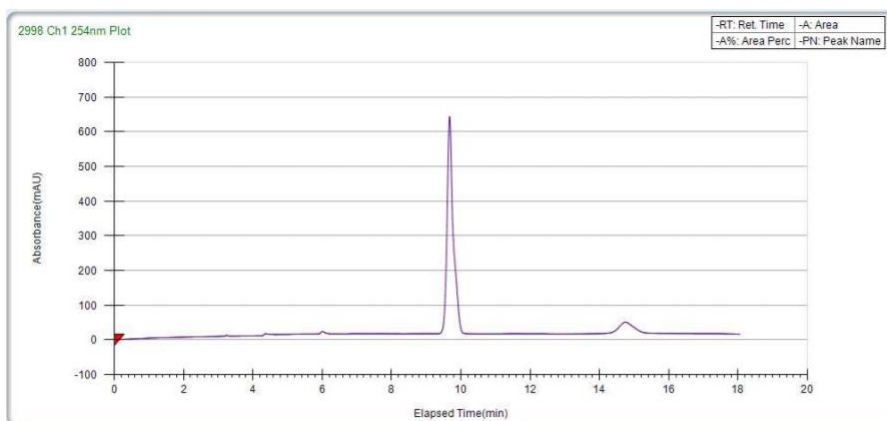


Figure 2.35: HPLC trace. **7c**, 254 nm. Method:

Time (min)	% A	% B
0	95	5
1	25	75
10	15	85
10.1	5	95
14	5	95
18	95	5

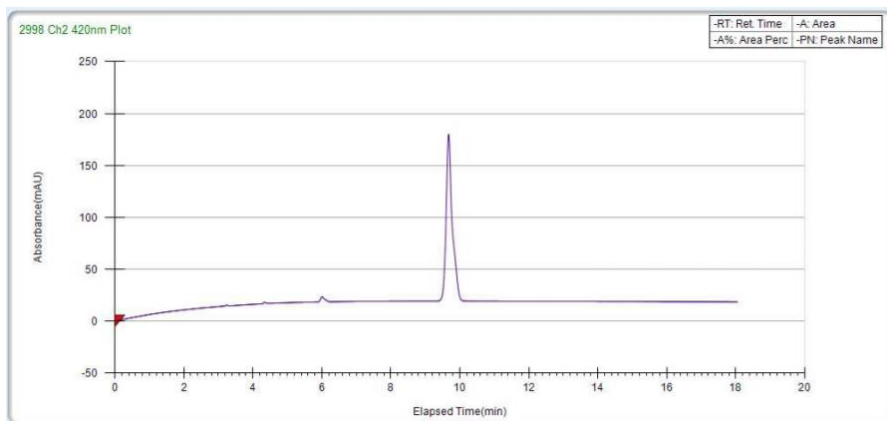


Figure 2.36: HPLC trace, **7c**, 420 nm. Method:

Time (min)	% A	% B
0	95	5
1	25	75
10	15	85
10.1	5	95
14	5	95
18	95	5

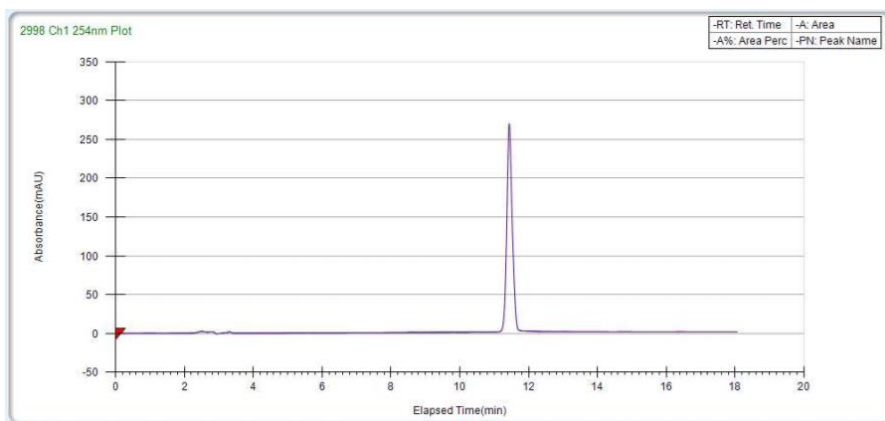


Figure 2.37: HPLC trace, 7d, 254 nm. Method:

Time (min)	% A	% B
0	45	55
10	5	95
14	5	95
18	95	5

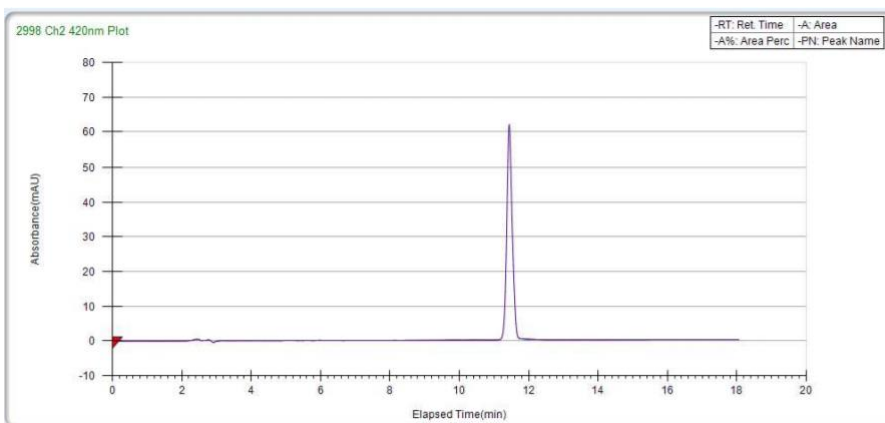


Figure 2.38: HPLC trace, 7d, 420 nm. Method:

Time (min)	% A	% B
0	45	55
10	5	95
14	5	95
18	95	5

Acknowledgements

We are grateful for support of this work by Iowa State University of Science and Technology and the Iowa State University Crop Bioengineering Consortium Seed Grant Initiative. We also thank the laboratory of Prof. Javier Vela for the use of their photoreactor.

References

1. Thooft, A. M.; Cassaidy, K.; VanVeller, B. *J. Org. Chem.* **2017**, *82*, 8842-8847.
2. Kymchenko, A. S.; Mely, Y. *Prog. Mol. Biol. Transl. Sci.* **2013**, *113*, 35-58.
3. Klymchenko, A. S. *Acc. Chem. Res.* **2017**, *50*, 366-375.
4. Loving, G. S.; Sainlos, M.; Imperiali, B. *Trends Biotechnol.* **2010**, *28*, 73-83.
5. Klymchenko, A. S.; Kreder, R. *Chem. Biol.* **2014**, *21*, 97-113.
6. Santos-Figueroa, L. E.; Moragues, M. E.; Climent, E.; Agostini, A; Martínez-Mañez, R.; Sancenón, F. *Chem. Soc. Rev.* **2013**, *42*, 3489-3613.
7. Han, J.; Burgess, K. *Chem. Rev.* **2010**, *110*, 2709-2728.
8. Nadler, A.; Schultz, C. *Angew. Chem. Int. Ed.* **2013**, *52*, 2408-2410.
9. Zhu, H.; Fan, J.; Du, J.; Peng, X. *Acc. Chem. Res.* **2016**, *49*, 2115-2126.
10. Li, X.; Gao, X.; Shi, W.; Ma, H. *Chem. Rev.* **2014**, *114*, 590-659.
11. Neto, B. A.; Carvalho, P. H.; Correa, J. R. *Acc. Chem. Res.* **2015**, *48*, 1560-1569.
12. Liu, T. K.; Hsieh, P. Y.; Zhuang, Y. D.; Hsia, C. Y.; Huang, C. L.; Lai, H. P.; Lin, H. S.; Chen, I. C.; Hsu, H. Y.; Tan, K. T. *ACS Chem. Biol.* **2014**, *9*, 2359-2365.
13. Uchiyama, S.; Santa, T.; Fukushima, T.; Homma, H.; Imai, K. *J. Chem. Soc., Perkin Trans. 2* **1998**, 2165-2173.
14. Uchiyama, S.; Takehira, K.; Kohtani, S.; Imai, K.; Nakagaki, R.; Tobita, S.; Santa, T. *Org. Biomol. Chem.* **2003**, *1*, 1067-1072.
15. Uchiyama, S.; Kimura, K.; Gota, C.; Okabe, K.; Kawamoto, K.; Inada, N.; Yoshihara, T.; Tobita, S. *Chem. – Eur. J.* **2012**, *18*, 9552-9563.
16. Haugland, R. P.; Spence, M. T. Z.; Johnson, I. D.; Basey, A. *The Handbook: A Guide to Fluorescent Probes and Labeling Technologies*, 10th ed.; Molecular Probes: Eugene, OR, 2005.
17. Gota, C.; Uchiyama, S.; Yoshihara, T.; Tobita, S.; Ohwada, T. *J. Phys. Chem. B* **2008**, *112*, 2829-2836.
18. Martin, E.; Pardo, A.; Guijarro, M. S.; Fernandez-Alonso, J. I. *J. Mol. Struct.* **1986**, *142*, 197-200.

19. Johnson, I. *Histochem. J.* **1998**, *30*, 123-140.
20. Salvati, M. E.; Balog, J. A.; Pickering, D. A.; Sören, G.; Fura, A.; Li, W.; Paterl, R. N.; Hanson, R. L. US Patent 20040077605A1, April 22, 2004.
21. (a) Cohen, D. T.; Buchwald, S. L. *Org. Lett.* **2015**, *17*, 202-205. (b) Benson, G. M.; Rutledge, M. C.; Widdowson, K. L. WO 0076501 A1, December 21, 2000.
22. Reichardt, C. *Chem. Rev.* **1994**, *94*, 2319-2358.
23. *Solvent and Solvent Effects in Organic Chemistry*, 4th ed.; Reichardt, C., Welton, T., Eds.; Wiley-VCH: Weinheim, 2011; pp 425-508.
24. Agneeswari, R.; Tamilavan, V.; Song, M. Hyun, M. H. *J. Mater. Chem. C.* **2014**, *2*, 8505-8524.
25. Grimm, J. B.; English, B. P.; Chen, J.; Slaughter, J. P.; Zhang, Z.; Revyakin, A.; Paterl, R.; Macklin, J. J.; Normanno, D.; Singer, R. H.; Lionnet, T. Lavis, L. D. *Nat. Methods* **2015**, *12*, 244-250.
26. Liu, X.; Qiao, Q.; Tian, W.; Liu, W.; Chen, J.; Lang, M. J.; Xu, Z. *J. Am. Chem. Soc.* **2016**, *138*, 6960-6963.
27. Saha, S.; Samanta, A. *J. Phys. Chem. A* **1998**, *102*, 7903-7912.
28. Salvati, M. E.; Balog, J. A.; Pickering, D. A.; Sören, G.; Fura, A.; Li, W.; Patel, R. N.; Hanson, R. L. US 20040077605 A1, April 22, 2004.
29. Matsunaga, H.; Santa, T.; Iida, T.; Fukushima, T.; Homma, H.; Imai, K. *Analyst*, **1997**, *122*, 931-936.

CHAPTER 3: CONTROLLING PHOTO-CLEAVAGE: THE MALLEABLE EXCITED STATES OF BENZOTHIADIAZOLE CHROMOPHORES

3.1 Abstract

Herein we report the synthesis of a nitrobenzoxadiazole (NBD) derivative with the possibility of it being used as a photocleavable protecting group (PPG). We were able to demonstrate that the degassed sample in benzene was unstable and underwent photodecomposition. However work is still ongoing with the PPG exposed to air as upon irradiation the NMR indicates the possible formation of an intermediate in the photocleave mechanism.

3.2 Introduction

Photocleavable protecting groups (PPGs) mask, or “cage,” functional groups and can be subsequently cleaved upon excitation with the correct wavelength of light. Examples of masked substrates include pharmaceutical drugs, fluorescent molecules, signaling molecules (e.g. neurotransmitters), as well as numerous other molecules of interest (Figure 3.1).¹⁻³ Photocleavable reactions are of interest because they allow the researcher to control the release of the active molecule via an external light stimulus without introduction of other materials which could negatively impact the environment of interest.

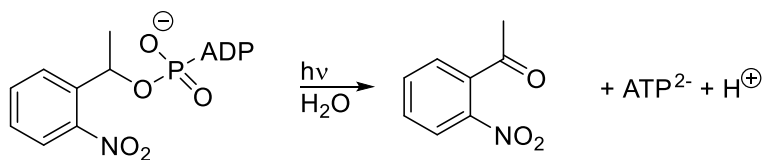


Figure 3.1 Examples of photochemical reactions used to release ATP.

There are several current limitations in the use of PPGs. The first is the requirement that if multiple PPGs are used in the same system, the absorbance maxes must be distinct with little overlap in order to only cleave one group at a time (Figure 3.2).² A second

limitation is that the researcher must deprotect in a sequence-specific order—from the longest wavelength to shortest wavelength. This order of deprotection is necessary due to overlapping absorptions at higher energy wavelengths due to functional group absorptions that occur at these same wavelengths. These overlapping absorbances mean that distinct PPGs cannot be selectively excited at higher energy wavelengths. If the reaction of one PPG could be turned off, however, this would allow for selective activation of one PPG in the presence of another because the absorbed light would only lead to photocleavage of one PPG. Subsequently, the reaction could then be turned back on at a later point to cleave the remaining PPG.⁴

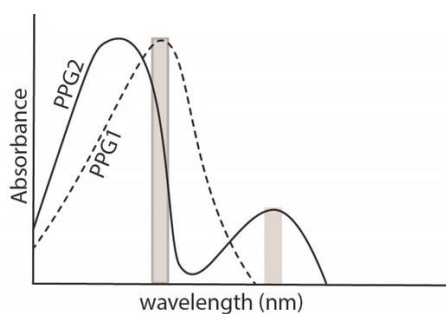


Figure 3.2 Model absorbances of multiple PPGs when used in the same system.

There are only a few PPG systems that have been reported where the order of PPG release can be reversed (deprotect from shortest to longest wavelength). The first system takes advantage of differing reaction rates between PPGs.⁵⁻⁶ This research group noticed that depending on the wavelength of excitation, certain PPGs reacted faster than others.

Consequently, if the right PPGs are chosen, the order of deprotection doesn't matter as only one PPG will be reactive at the specific wavelength (Figure 3.3). The second system took advantage of the kinetic isotope effect when comparing hydrogen to deuterium containing atoms molecules.⁷ Again this system takes advantage of various reaction rates that result from the different bond strengths of a C-H bond versus a C-D bond.

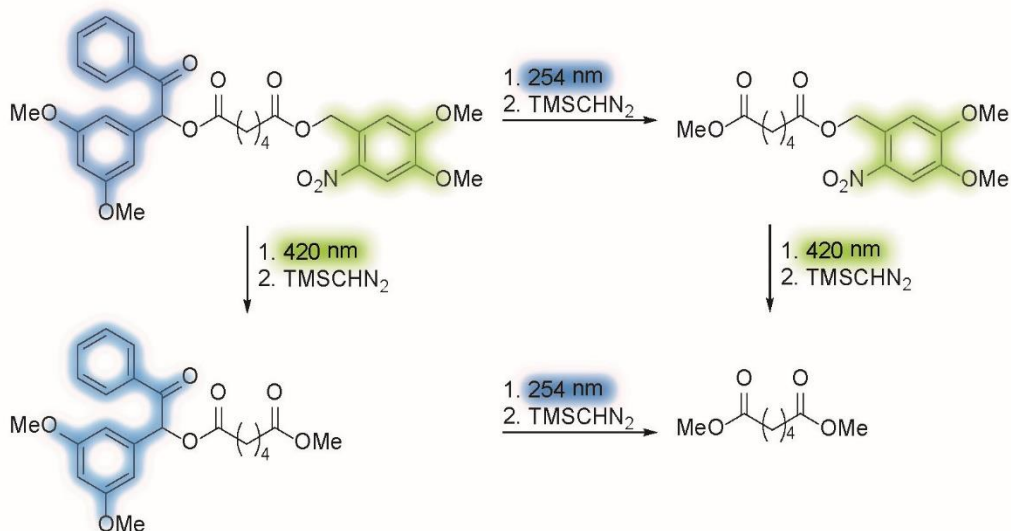


Figure 3.3 One of the few examples where PPGs can be deprotected in either order.⁵⁻⁶

One of the most common photocleavable protecting groups is the ortho-nitrobenzyl protecting group (**1**).^{1,8-9} The popularity of **1** is due to its small size, minimizing steric interactions, as well as relatively high quantum yield of photocleavage. The mechanism (Figure 3.4) involves excitation of the nitro group in **1** to form the excited state (**1***). This excited state can then undergo hydrogen abstraction to form the orthoquinone derivative **2-Z**. The orthoquinone **2-Z** can isomerize to **2-E** which subsequently cyclize to **3**. Ring opening of **3** yields alcohol **4**, which readily forms the carbonyl, ejecting the leaving group to yield the nitroso aldehyde (**5**).¹⁰⁻¹⁵

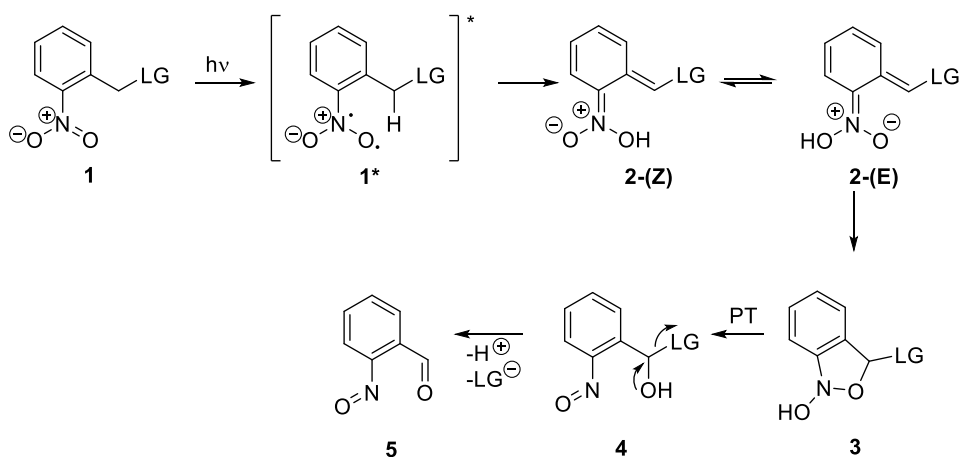


Figure 3.4 o-nitrobenzyl PPG photocleavage mechanism.

The base structure of the ortho-nitrobenzyl PPG **1** absorbs light at approximately 300 nm. This high energy absorbance wavelength means when this photocleavable protecting group (PPG) is used with other PPGs in the same system, it will most likely need to be photocleaved last as photocleavage needs to occur from longest to shortest wavelength (Figure 3.5A). Attempts to redshift the absorbance, by creating a push-pull system, have been somewhat successful. Addition of electron donating groups, such as methoxy groups, redshifts the absorbance to approximately 350 nm, but the quantum yield of photo-release also decreases.¹⁶⁻¹⁷ Ultimately, addition of even more electron donating groups such as dimethylamine further redshifts the absorption to approximately 390 nm, but hydrogen abstraction no longer occurs. The lack of hydrogen abstraction with **8** is due to the excited state of **8** adopting a charge-transfer (CT) state which cannot undergo the hydrogen abstraction, which is the $n \rightarrow \pi^*$ state, necessary for photocleavage (Figure 3.5B).⁵

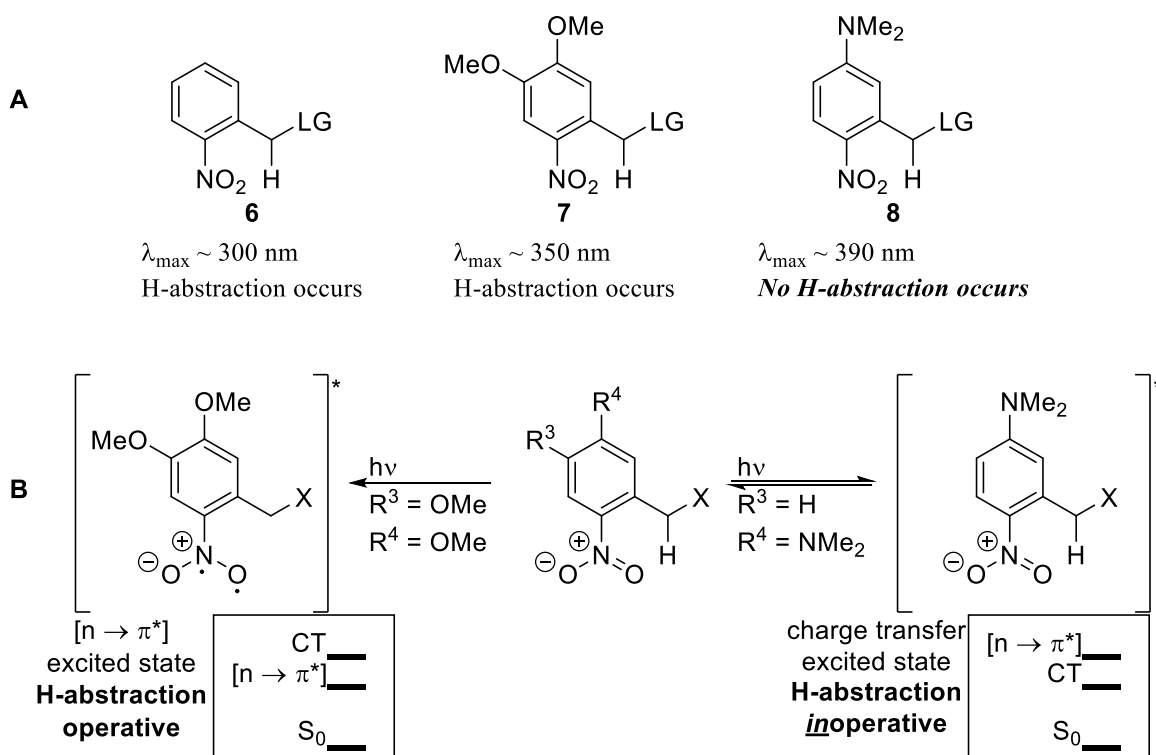


Figure 3.5 (A) Absorption wavelengths of various nitro PPGs and ability to photocleave. (B) Charge transfer state of dimethylamine PPG instead of hydrogen abstraction leading to photocleavage.

A commonly used fluorophore in chemistry is nitrobenzoxadiazole (**NBD**).¹⁸ This fluorescent molecule is of interest due to its small size, minimizing steric interactions, and green fluorescence, shifting it past the autofluorescence of the cell. Much work has been done looking into shifting the wavelength by altering the electron donating group (EDG) on the system (Figure 3.6).¹⁹⁻²¹

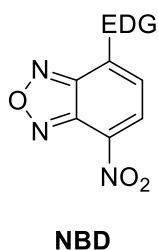


Figure 3.6 Basic structure of NBD fluorophore.

Saha and Samanta looked into how changing the amine effected the nonradiative deactivation, quantum yield and other photophysical measurements. During their investigation, they came across an interesting observation. They observed a dramatic decrease in quantum yields of NBD-NH₂ in toluene when compared to dioxane. These data were in contradiction with all of the other amino EDG molecules they investigated which typically show decreasing quantum yield as polarity increases. Saha and Samanta hypothesized that NBD-NH₂ has two close-lying excited state energy levels: the $n \rightarrow \pi^*$ and the CT excited states. In non-polar solvents the $n \rightarrow \pi^*$ state is lower in energy, while in polar solvents the CT excited state is stabilized and becomes lower in energy (Figure 3.7).²²

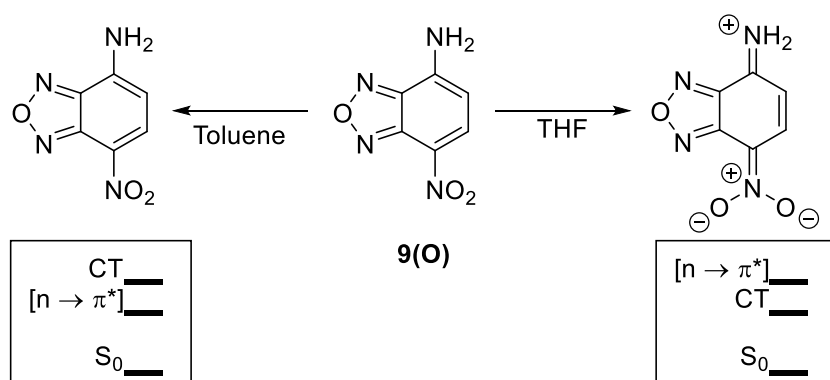


Figure 3.7 Proposed excited states of NBD-NH₂ in different solvents.

We propose combining the NBD fluorophore with the ortho-nitrobenzyl protecting group to produce a new photocleavable protecting that can be turned on/off by altering the environmental polarity (**10**, Figure 3.8). When this benzothiadiazole based PPG is in a non-polar environment, the photocleavage reaction will occur as the $n \rightarrow \pi^*$ excited state is lower in energy than the CT excited state. On the other hand if the PPG is in a polar solvent, photocleavage will not occur due to the CT excited state now being lower in energy than the $n \rightarrow \pi^*$ excited state.

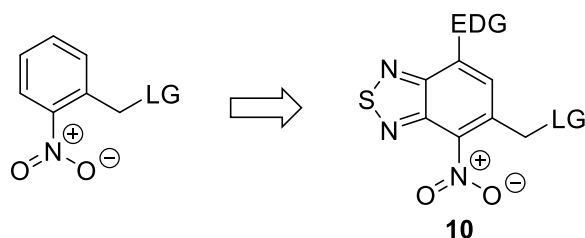


Figure 3.8 Proposed ortho-nitrobenzyl PPG using benzothiadiazole as a scaffold.

3.3 Results and Discussion

Our initial studies focused on the core benzothiadiazole (**9(S)**, Figure 3.9) instead of the benzoxadiazole (**9(O)**, Figure 3.7) because the benzothiadiazoles have been shown to have greater photostability.²¹ We began by irradiating the structure, with no leaving group, in benzene. We were surprised to observe decomposition over the 20 min the sample was irradiated (Figure 3.9A). However, when the sample was degassed and irradiated, very little photodecomposition was observed (Figure 3.9B). Consequently we remained hopeful our proposed PPG would be successful as long as the solution was degassed when irradiation occurred.

To test our hypothesis we started by protecting the amine of 2-fluoro-4-methylaniline (**11**), followed by nitration and subsequent deprotection to yield **12**.²³ The benzothiadiazole was then achieved by nitro reduction using tin (II) chloride²⁴⁻²⁵ and ring closure with N-thionylaniline yielding **13**.²⁶ The NBD structure could readily be obtained by nitration²⁷ followed by amination with ammonium hydroxide²⁸ and boc protection to give **15**.

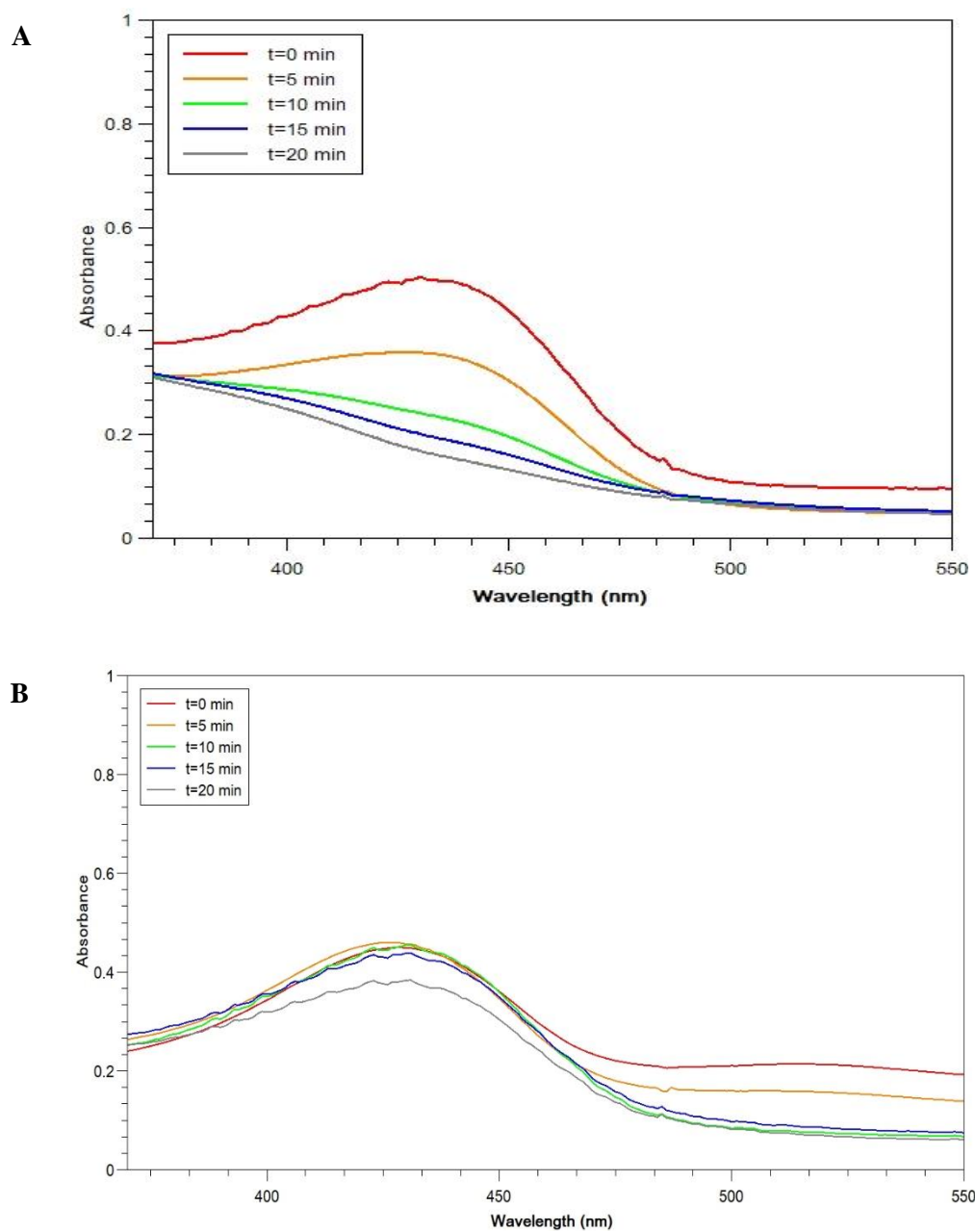
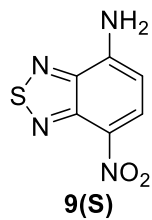
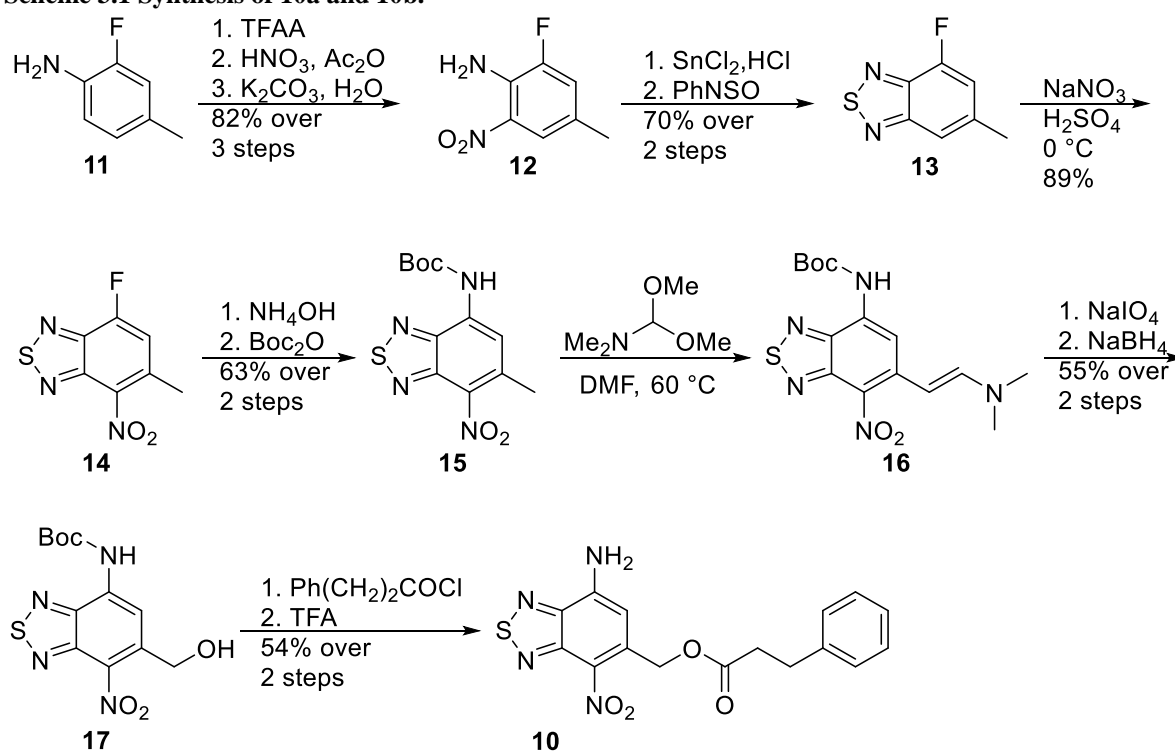


Figure 3.9 (A) Photoirradiation of **9(S)** at 455 nm for 20 min in benzene. (B) Photoirradiation of **9(S)** at 455 nm for 20 min in degassed benzene.

With the NBD core now in hand, we could turn our attention to installation of the leaving group to be photocleaved. To install the leaving group, we first reacted **15** with DMFDMA to obtain enamine (**16**)²⁹ which could be hydrolyzed³⁰ to yield the aldehyde which underwent a sodium borohydride reduction to yield alcohol **17**. Finally 3-phenylpropanoyl chloride was added followed by boc deprotection to yield our hypothesized NBD PPG (**10**).

Scheme 3.1 Synthesis of 10a and 10b.



With our new PPG in hand we could now test our hypothesis. We made a 1 mg/mL solution of our PPG in deuterated benzene, degassed the sample and irradiated the sample at 455 nm with ¹H NMR spectra taken every 5 min. We were surprised to see the degassed sample had very poor photostability. We didn't see any evidence of photocleavage but only photodecomposition (Figure 3.10).

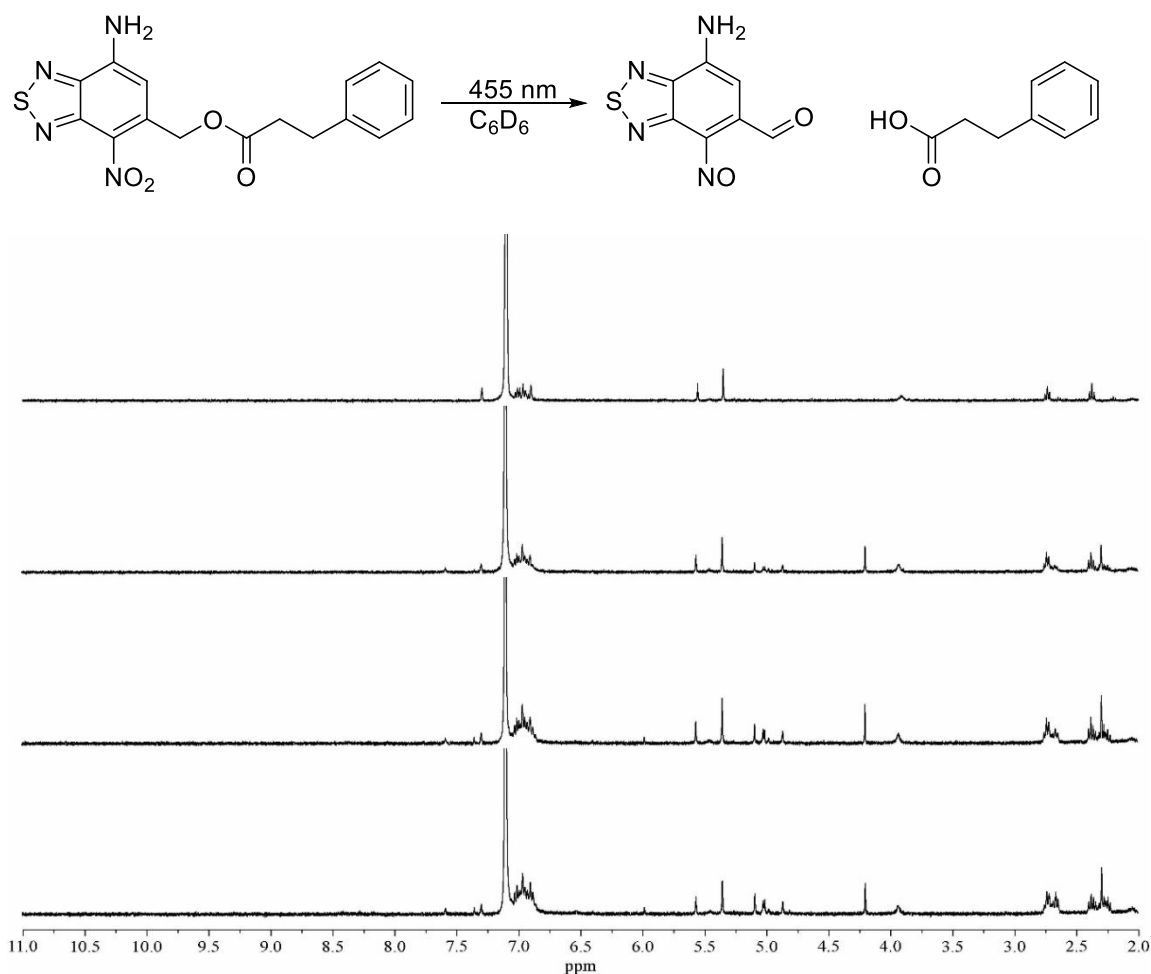


Figure 3.10 Irradiation at 455 nm in degassed benzene.

We then did the same experiment but this time the sample was open to air. Unfortunately we did not see any aldehyde or carboxylic acid signal that would correspond with the desired photocleavage product. However we do see new peaks come in that are shifted in relation to the starting material. This seems to indicate that we may be forming an intermediate in the photocleavage mechanism. Work is currently undergoing in our lab to confirm if this photocleaving mechanism is at work or not.

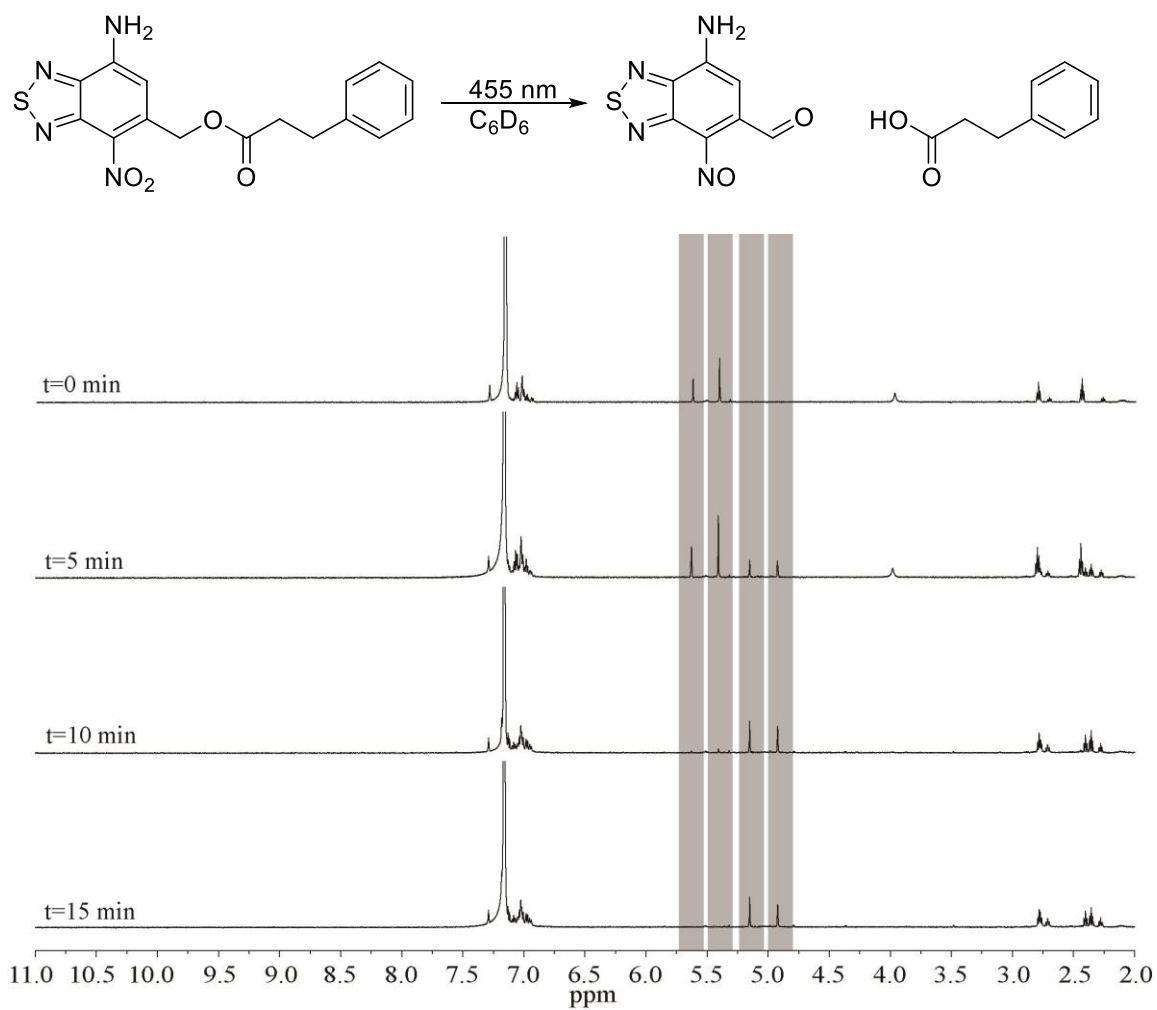


Figure 3.11 Irradiation at 455 nm in benzene exposed to air.

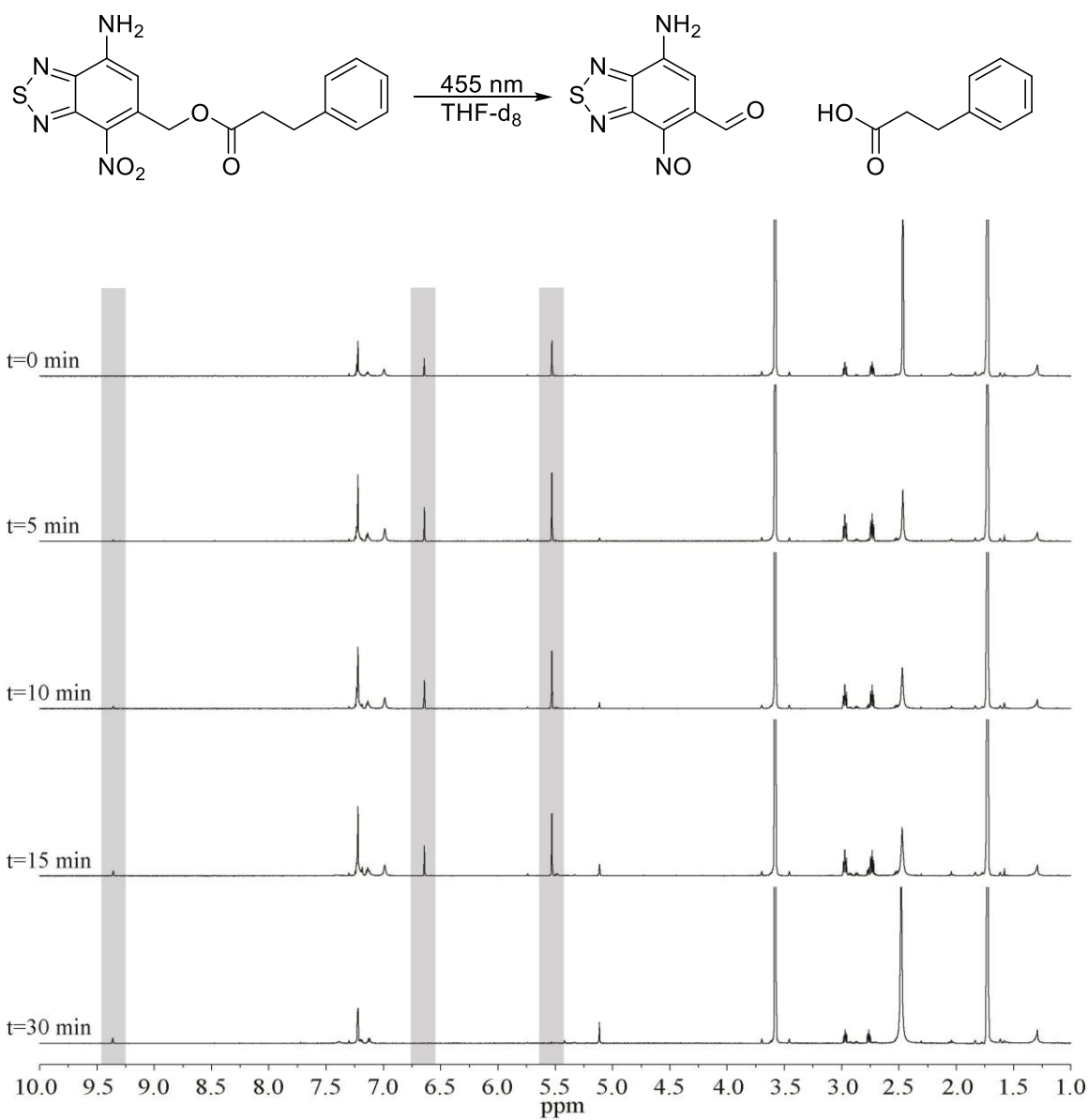


Figure 3.12 Irradiation at 455 nm in THF-d₈ exposed to air.

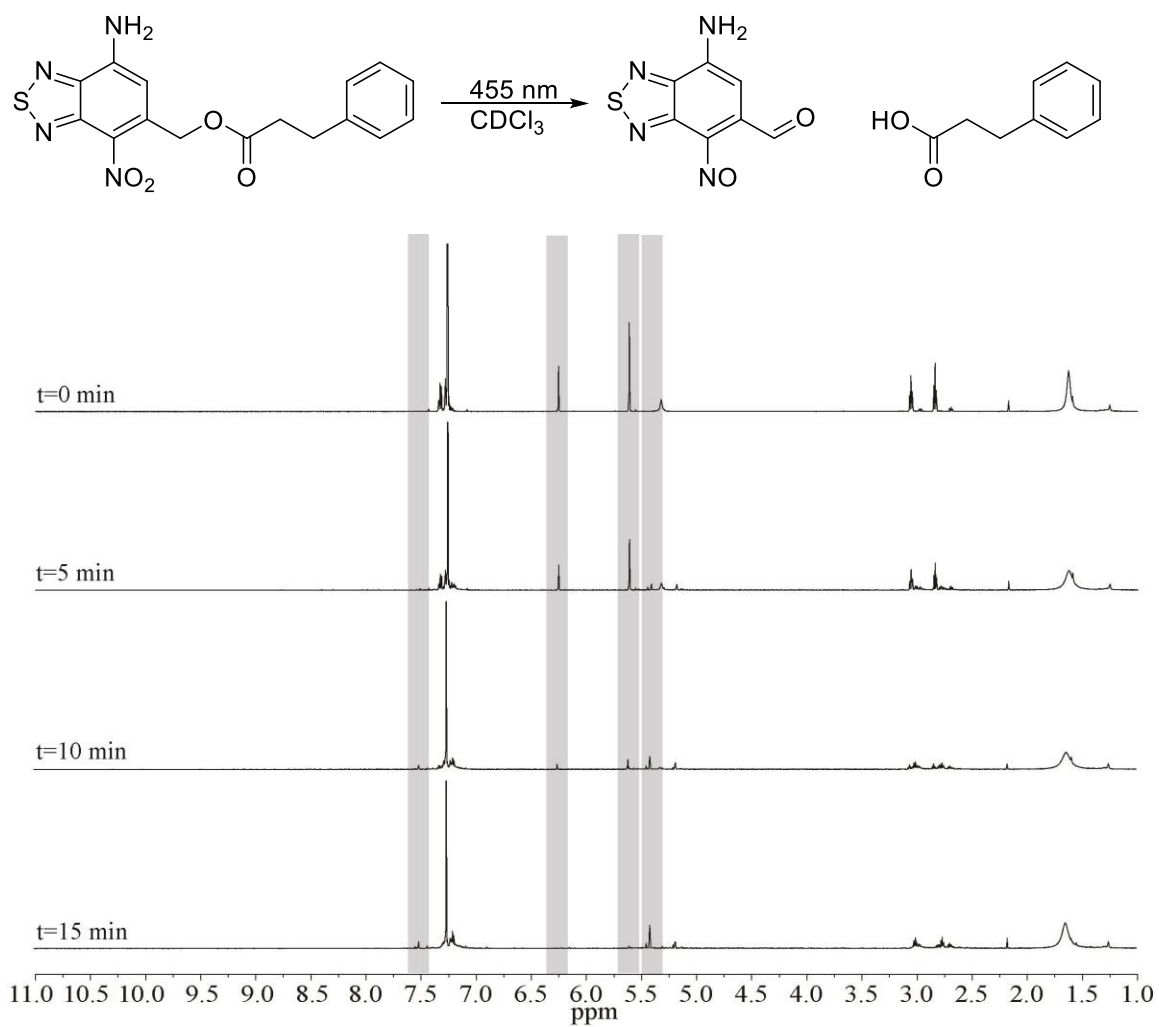


Figure 3.13 Irradiation at 455 nm in CDCl₃ exposed to air.

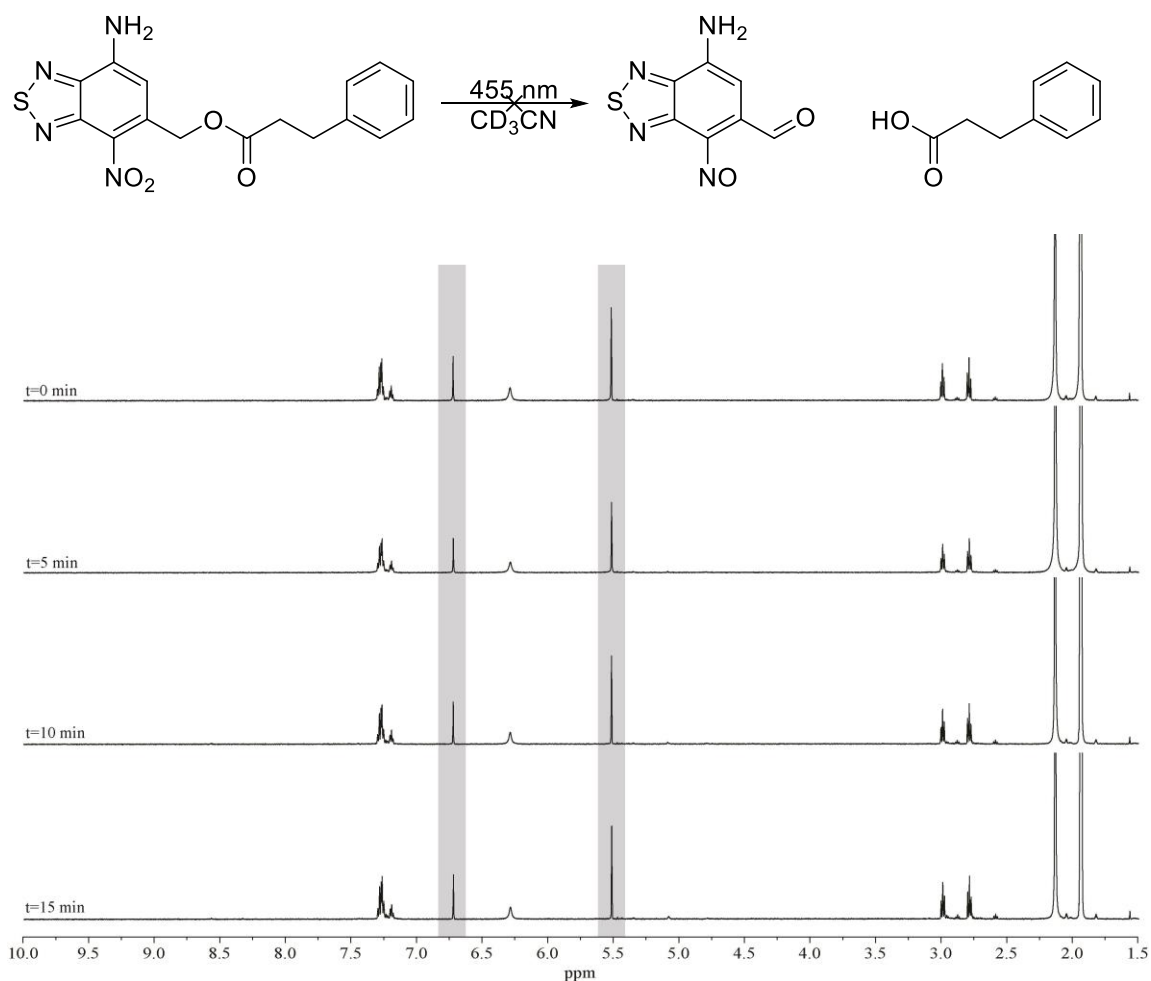


Figure 3.14 Irradiation at 455 nm in CD₃CN exposed to air.

3.4 Conclusions

We report here a new NBD derivative containing an appendage off of the 6-membered ring. Our initial studies seem to indicate that in irradiated samples exposed to air, we may be forming an intermediate in the photocleavage mechanism. Work is currently undergoing to determine if our NBD PPG functions as a viable PPG or not.

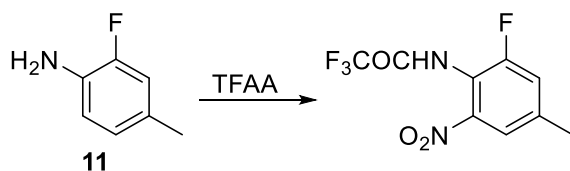
3.5 Experimental

Silica gel (40 μm) was purchased from Grace Davison. All solvents used for photophysical experiments were reagent grade. 4-chloro-7-nitrobenzofurazan (**2**) and 4,7-dibromobenzo[c]-1,2,5-thiadiazole (used to synthesize **6**) were purchased from Alfa Aesar.

All other reagents were purchased from Sigma Aldrich and used without further purification. ^1H and ^{13}C NMR spectra for all compounds were acquired in deuterated solvents (as indicated) on a Bruker Spectrometer at the field strengths reported in the text. The chemical shift data are reported in units of δ (ppm) relative to residual solvent. Fluorescence spectra were measured on an Agilent Technologies Car Eclipse Fluorescence Spectrophotometer using right-angle detection. Ultraviolet-visible absorption spectra were measured with an Agilent Technologies Cary 8454 UV-Vis Diode Array System and corrected for background signal with a cuvette containing the same solvent used for analysis. Fluorescent quantum yields were determined relative to the fluorescence standard reported in the text and are corrected for solvent refractive index and absorption differences at the excitation wavelength.

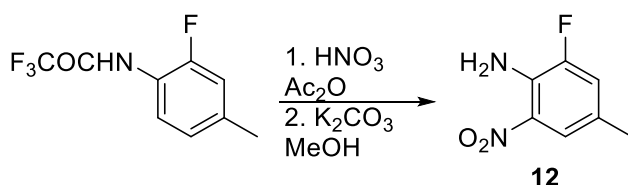
3.5.1 Synthetic Procedures

Scheme 3.2



Synthesis of 2,2,2-trifluoro-N-(2-fluoro-4-methylphenyl)acetamide: Based on a previously published procedure,²³ 2-fluoro-4-methylaniline (9 mL, 80 mmol, 1 eq) was dissolved in dioxane (32 mL) and cooled to 0 °C. Trifluoroacetic anhydride (12.2 mL, 88 mmol, 1.1 eq) was added dropwise, and the solution was stirred at room temperature for 3 hrs. Upon completion of the reaction, the product was diluted with EtOAc and washed with water before concentrated under reduced pressure. Product purified using trituration with hexane to yield 2,2,2-trifluoro-N-(2-fluoro-4-methylphenyl)acetamide (75%). Physical and spectroscopic data were in agreement with those previously reported (Scheme 3.2).²³

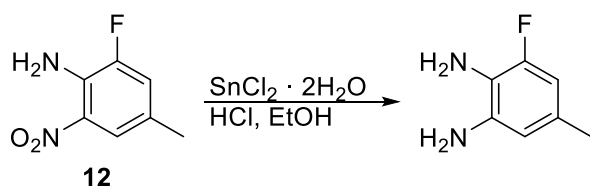
Scheme 3.3



Synthesis of 2-fluoro-4-methyl-6-nitroaniline: Based on a previously published procedure, 2,2,2-trifluoro-N-(2-fluoro-4-methylphenyl)acetamide (5.046 g, 22.6 mmol, 1 eq) was dissolved in acetic anhydride (15 mL) and cooled to 0 °C. Nitric acid (5 mL, 79.1 mmol, 3.5 eq) was added dropwise and the solution was stirred at 55 °C for 14 hrs. The reaction was cooled to room temperature, diluted with water and extracted with EtOAc before concentrated under reduced pressure.

The residue was redissolved in MeOH (57 mL) and water (28 mL). Potassium carbonate (7.734 g, 55.6 mmol, 2.5 eq) was added and the reaction was stirred at 70 °C for 4 hrs. The reaction was diluted with water, extracted with EtOAc (X2) and concentrated under reduced pressure. The product was purified using silica gel chromatography (1:1 hexanes:DCM) to yield 2-fluoro-4-methyl-6-nitroaniline (82%). Physical and spectroscopic data were in agreement with those previously reported (Scheme 3.3).²³

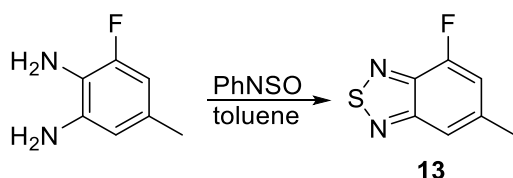
Scheme 3.4



Synthesis of 3-fluoro-5-methylbenzene-1,2-diamine: Based on a previously published procedure,²⁴ 2-fluoro-4-methyl-6-nitroaniline (1.004 g, 5.9 mmol, 1 eq) and tin (II) chloride dihydrate (6.796, 29.5 mmol, 5 eq) were dissolved in ethanol (7.7 mL) and hydrochloric acid (2 mL). The solution was degassed and put under nitrogen. The reaction

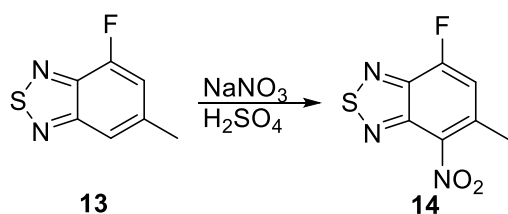
was stirred at 60 °C for 18 hrs before cooling to room temperature. The reaction was quenched with 2 M sodium hydroxide, extracted with EtOAc (X2) and concentrated under reduced pressure. Purified using silica gel chromatography (20:3 DCM:EtOAc) to yield 3-fluoro-5-methyl-1,2-diamine (88%). Physical and spectroscopic data were in agreement with those previously reported (Scheme 3.4).²⁵

Scheme 3.5



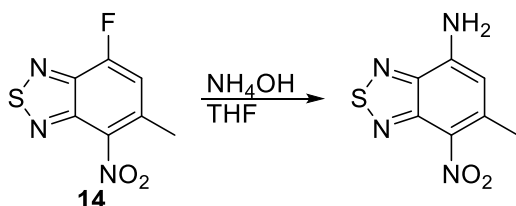
Synthesis of 4-fluoro-6-methylbenzothiadiazole: Based on a previously published procedure,²⁶ 3-fluoro-5-methylbenzene-1,2-diamine (1.721 g, 12.2 mmol, 1 eq) was dissolved in toluene (18 mL). N-thionylaniline (15.1 mL, 134.2 mmol, 11 eq) was added and the solution was stirred at reflux for 2 hrs. The reaction was cooled to room temperature, and concentrated under reduced pressure. The product was purified using silica gel chromatography (10:3 hexanes:DCM) to yield 4-fluoro-6-methylbenzothiadiazole (79%). ¹HNMR (CDCl₃, 600MHz) δ 7.49 (s, 1H), 7.01 (d, *J* = 12 Hz, 1H), 2.48 (s, 3H). ¹³C NMR (CDCl₃, 150 MHz) δ 157.0 (d, *J*_{CF}=2.4), 152.3 (d, *J*_{CF}=261.2), 144.7 (d, *J*_{CF}=15.6), 140.6 (d, *J*_{CF}=5.9), 116.0 (d, *J*_{CF}=4.7), 114.7 (d, *J*_{CF}=15.5), 22.2 (d, *J*_{CF}=1.8). HRMS (ESI-TOF) *m/z*: [M+H]⁺ Calcd. for C₇H₅N₂FSH 169.0230; found 169.0231 (Scheme 3.5).

Scheme 3.6



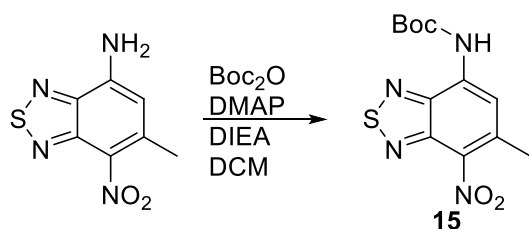
Synthesis of 7-fluoro-5-methyl-4-nitrobenzothiadiazole: Based on a previously published procedure,²⁷ 4-fluoro-6-methylbenzothiadiazole (0.508 g, 3 mmol, 1 eq) was dissolved in concentrated sulfuric acid (6 mL) and cooled to 0 °C. Sodium nitrate (1.315 g, 15.5 mmol, 5.2 eq) was added slowly and the solution was stirred at 0 °C for 2 hrs. The reaction was poured into ice water, filtered by vacuum filtration and rinsed with water to yield 7-fluoro-5-methyl-4-nitrobenzothiadiazole as a yellow powder (89%). Product was used without further purification. ¹HNMR (CDCl₃, 400MHz) δ 7.22 (d, J=9.6 Hz, 1 H), 2.67 (s, 3H). ¹³C NMR (DMSO, 150 MHz) δ 152.3 (d, J_{CF}=264.8), 148.2 (d, J_{CF}=3.9), 143.9 (d, J_{CF}=16.5), 136.7 (d, J_{CF}=5.9), 136.3 (d, J_{CF}=8.7), 115.8 (d, J_{CF}=19.1), 18.2 (d, J_{CF}=0.8). Compound did not ionize during HRMS (Scheme 3.6).

Scheme 3.7



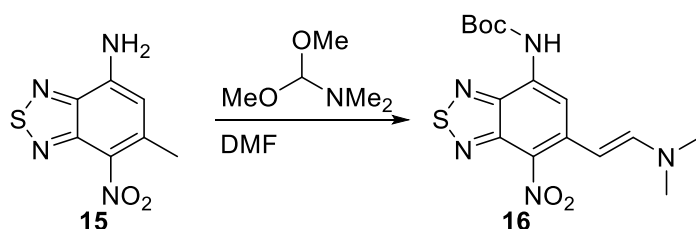
Synthesis of 4-amino-6-methyl-7-nitrobenzothiadiazole: Based on a previously published procedure,²⁸ 7-fluoro-5-methyl-4-nitrobenzothiadiazole (0.331 g, 1.5 mmol, 1 eq) was dissolved THF (15 mL). Ammonium hydroxide (0.4 mL, 3 mmol, 2 eq) was added and the solution was stirred at room temperature for 18 hrs. The reaction was diluted with EtOAc, washed with water and concentrated under reduced pressure. The product was used in the next step without further purification (Scheme 3.7).

Scheme 3.8



Synthesis of tert-butyl (6-methyl-7-nitrobenzothiadiazol-4-yl)carbamate: 4-amino-6-methyl-7-nitrobenzothiadiazole (3.153 g, 15 mmol, 1 eq) was dissolved in DCM (75 mL). DMAP (0.037 g, 0.3 mmol, 0.2 eq), DIEA (26 mL, 150 mmol, 10 eq) and Boc₂O (17 mL, 75 mmol, 5 eq) were added and the solution was stirred at room temperature for 22 hrs. Unreacted Boc₂O was quenched using ethanolamine (1 mL) before concentration under reduced pressure. The reaction was purified using silica gel chromatography (DCM) to yield tert-butyl (6-methyl-7-nitrobenzothiadiazol-4-yl)carbamate (69%).¹HNMR (DMSO, 600MHz) δ 9.78 (s, 1H), 8.00 (s, 1H), 2.59 (s, 3H), 1.53 (s, 9H). ¹³C NMR (DMSO, 150 MHz) δ 152.2, 146.9, 146.4, 137.7, 134.0, 133.8, 116.1, 81.0, 27.9, 19.3. HRMS (ESI-TOF) m/z: [M-H]⁻ Calcd. for C₁₂H₁₃N₄O₄S 309.0664; found 309.0663 (Scheme 3.8).

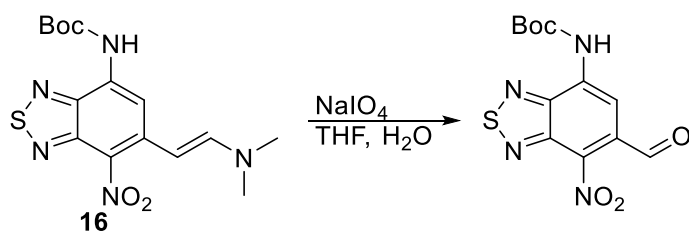
Scheme 3.9



Synthesis of tert-butyl (E)-(6-(2-(dimethylamino)vinyl)-7-nitrobenzothiadiazole)carbamate: Based on a previously published procedure,²⁹ tert-butyl (6-methyl-7-nitrobenzothiadiazole)carbamate (2.514 g, 8.1 mmol, 1 eq) and DMFDMA (2.5 mL, 18.6 mmol, 2.3 eq) were dissolved in DMF (27 mL). The reaction was stirred at 60 °C

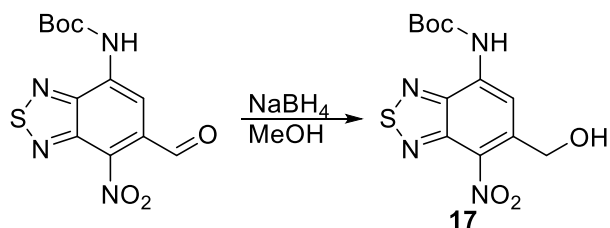
for 4 hrs. The solution was concentrated under reduced pressure and used immediately in the next step without purification (Scheme 3.9).

Scheme 3.10



Synthesis of *tert*-butyl (6-formyl-7-nitrobenzothiadiazole)carbamate: Based on a previously published procedure,³⁰ *tert*-butyl (E)-(6-(2-(dimethylamino)vinyl)-7-nitrobenzothiadiazole)carbamate (2.960 g, 8.1 mmol, 1 eq) and sodium periodate (5.198 g, 24.3 mmol, 3 eq) were dissolved in THF (40 mL) and H₂O (40 mL). The solution was stirred at 60 °C for 3 hrs. The reaction was filtered, washed with sodium bicarbonate (X2) and concentrated under reduced pressure. The product was used immediately in the next step without purification (crude yield 89% over two steps. Scheme 3.10).

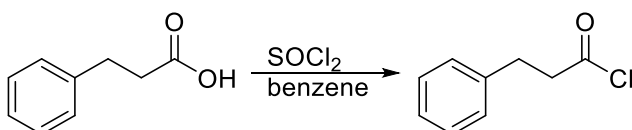
Scheme 3.11



Synthesis of *tert*-butyl (6-(hydroxymethyl)-7-nitrobenzothiadiazole)carbamate: *tert*-butyl (6-formyl-7-nitrobenzothiadiazole)carbamate (0.486 g, 1.5 mmol, 1 eq) was dissolved in MeOH (5 mL). The solution was cooled to 0 °C and sodium borohydride (0.057 g, 1.5 mmol) was slowly added. The solution was stirred at 0 °C for 1 hr and quenched with water before concentrated under reduced pressure. The product was purified using silica gel

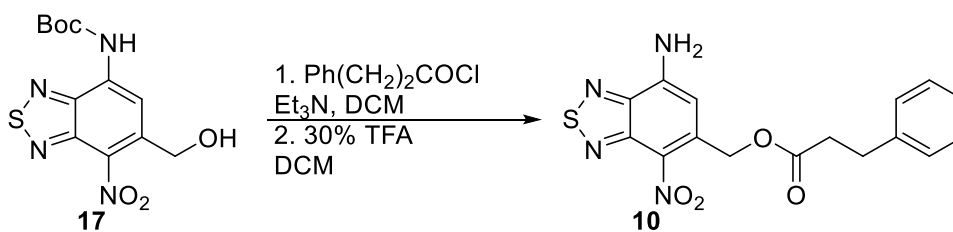
chromatography (20:1 DCM:EtOAc) to yield *tert*-butyl (6-hydroxymethyl)-7-nitrobenzothiadiazole)carbamate (55%). ¹HNMR (DMSO, 400MHz) δ 9.87 (s, 1H), 8.48 (s, 1H), 5.85 (t, J=5.6 Hz, 1H), 4.87 (d, J=8 Hz, 2H), 1.53 (s, 9H). ¹³C NMR (DMSO, 150 MHz) δ 152.1, 147.0, 146.8, 143.4, 134.5, 131.7, 112.3, 81.1, 59.8, 27.9. HRMS (ESI-TOF) m/z: [M+H]⁺ Calcd. for C₁₂H₁₄N₄O₅SH 327.0758; found 327.0759 (Scheme 3.11).

Scheme 3.12



Synthesis of 3-phenylpropanoyl chloride: Using a previously published procedure,³¹ 3-phenylpropionic acid (1.007 g, 6.7 mmol, 1 eq) was dissolved in benzene (1.7 mL). Thionyl chloride (3.4 mL, 46.9 mmol, 7 eq) was slowly added and the solution was refluxed for 3 hrs before concentrated under reduced pressure. Product was used without further purification. Spectra matched those previously reported (Scheme 3.12).

Scheme 3.13



Synthesis of (7-amino-4-nitrobenzothiadiazol-5-yl)methyl 3-phenyl propanoate: *tert*-butyl (6-hydroxymethyl)-7-nitrobenzothiadiazole)carbamate (0.049 g, 0.15 mmol, 1 eq), 3-phenylpropanoyl chloride (0.076 g, 0.45 mmol, 3 eq) and triethylamine (0.13 mL, 0.90 mmol, 6 eq) were dissolved in DCM (0.75 mL). The solution was stirred for 30 min before concentrated under reduced pressure.

The product was then redissolved in DCM (1 mL) and TFA (0.3 mL) was added. The solution was stirred at room temperature for 2.5 hrs before concentrated under reduced pressure. The product was purified using silica gel chromatography (20:1 DCM:EtOAc) to yield (7-amino-4-nitrobenzothiadiazol-5-yl)methyl 3-phenyl propanoate (54%). ^1H NMR (DMSO, 600MHz) δ 8.06 (s, 2H), 7.24 (m, 5H), 6.73 (s, 1H), 5.54 (s, 2H), 2.95 (t, J=6 Hz, 2H), 2.80 (t, J=6 Hz, 2H). ^{13}C NMR (DMSO, 150 MHz) δ 171.8, 149.4, 146.8, 145.0, 142.4, 140.3, 128.4, 128.2, 126.1, 125.3, 102.1, 63.1, 35.0, 30.1. HRMS (ESI-TOF) m/z: $[\text{M}+\text{H}]^+$ Calcd. for $\text{C}_{16}\text{H}_{14}\text{N}_4\text{O}_4\text{SH}$ 359.0809; found 359.0810 (Scheme 3.13).

3.5.2 NMR Spectra

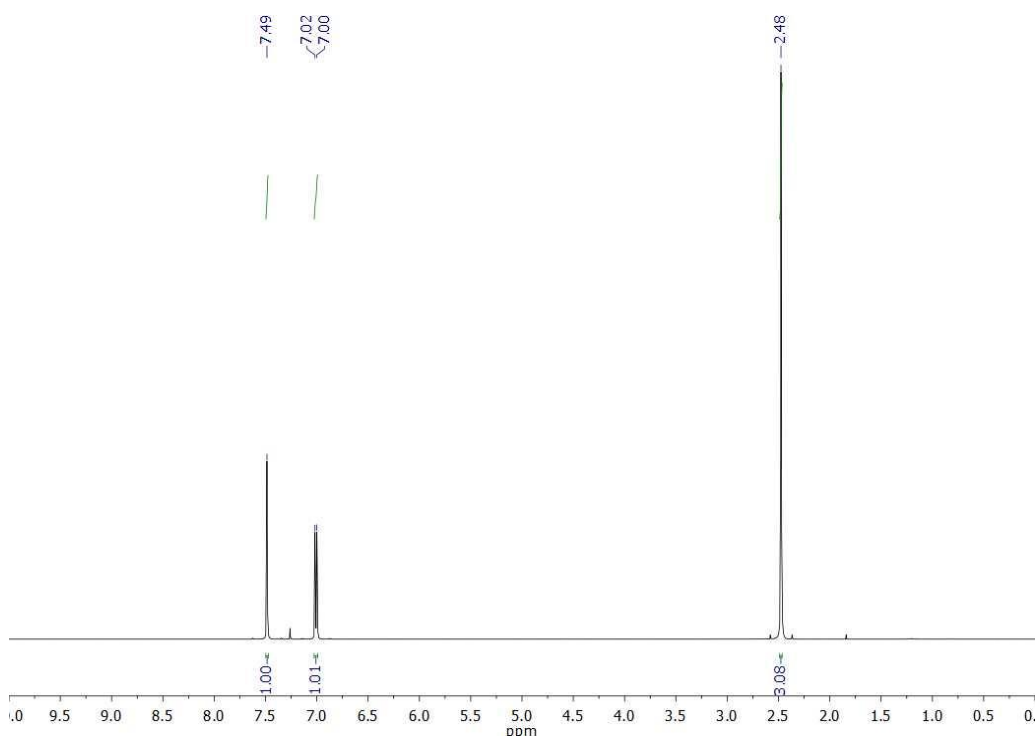


Figure 3.12: ^1H NMR spectra of **13** (600 MHz, CDCl_3).

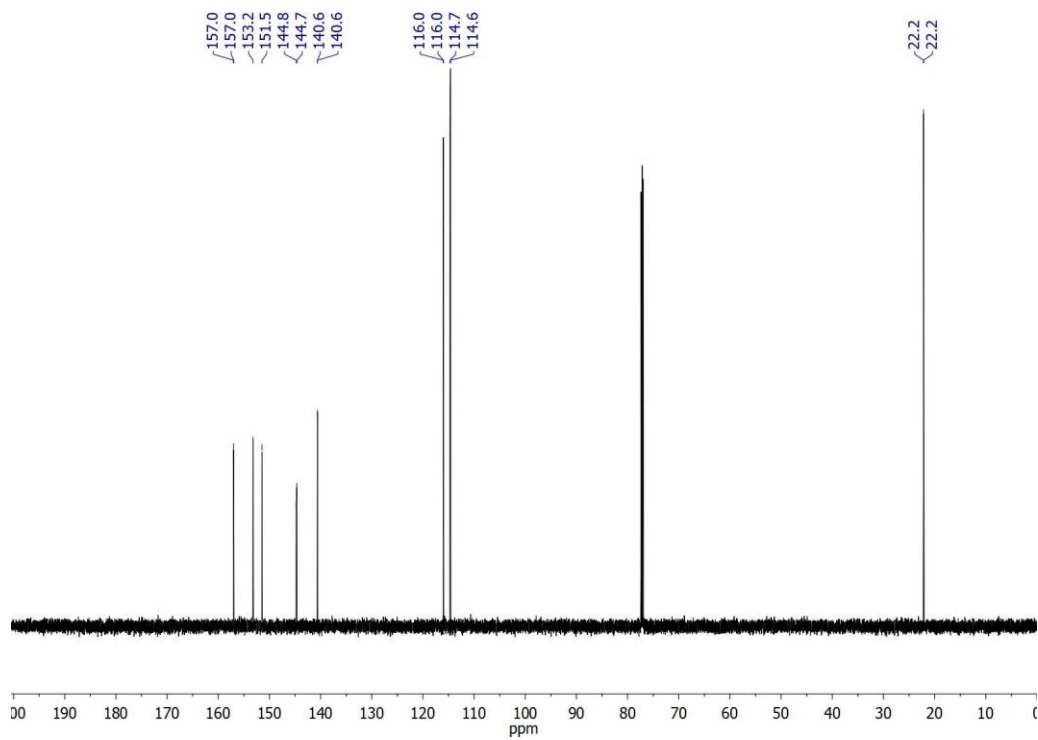


Figure 3.13: ¹³C NMR spectra of **13** (150 MHz, CDCl₃).

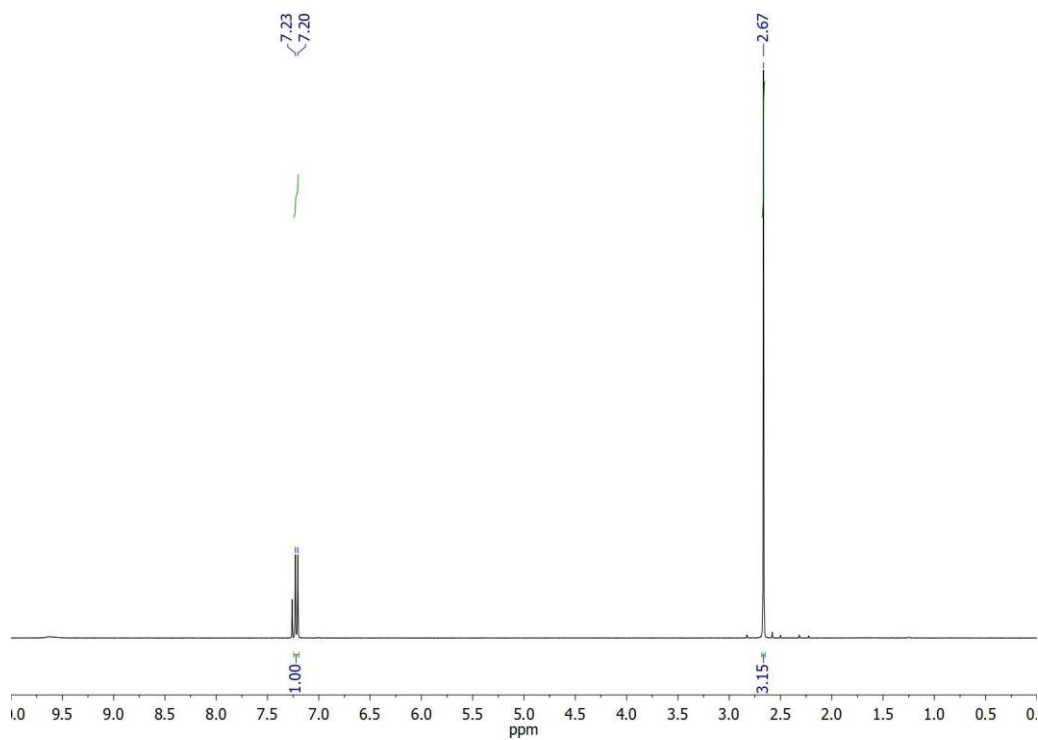


Figure 3.14: ¹H NMR spectra of **14** (400 MHz, CDCl₃).

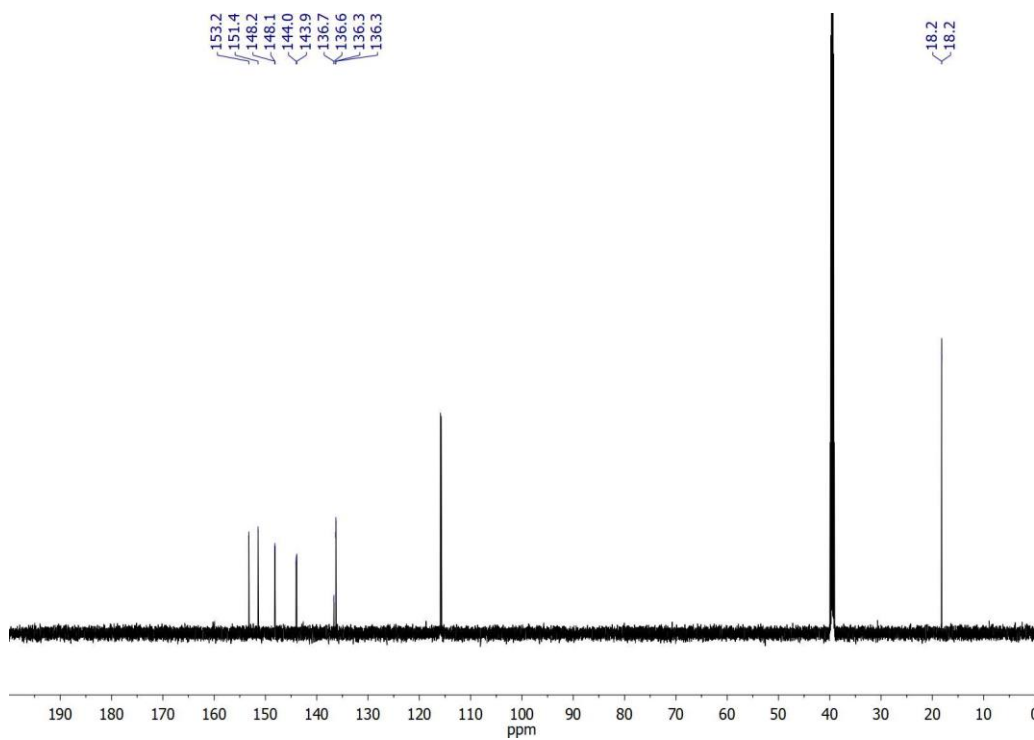


Figure 3.15: ^{13}C NMR spectra of **14** (150 MHz, DMSO).

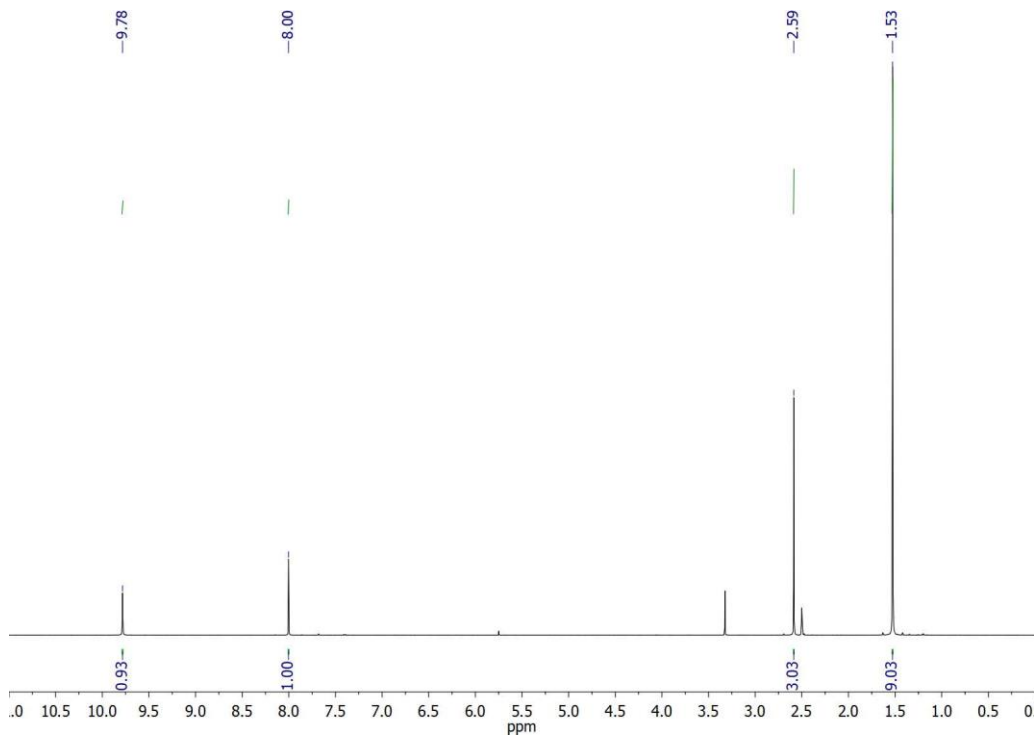


Figure 3.16: ^1H NMR spectra of **15** (600 MHz, DMSO).

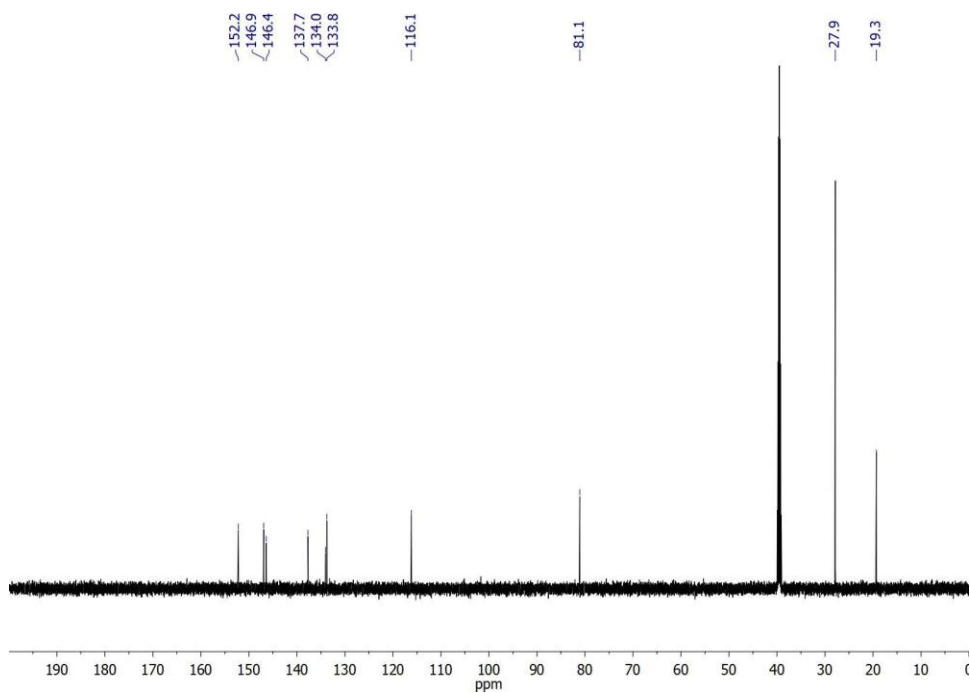


Figure 3.17: ^{13}C NMR spectra of **15** (150 MHz, DMSO).

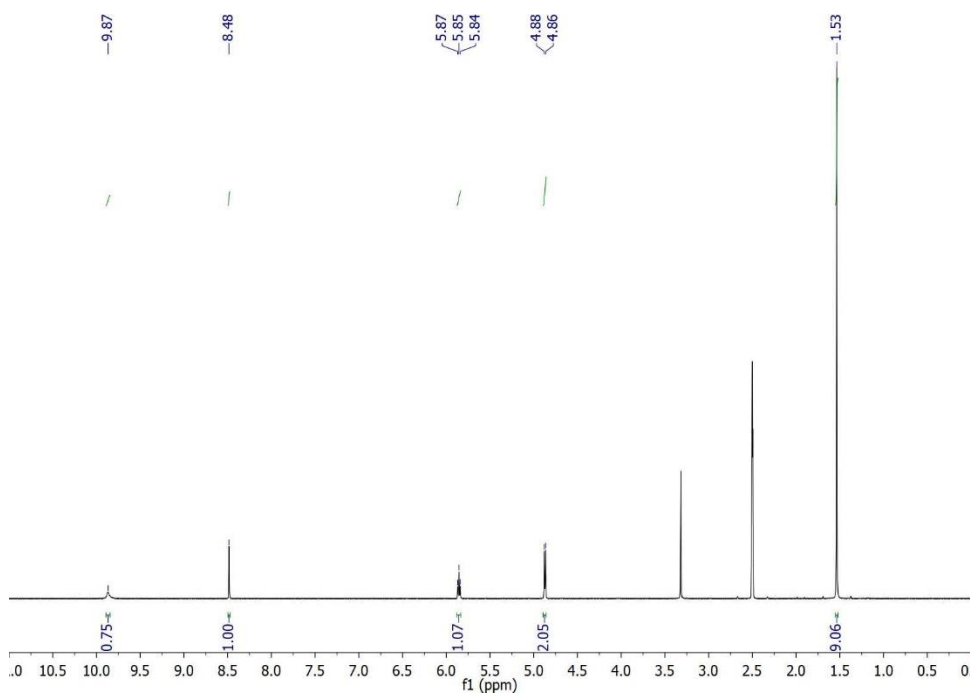


Figure 3.18: ^1H NMR spectra of **17** (400 MHz, DMSO).

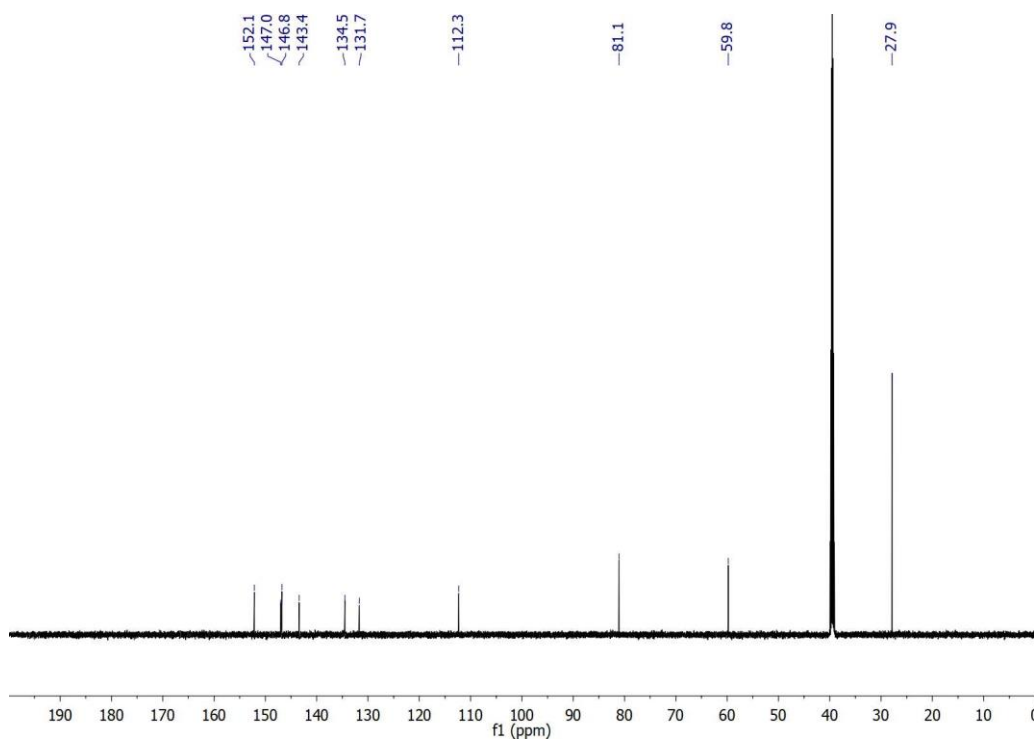


Figure 3.19: ^{13}C NMR spectra of **17** (150 MHz, DMSO).

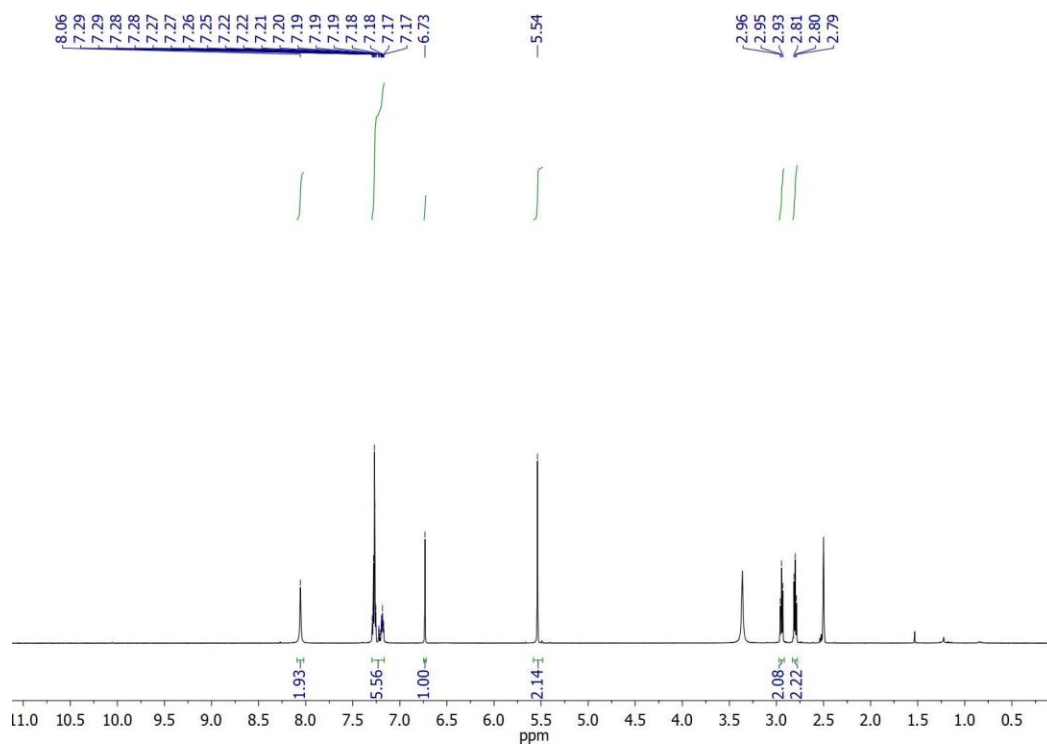


Figure 3.20: ^1H NMR spectra of **10** (600 MHz, DMSO).

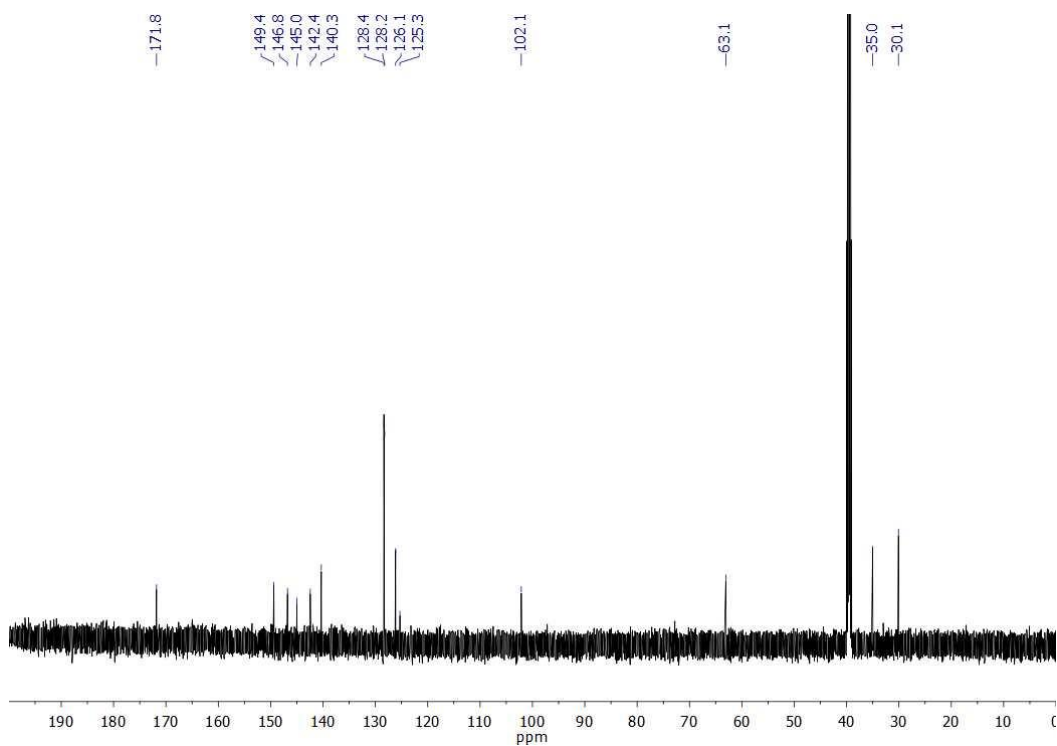


Figure 3.21: ^{13}C NMR spectra of **10** (150 MHz, DMSO).

Acknowledgements

Many thanks to Caroline Warner and Selin Demirci for their help on this project.

3.6 References

1. Klán, P.; Šolomek, T.; Bochet, C. G.; Blanc, A.; Givens, R.; Rubina, M.; Popik, V.; Kostikov, A.; Wirz, J. *Chem. Rev.* **2013**, *113*, 119-191.
2. Hansen, M. J.; Velema, W. A.; Lerch, M. M.; Szymanski, W.; Feringa, B. L. *Chem. Soc. Rev.* **2015**, *44*, 3358-3377.
3. Yu, H.; Li, J.; Wu, D.; Qiu, Z.; Zhang, Y. *Chem. Soc. Rev.* **2010**, *39*, 464-473.
4. Miguel, V. S.; Bochet, C. G.; del Campo, A. *J. Am. Chem. Soc.* **2011**, *133*, 5380-5388.
5. Bochet, C. G.; *Tet. Lett.* **2000**, *41*, 6341-6346.
6. Blanc, A.; Bochet, C. G. *J. Org. Chem.* **2002**, *67*, 5567-5577.
7. Blanc, A.; Bochet, C. G. *J. Am. Chem. Soc.* **2004**, *126*, 7174-7175.
8. *Dynamic Studies in Biology*; Goeldner, M.; Givens, R. Eds.; Wiley-VCH, 2005.

9. Walker, J. W.; Reid, G. P.; McCray, J. A.; Trentham, D. R. *J. Am. Chem. Soc.* **1988**, *110*, 7170-7177.
10. Schmierer, T.; Laimgruber, S.; Haiser, K.; Kiewisch, K.; Neugebauer, J.; Gilch, P. *Phys. Chem. Chem. Phys.* **2010**, *12*, 15653-15664.
11. Schmierer, T.; Bley, F.; Schaper, K.; Gilch, P. *J. Photochem. Photobiol. A* **2011**, *217*, 363-368.
12. Fröbel, S.; Gilch, P. *J. Photochem. Photobiol. A* **2016**, *318*, 150-159.
13. Schmierer, T.; Ryseck, G.; Villnow, T.; Regner, N.; Gilch, P. *Photochem. Photobiol. Sci.* **2012**, *11*, 1313-1321.
14. Il'ichev, Y. V.; Wirz, J. *J. Phys. Chem. A* **2000**, *104*, 7856-7870.
15. Il'ichev, Y. V.; Schwörer, M. A.; Wirz, J. *J. Am. Chem. Soc.* **2004**, *126*, 4581-4595.
16. Charier, S.; Ruel, O.; Baudin, J.-B.; Alcor, D.; Allemand, J.-F.; Meglio, A.; Jullien, L. *Chem. Eur. J.* **2006**, *12*, 1097-1113.
17. Görner, H. *Photochem. Photobiol. Sci.* **2005**, *4*, 822-828.
18. Ghosh, P. B.; Whitehouse, M. W. *Biochem. J.* **1968**, *108*, 155-156.
19. Uchiyama, S.; Santa, T.; Fukushima, T.; Homma, H.; Imai, K. *J. Chem. Soc. Perkin Trans. 2* **1998**, 2165-2174.
20. Uchiyama, S.; Takehira, K.; Kohtani, S.; Imai, K.; Nakagaki, R.; Tobita, S.; Santa, T. *Org. Biomol. Chem.* **2003**, *1*, 1067-1072.
21. Uchiyama, S.; Kimura, K.; Gota, C.; Okabe, K.; Kawamoto, K.; Inada, N.; Yoshihara, T.; Tobita, S. *Chem. Eur. J.* **2012**, *18*, 9552-9563.
22. Saha, S.; Samanta, A. *J. Phys. Chem. A*, **1998**, *102*, 7903-7912.
23. Zhang, N.; Zhang, X.; Zhu, J.; Turpoff, A.; Chen, G.; Morrill, C.; Huang, S.; Lennox, W.; Kakarla, R.; Liu, R.; Li, C.; Ren, H.; Almstead, N.; Venkatraman, S.; Njoroge, F. G.; Gu, Z.; Clausen, V.; Graci, J.; Jung, S. P.; Zheng, Y.; Colacino, J. M.; Lahser, F.; Sheedy, J.; Mollin, A.; Weetall, M.; Nomeir, A.; Karp, G. M. *J. Med. Chem.* **2014**, *57*, 2121-2135.
24. Yasui, Y.; Frantz, D. K.; Siegel, J. S. *Org. Lett.* **2006**, *8*, 4989-4992.
25. O'Neill, B. M.; Ratto, J. E.; Good, K. L.; Tahmassebi, D. C.; Helquist, S. A.; Morales, J. C.; Kool, E. T. *J. Org. Chem.* **2002**, *67*, 5869-5875.

26. Uchiyama, S.; Kawamoto, K. *Chem. Lett.* **2012**, *41*, 1451-1452.
27. Sharma, K. S.; Singh, V.; Singh, P. *Indian J. Chem.* **1978**, *16B*, 892-894.
28. Yan, Y.; Liu, Z.; Zhang, J.; Xu, R.; Hu, X.; Gang, L. **2011**, *21*, 4189-4192.
29. Edin, M.; Grivas, S. *Arkivoc*, **2000**, 1-5.
30. Riesgo, E. C.; Jin, X.; Thummel, R. P. *J. Org. Chem.* **1996**, *61*, 3017-3022.
31. Sguazzini, E.; Schmidt, H. R.; Iyer, K. A.; Kruse, A. C.; Dukat, M. *Bioorg. Med. Chem. Lett.* **2017**, *27*, 2912-2919.

CHAPTER 4: TURNING PHOTOREACTIONS ON AND OFF FOR SEQUENCE- INDEPENDENT PHOTOCHEMISTRY

4.1 Abstract

Herein we report the synthesis of a new photocleavable protecting group (PPG). This new PPG displays photocleavage that is dependent on the solvent environment. In nonpolar solvents photocleavage readily occurs, while in polar solvents no photocleavage is seen in polar solvents.

4.2 Introduction

Photocleavable protecting groups (PPGs) are an exciting area in chemistry as they offer the ability to release a masked substrate in order to provide control over a chemistry of interest. A benefit of using photochemistry to achieve the desired reactivity is it allows the chemistry to be completed without addition of outside reagents which may interfere with the system under study.¹⁻³ Additionally, a researcher can avoid undesired side reactions by using light to activate the system instead of adding other activating reagents.

Due to the vast number of PPGs currently known as well as the various functional groups that can house a PPG, it is becoming increasingly common to use multiple PPGs in the same system. When multiple photocleavable protecting groups are used simultaneously, there are a few factors the researcher needs to consider. The most obvious is the absorbance maxes of the two groups need to be distinctly different so as to activate one group while the other remains intact (Figure 4.1).²

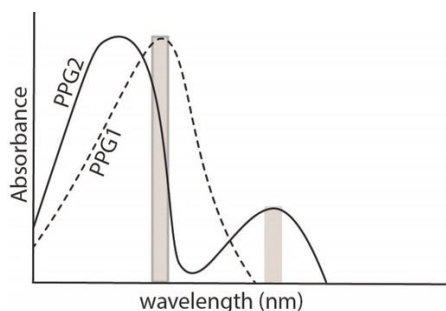


Figure 4.1 Sample spectra displaying different absorbances of two different PPGs.

A less obvious consideration is the limitation of deprotecting in order from longest to shortest wavelength. This requirement is due to multiple chromophores absorbing in the shorter wavelength region of the spectrum. Consequently, it is more likely that multiple PPGs will cleave simultaneously if the researcher starts with photocleaving the shorter wavelength absorbing PPG. Finally, once PPGs are installed in a system, the photoreaction cannot be turned on or off. Therefore the researcher must put great forethought when designing their system so only the desired PPG is cleaved when it is necessary.⁴

There are currently only a couple of PPGs that have been published where the order of photocleavage can be reversed: deprotect from shortest to longest wavelength (Figure 4.2).⁵⁻⁶ These systems take advantage of the fact different PPGs react at different rates depending on the wavelength of deprotection. At lower wavelengths the ortho-nitrobenzyl PPG had a faster reaction rate than the dimethoxy PPG. That order of reaction is reversed at higher wavelengths. Therefore the researcher is not restricted to only one order of deprotection.

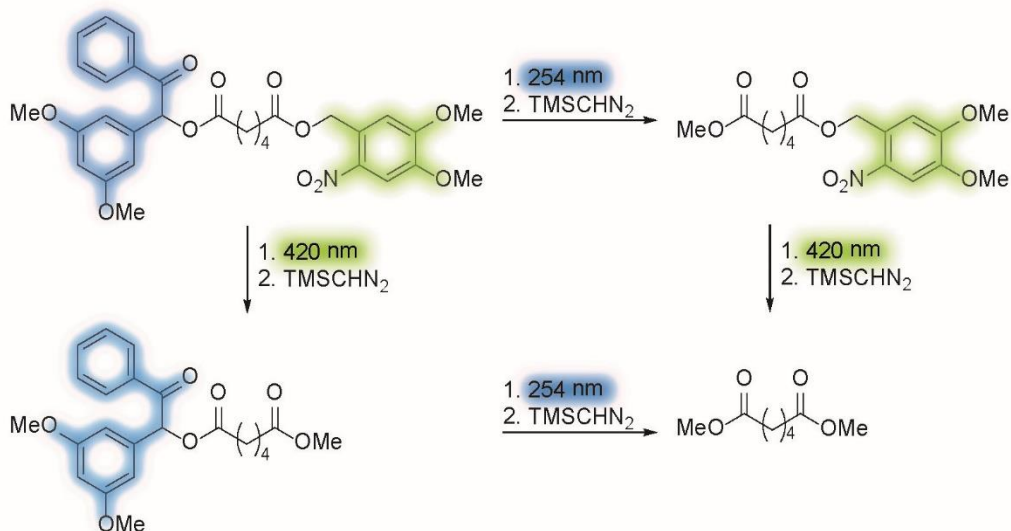


Figure 4.2 One of the few examples where PPGs can be deprotected in either order.⁶

The research in our lab has been interested in exploring new PPGs based on the benzothiadiazole fluorophore. Benzo(heteroatom)diazoles display large solvatochromism properties being highly fluorescent in nonpolar solvents while almost entirely non-fluorescent in polar solvents such as water.⁷ Saha and Samanta proposed in one of their publications that in benzoxadiazoles (**1**) the charge transfer (CT) and $n \rightarrow \pi^*$ excited states are very close in energy to the point at which in nonpolar solvents the $n \rightarrow \pi^*$ state dominates while in polar solvents the CT state dominates (Figure 4.3).⁸

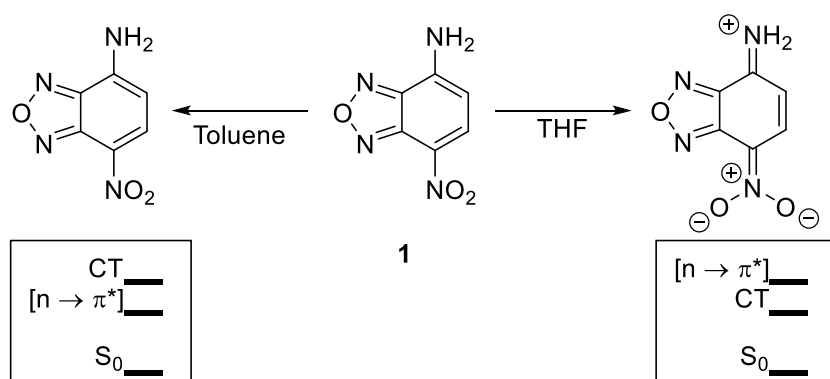


Figure 4.3 Different excited states of benzoxadiazoles.

One of the most common PPG is based on the ortho-nitrobenzoxadiazole (Figure 4.4A, **2**) scaffold.^{1,9-10} The popularity of this PPG is due to its small size, thus minimizing steric hindrance, and high quantum yield of photocleavage. The basic structure undergoes H-abstraction at approximately 300 nm. The absorption wavelength can be further red-shifted by addition of EDG (Figure 4.4A, **3**) but at the cost of reducing the quantum yield of cleavage.¹¹⁻¹² Addition of better EDG such as an amine can further red-shift the absorption but the structure can no longer undergo H-abstraction (Figure 4.4A, **4**). This lack of photochemical reaction is due to the CT nature dominating the excited state, which will not undergo H-abstraction (Figure 4.4B).⁵

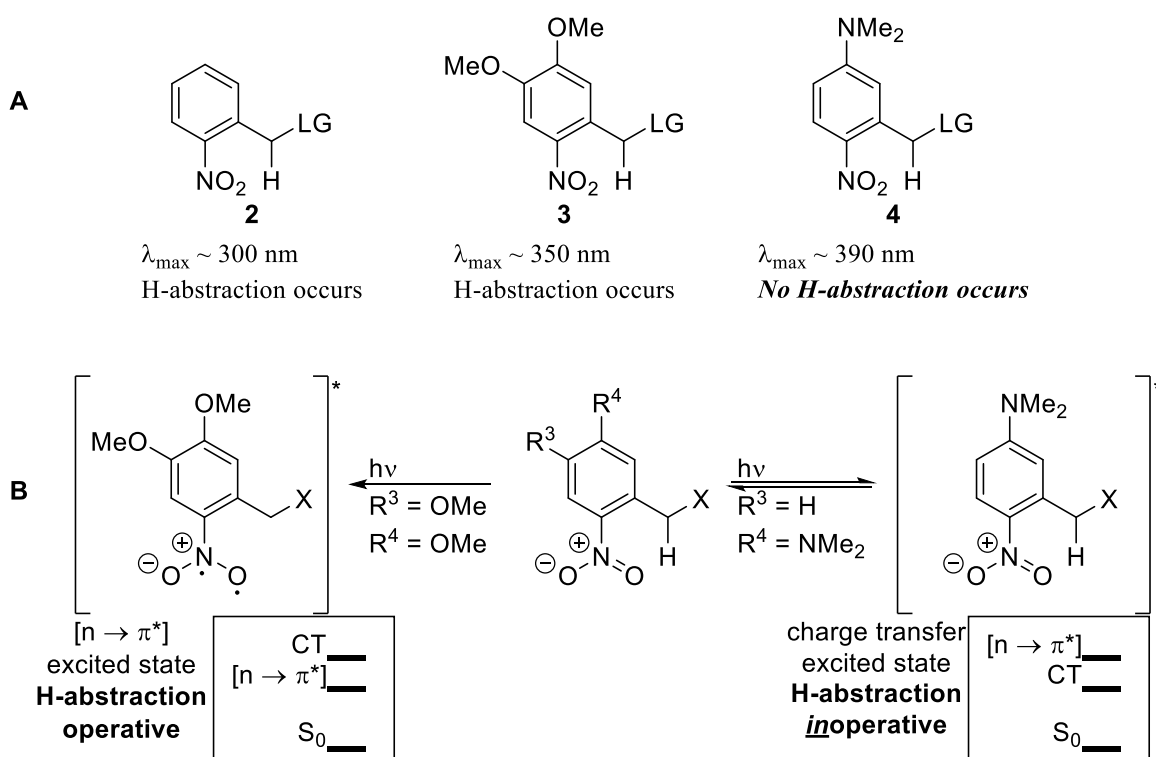


Figure 4.4 (A) Absorption wavelengths of various nitro PPGs and ability to photocleave. (B) Charge transfer state of dimethylamine PPG instead of hydrogen abstraction leading to photocleavage.

We propose use of the benzothiadiazole scaffold, which have been shown to be more photostable,¹³ and combining it with the ortho-nitrobenzyl PPG to create a new class of

photocleavable protecting groups (Figure 4.5). We propose in nonpolar solvents, the n,π^* excited state would dominate and photocleavage would occur. However in more polar solvents, the CT excited state would dominate resulting in no photocleavage. Thus we propose the synthesis of a new PPG which can be turned on and off simply by changing the polarity of the environment.

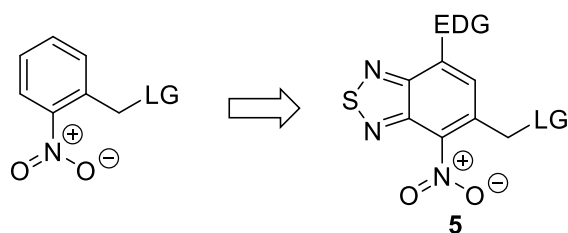
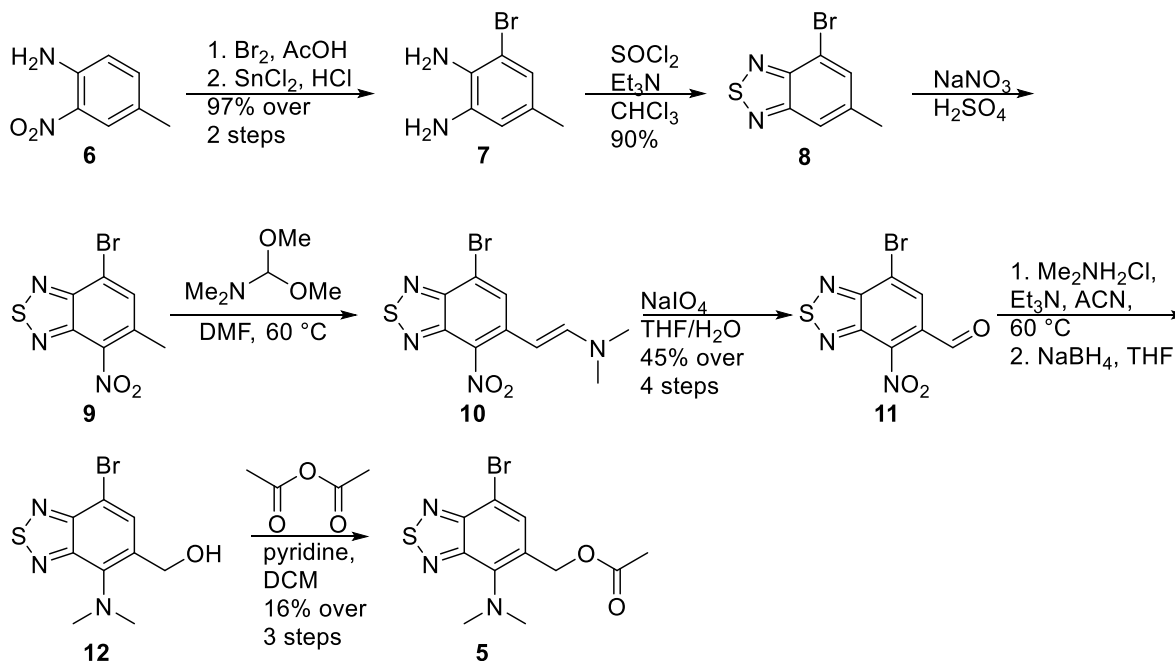


Figure 4.5 Benzothiadiazole scaffold as a PPG.

4.3 Results and Discussion

Scheme 4.1



The synthesis of our PPG (Scheme 4.1) started with readily available 4-methyl-2-nitroaniline which readily underwent monobromination¹⁵ followed by tin reduction to yield

the diamine.¹⁵ The diamine then rapidly ring closed with thionyl chloride to yield the benzothiadiazole which was nitrated using sodium nitrated in concentrated sulfuric acid.¹⁷

In order to eventually obtain the acetate group, the methyl group on the benzothiadiazole needed to be functionalized. The dimethyleneamine was formed by reaction with DMFDMA over 2 hrs,¹⁸ followed by hydrolysis with sodium periodate to yield the aldehyde.¹⁹

An unanticipated reaction occurred upon amination. Instead of displacement of the bromine, which was intended, the substitution occurred at the nitro position.²⁰ This diaminobenzothiadiazole readily underwent a sodium borohydride reduction to form the alcohol followed by acetylation to form the ester.²¹

With our target molecule now in hand, we set out to run some photocleavage studies by irradiating a 1 mg/mL sample in CDCl₃ at 420 nm and analyzing by ¹H NMR every 5 min. Within the first 5 min, a new peak corresponding to acetic acid can be seen growing in as well as a signal in the aldehyde region of the NMR spectra. This trend continues over the 15 min the sample is irradiated, with the remaining signals from the PPG appearing to decompose (Figure 4.6).

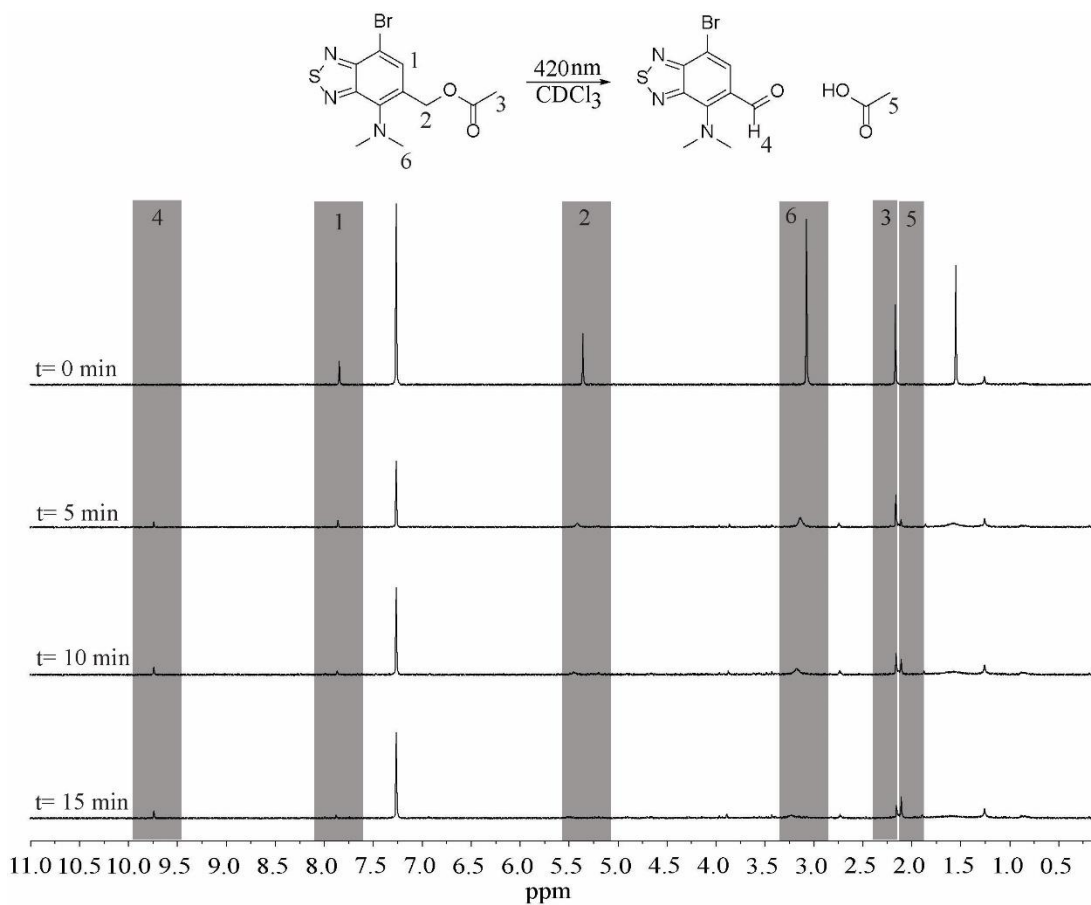


Figure 4.6 PPG irradiated at 420 nm for 15 min.

To confirm the reaction was caused by photolysis and not by instability of the molecule in solution, several control studies were run. First the sample was dissolved in solution and left in the dark overnight (Figure 4.7). Over the 24 h period, there was no detectable change seen in the ^1H NMR spectra.

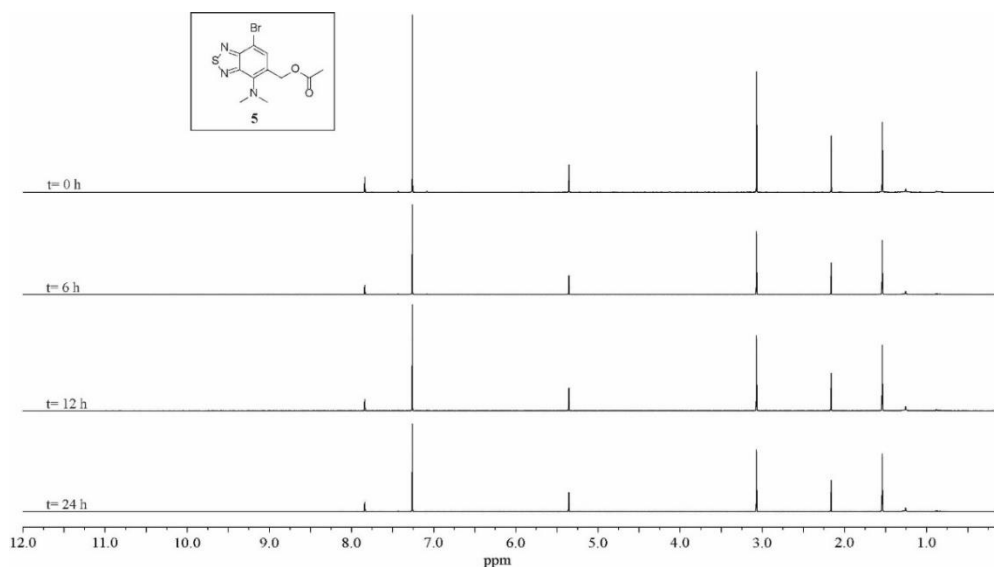


Figure 4.7 PPG in CDCl₃ in the dark for 24 h.

We observed during the photoirradiation of **5**, the water peak was shown to decrease with time. To verify the role water played in the photocleavage, we dried CDCl₃ and irradiated the sample under the same conditions. While there was a small amount of photocleavage product observed due to incomplete drying of the solvent, most of compound **5** simply decomposed (Figure 4.8).

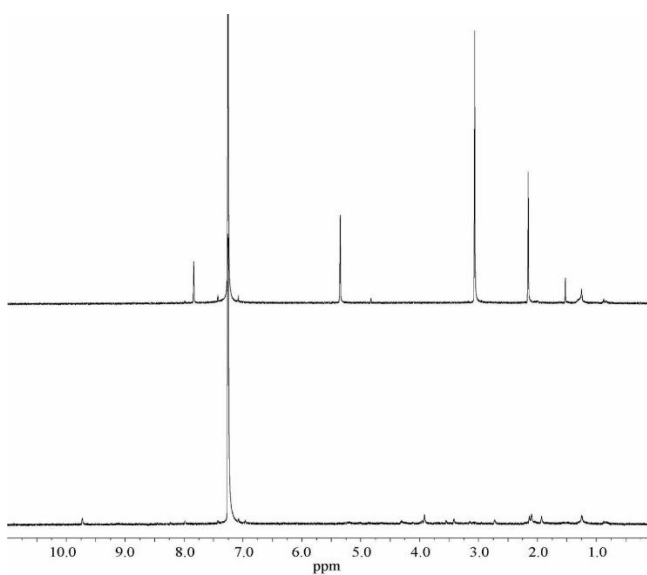


Figure 4.8 Photoirradiation of **5** in dry CDCl₃ over 15 min.

Next the temperature of the sample was increased to 55 °C and stirred for 1 h to confirm the reaction wasn't due to thermal cleavage. Again over the time period analyzed, no change could be seen in the ^1H NMR (Figure 4.9). These results were encouraging as it confirmed our hypothesis that the reaction was due to excitation by the light source.

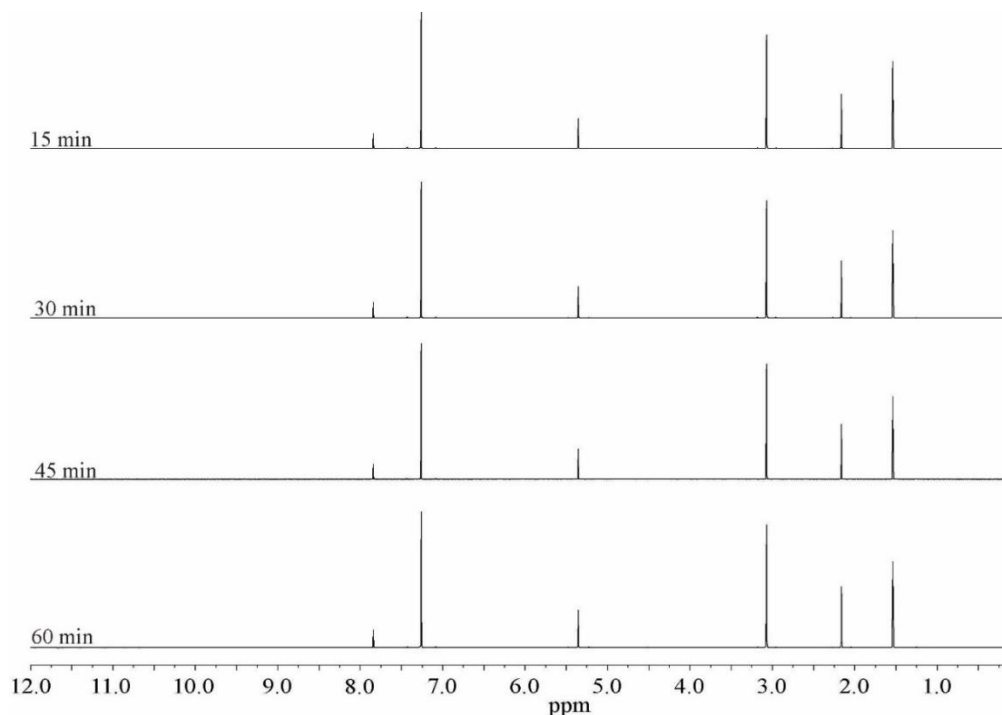


Figure 4.9 PPG stirred at 55 °C for 60 min.

We were then curious to see if photocleavage would not occur, as we predicted it wouldn't, in a more polar solvent such as D_2O . The same test was run (1 mg/mL sample in D_2O irradiated at 420 nm and analyzed by ^1H NMR every 5 min) with surprising results. Over the same time frame as the test that was run in CDCl_3 , no release of acetic acid was seen (Figure 4.10).

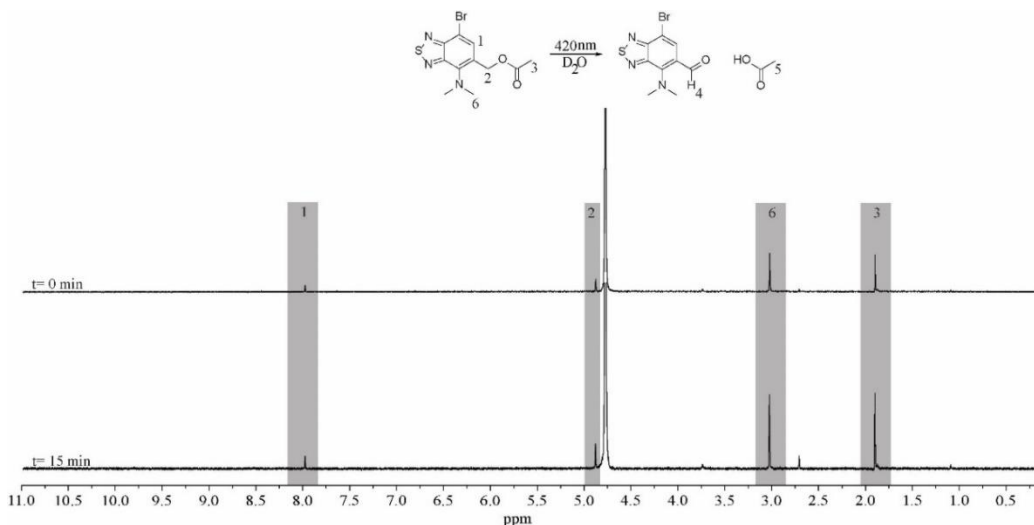


Figure 4.10 PPG in D_2O irradiated at 420 nm for 15 min.

With molecule **5** demonstrating on/off photodeprotection, we then had to look into the mechanism of photoceprotection. We propose the photoreaction is turned on or off due to different rates being active or inactive depending on the solvent (Figure 4.11). In nonpolar solvents, the photodeprotection rate is faster than the fluorescence rate to return to the ground state. As a result we observe the photocleaved product in $CDCl_3$. However in polar solvents the nonradiative emission rate is more rapid than the photodeprotection rate. Consequently no photocleaved product is observed in D_2O . Work is currently underway in our lab to investigate if this is in fact the mechanism of photodeprotection.

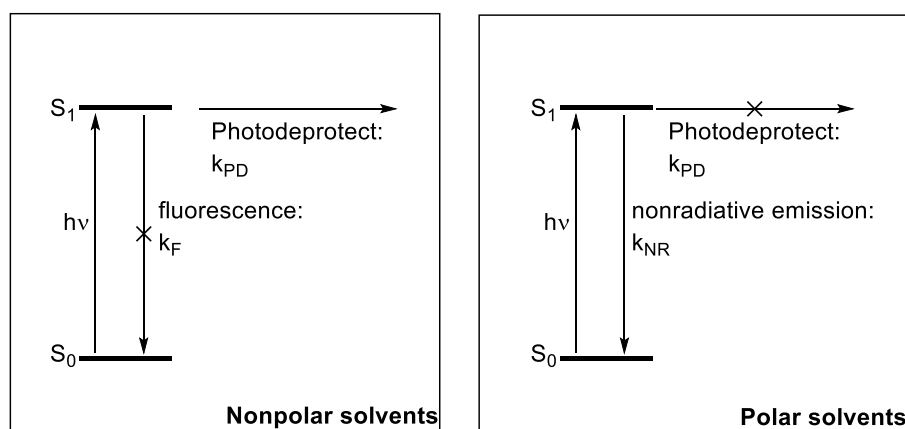


Figure 4.11 Proposed explanation for the difference in reactivity of **5** in nonpolar and polar solvents.

4.4 Conclusions

In conclusion, we demonstrated a photocleavable protecting group which can be turned on/off by changing the polarity of the solvent. To our knowledge this is the only system to demonstrate such properties. Work is currently undergoing in our lab to demonstrate selective deprotection in a system with multiple PPGs present (Figure 4.12). We are also exploring modifications of the PPG structure to better understand what structural properties of our PPG are necessary for optimal selective photocleavage.

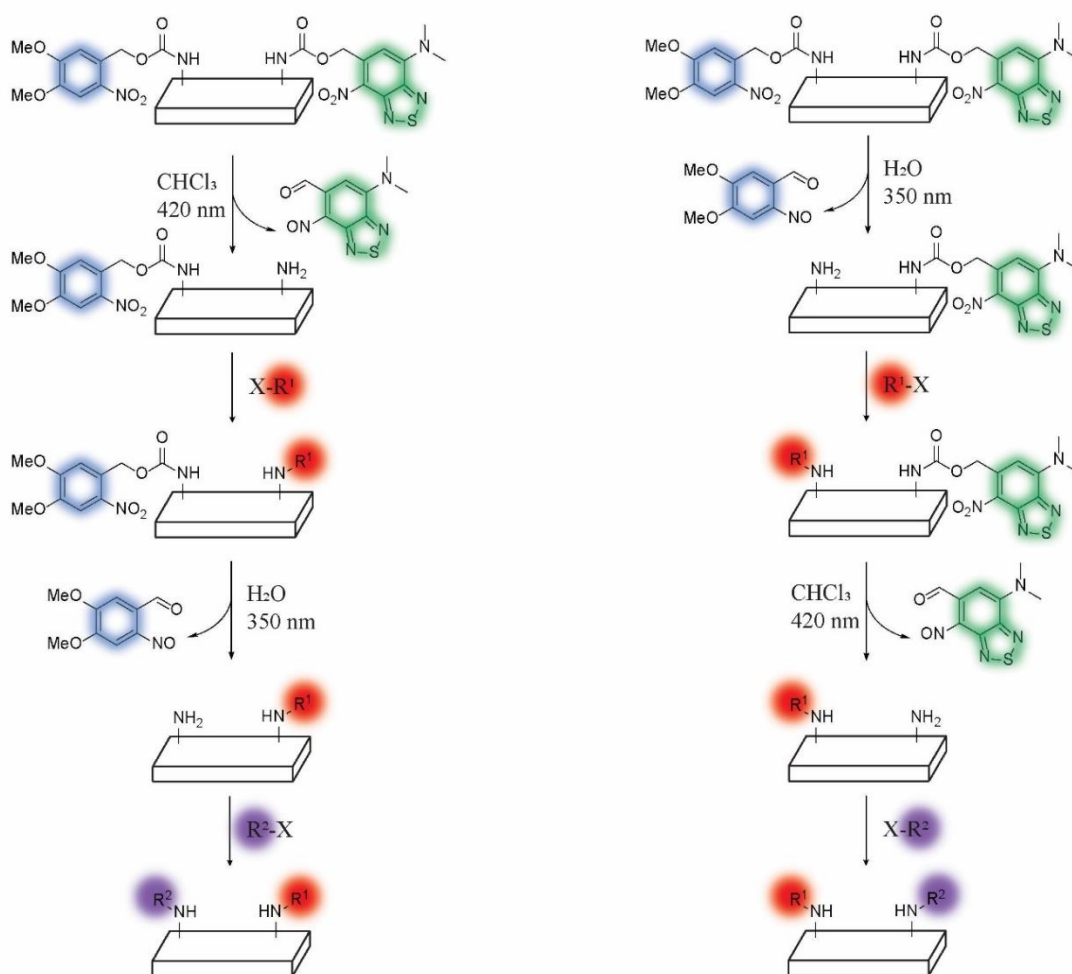


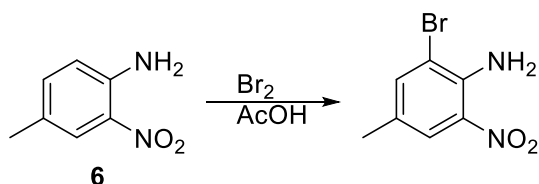
Figure 4.12 Differential deprotection of PPGs in the same system by altering solvent environment.

4.5 Experimental

Silica gel (40 μm) was purchased from Grace Davison. All solvents used for photophysical experiments were reagent grade. 4-chloro-7-nitrobenzofurazan (**2**) and 4,7-dibromobenzo[c]-1,2,5-thiadiazole (used to synthesize **6**) were purchased from Alfa Aesar. All other reagents were purchased from Sigma Aldrich and used without further purification. ^1H and ^{13}C NMR spectra for all compounds were acquired in deuterated solvents (as indicated) on a Bruker Spectrometer at the field strengths reported in the text. The chemical shift data are reported in units of δ (ppm) relative to residual solvent. Fluorescence spectra were measured on an Agilent Technologies Car Eclipse Fluorescence Spectrophotometer using right-angle detection. Ultraviolet-visible absorption spectra were measured with an Agilent Technologies Cary 8454 UV-Vis Diode Array System and corrected for background signal with a cuvette containing the same solvent used for analysis. Fluorescent quantum yields were determined relative to the fluorescence standard reported in the text and are corrected for solvent refractive index and absorption differences at the excitation wavelength.

4.5.1 Synthetic Procedures

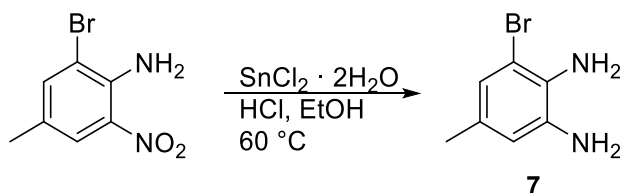
Scheme 4.2



Synthesis of 2-bromo-4-methyl-6-nitroaniline: Using a previously published procedure,¹⁵ 4-methyl-2-nitroaniline (20 g, 131.5 mmol, 1 eq) in glacial acetic acid (200 mL) was heated at 50 °C until a clear orange solution was formed. The reaction was removed from heat and bromine (7.41 mL, 144.6 mmol, 1.1 eq) was added slowly yielding an orange

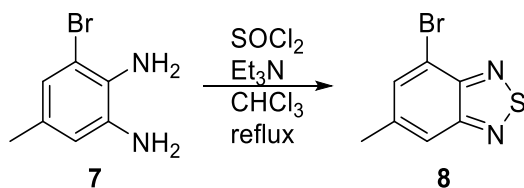
precipitate was obtained. The suspension was stirred for 30 min, and then poured into ice water. The solid was collected by filtration, washed with water and dried in vacuo to yield 2-bromo-4-methyl-6-nitroaniline as an orange solid (90%). The product was used without further purification (Scheme 4.2).

Scheme 4.3



Synthesis of 3-bromo-5-methylbenzene-1,2-diamine: Using a previously published procedure,¹⁶ 2-bromo-4-methyl-6-nitroaniline (5.000 g, 21.6 mmol, 1 eq) and tin (II) chloride dihydrate (24.470 g, 108 mmol, 5 eq) were dissolved in ethanol (28 mL) and concentrated hydrochloric acid (7.2 mL). The reaction was degassed and put under nitrogen. The solution was stirred at 60 °C for 3 hrs before being quenched with 2M sodium hydroxide. The product was extracted with DCM and concentrated under reduced pressure. The product was purified using silica gel chromatography in 1:1 EtOAc:hexanes to yield 3-bromo-5-methylbenzene-1,2-diamine (97%). Spectra match those previously reported (Scheme 4.3).¹⁶

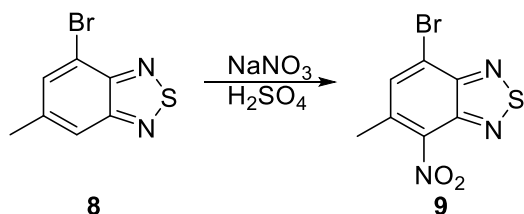
Scheme 4.4



Synthesis of 4-bromo-6-methyl-2,1,3-benzothiadiazole: Using a previously published procedure,¹⁷ 3,4-diamino-5-bromotoluene (5.00 g, 24.92 mmol, 1 eq) and triethylamine (17.4 mL, 124.61 mmol, 5 eq.) were dissolved in chloroform (150 mL). The

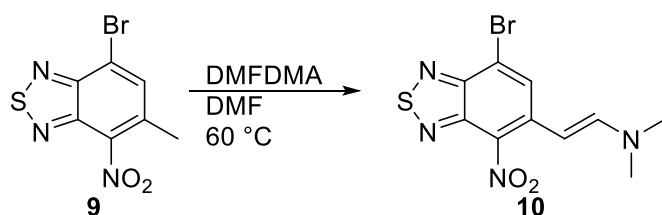
solution was cooled to 0 °C after which thionyl chloride (9.05 mL, 124.61 mmol, 5 eq.) was added slowly. After addition, the solution was stirred at reflux for 1 h. The product was then washed with 1M HCl (X2), dried with MgSO₄ and concentrated under reduced pressure to yield an orange-red solid. The product was used without further purification (Scheme 4.4).

Scheme 4.5



Synthesis 7-bromo-5-methyl-4-nitrobenzothiadiazole: Using a previously published procedure,¹⁷ 4-Bromo-6-methylbenzo-2,1,3-thiadiazole (1.00 g, 4.36 mmol, 1 eq) was dissolved in a minimum quantity of H₂SO₄ (8.73 mL) at 0°C. Sodium nitrate (1.855 g, 21.83 mmol, 5 eq.) was slowly added. The reaction was stirred for 2 h at 0°C. The solution was then poured into 100 mL of ice-water. The precipitate was collected by filtration, washed with water and dried to yield a 7-bromo-5-methyl-4-nitrobenzothiadiazole. The product was used without further purification. Spectra matched those previously reported (Scheme 4.5).¹⁷

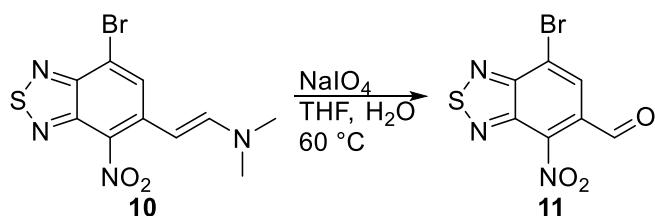
Scheme 4.6



Synthesis of (E)-2-(7-bromo-4-nitrobenzothiadiazol-5-yl)-N,N-dimethylethan-1-amine: Based on a previously published procedure,¹⁸ 7-bromo-5-methyl-4-nitrobenzothiadiazole (0.101 g, 0.36 mmol, 1 eq) was dissolved in DMF (1.2 mL). DMFDMA (0.11 mL, 0.83 mmol, 2.3 eq) was added, the solution was degassed and put

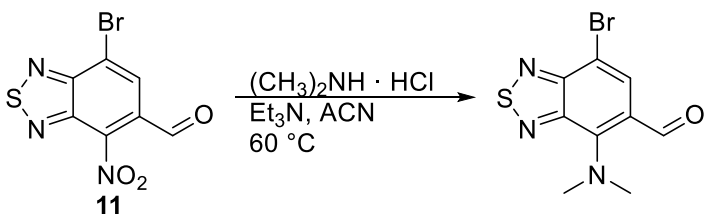
under nitrogen, and the temperature was increased to 60 °C. The reaction was stirred at 60 °C for 1.5 hrs and concentrated under reduced pressure to yield (E)-2-(7-bromo-4-nitrobenzothiadiazol-5-yl)-N,N-dimethylethen-1-amine as a red solid. The product was used without further purification (Scheme 4.6).

Scheme 4.7



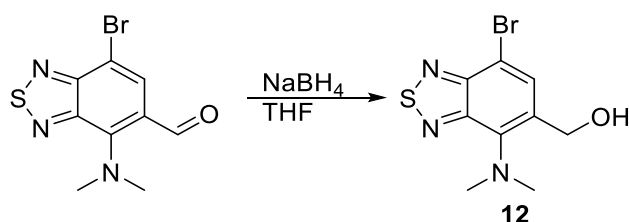
Synthesis of 7-bromo-4-nitrobenzothiadiazole-5-carbaldehyde: Based on a previously published procedure,¹⁹ (E)-2-(7-bromo-4-nitrobenzothiadiazol-5-yl)-N,N-dimethylethen-1-amine (0.530 g, 1.6 mmol, 1 eq) and sodium periodate (1.035 g, 4.8 mmol, 3 eq) were dissolved in THF (8 mL) and water (8 mL). Solution was stirred at 60 °C for 1.5 hrs. The reaction was filtered, precipitate rinsed with EtOAc, and the filtrate was washed with saturated sodium bicarbonate x2. The organic layer was concentrated under reduced pressure. The product was purified using silica gel chromatography (4:1 hexanes:EtOAc) to yield 7-bromo-4-nitrobenzothiadiazole-5-carbaldehyde as an orange powder (45%). ¹HNMR (CDCl₃, 600MHz) δ 10.35 (s, 1 H), 8.42 (s, 1H). ¹³C NMR (CDCl₃, 150 MHz) δ 185.1, 156.1, 145.8, 129.0, 129.0, 128.9, 120.4. Compound did not ionize in HRMS (Scheme 4.7).

Scheme 4.8



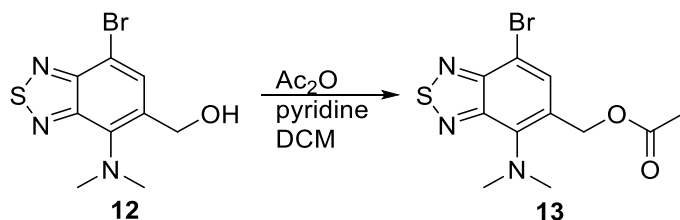
Synthesis of 7-dimethylamino-4-nitrobenzothiadiazole-5-carbaldehyde: 7-bromo-4-nitrobenzothiadiazole-5-carbaldehyde (0.100 g, 0.34 mmol, 1 eq) and dimethylamine hydrochloride (0.060 g, 0.68 mmol, 2 eq) were dissolved in acetonitrile (1.8 mL). Triethylamine (0.20 mL, 1.44 mmol, 4 eq) was added and the solution was stirred at 60 °C for 1 hrs. The reaction was diluted with EtOAc and washed with water before concentrated under reduced pressure to yield 7-dimethylamino-4-nitrobenzothiadiazole-5-carbaldehyde. The product was used without further purification (Scheme 4.8).

Scheme 4.9



Synthesis of 7-dimethylamino-4-nitrobenzothiadiazole-5-methanol: 7-dimethylamino-4-nitrobenzothiadiazole-5-carbaldehyde (0.086 g, 0.34 mmol, 1 eq) and sodium borohydride (0.015 g, 0.34 mmol, 1 eq) were put under nitrogen. In a separate vial, THF (1.1 mL) was degassed and put under nitrogen before being added to the solids. The reaction was stirred for 22 hrs at room temperature before being quenched with water and concentrated under reduced pressure to yield 7-dimethylamino-4-nitrobenzothiadiazole-5-methanol. The product was used without further purification (Scheme 4.9).

Scheme 4.10



Synthesis of (7-dimethylamino-4-nitrobenzothiadiazol-5-yl)methyl acetate: Based on a previously published procedure,²¹ 7-dimethylamino-4-nitrobenzothiadiazole-5-methanol (0.086 g, 0.34 mmol, 1 eq), acetic anhydride (0.13 mL, 1.36 mmol, 4 eq), and pyridine (0.22 mL, 2.72 mmol, 8 eq) were dissolved in DCM (1.7 mL). The solution was stirred for 20 hrs at room temperature before concentrated under reduced pressure. The product was purified using silica gel chromatography (10:1 hexanes:EtOAc) to yield (7-dimethylamino-4-nitrobenzothiadiazol-5-yl)methyl acetate as an orange powder (31%). ¹H NMR (CDCl₃, 600 MHz) δ 7.84 (s, 1H), 5.36 (s, 2H), 3.07 (s, 6H), 2.16 (s, 3H). ¹³C NMR (CDCl₃, 150 MHz) δ 171.0, 154.7, 152.4, 143.5, 133.7, 131.7, 108.6, 62.3, 44.8, 21.2. HRMS (ESI-TOF) m/z: [M+H]⁺ Calcd. for C₁₁H₁₂BrN₃O₂SH 329.9906, found 329.9906 (Scheme 4.10).

4.5.2 NMR Spectra

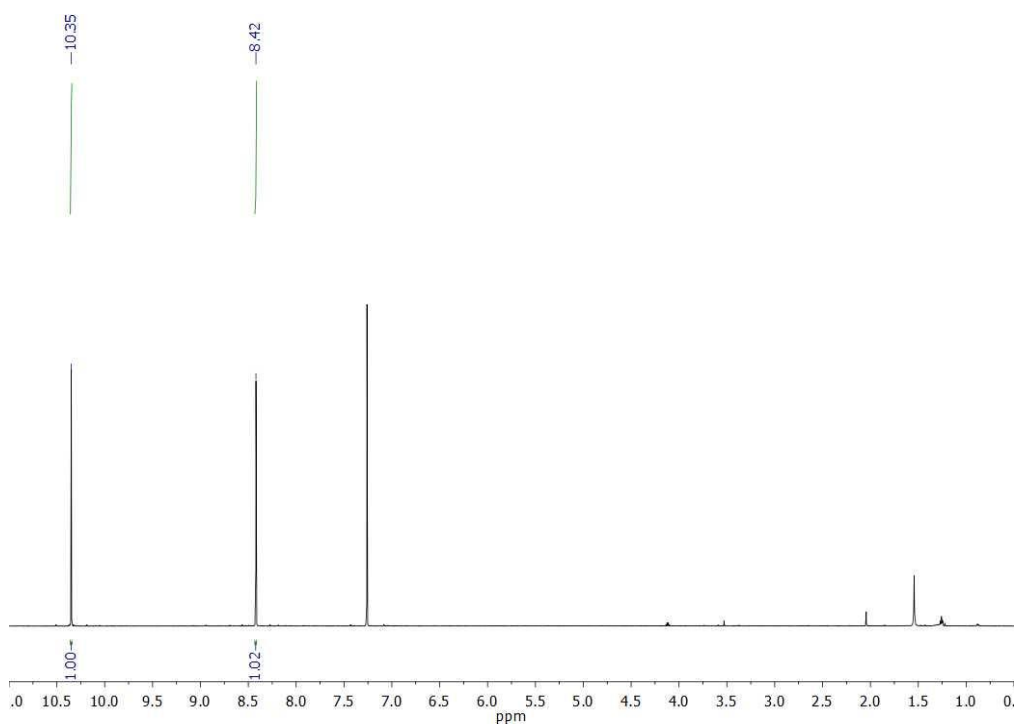


Figure 4.11 ¹H NMR **11** (CDCl₃, 600 MHz).

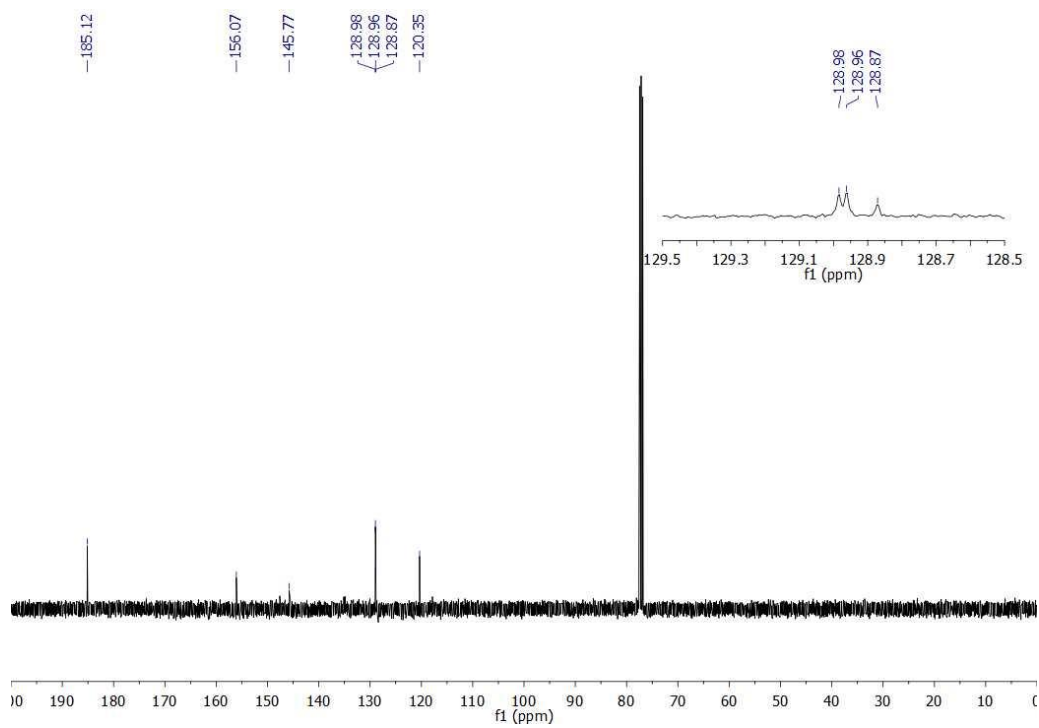


Figure 4.12 ^{13}C NMR 11 (CDCl_3 , 600 MHz).

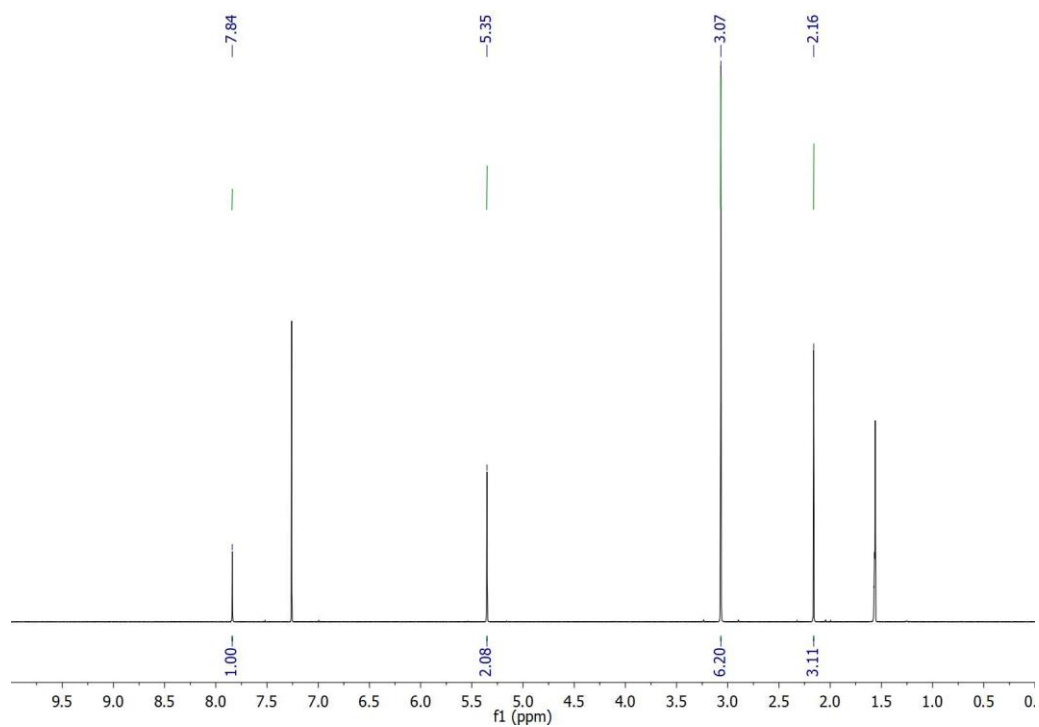


Figure 4.13 ^1H NMR 13 (CDCl_3 , 600 MHz).

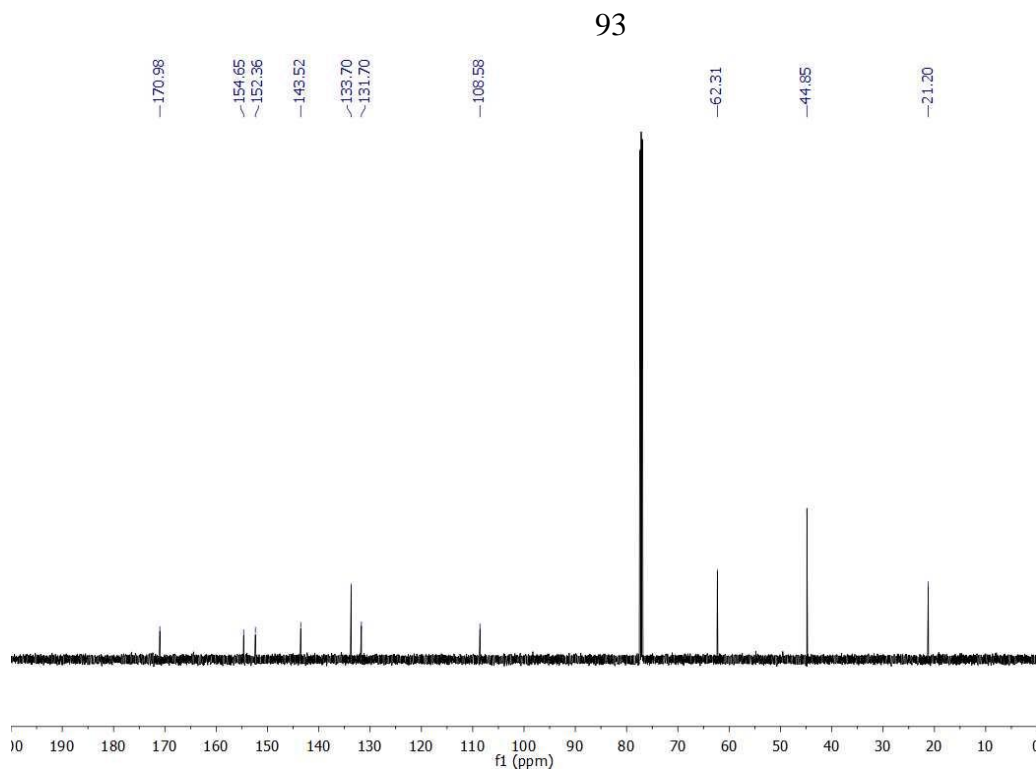


Figure 4.14 ^{13}C NMR **13** (CDCl_3 , 600 MHz).

Acknowledgments

Many thanks to Selin Demirci and Yen Nguyen for their help on this project.

4.6 References

1. Klán, P.; Šolomek, T.; Bochet, C. G.; Blanc, A.; Givens, R.; Rubina, M.; Popik, V.; Kostikov, A.; Wirz, J. *Chem. Rev.* **2013**, *113*, 119-191.
2. Hansen, M. J.; Velema, W. A.; Lerch, M. M.; Szymanski, W.; Feringa, B. L. *Chem. Soc. Rev.* **2015**, *44*, 3358-3377.
3. Yu, H.; Li, J.; Wu, D.; Qiu, Z.; Zhang, Y. *Chem. Soc. Rev.* **2010**, *39*, 464-473
4. Miguel, V. S.; Bochet, C. G.; del Campo, A. **2011**, *133*, 5380-5388.
5. Bochet, C. G. *Tet. Lett.* **2000**, *41*, 6341-6346.
6. Blanc, A.; Bochet, C. G. *J. Org. Chem.* **2002**, *67*, 5567-5577.
7. Neto, B. A. D.; Carvalho, P. H. P. R.; Correa, J. R. *Acc. Chem. Res.* **2015**, *48*, 1560-1569.

8. Liu, T.-K.; Hsieh, P.-Y.; Zhuang, Y.-D.; Hsia, C.-Y.; Huang, C.-L.; Lai, H.-P.; Lin, H.-S.; Chen, I.-C.; Hsu, H.-Y.; Tan, K.-T. *ACS Chem. Biol.* **2014**, *9*, 2359-2365.
9. Saha, S.; Samanta, A. *J. Phys. Chem. A* **1998**, *102*, 7903-7912.
10. *Dynamic Studies in Biology*; Goeldner, M.; Givens, R. Eds.; Wiley-VCH, 2005.
11. Walker, J. W.; Reid, G. P.; McCray, J. A.; Trentham, D. R. *J. Am. Chem. Soc.* **1998**, *110*, 7170-7177.
12. Charier, S.; Ruel, O.; Baudin, J.-B.; Alcor, D.; Allemand, J.-F.; Meglio, A.; Jullien, L.; Valeur, B. *Chem. Eur. J.* **2006**, *12*, 1097-1113.
13. Görner, H. *Photochem. Photobiol. Sci.* **2005**, *4*, 822-828.
14. Uchiyama, S.; Kimura, K.; Gota, C.; Okabe, K.; Kawamoto, K.; Inada, N.; Yoshihara, T.; Tobita, S. *Chem. Eur. J.* **2012**, *18*, 9552-9563.
15. Zhu, D.; Liu, P.; Lu, W.; Wang, H.; Luo, B.; Hu, Y.; Huang, P.; Wen, S. *Chem. Eur. J.* **2015**, *17*, 18915-18920.
16. Yasui, Y.; Frantz, D. K.; Siegel, J. S. *Org. Lett.* **2006**, *8*, 4989-4992.
17. Sharma, K. S.; Singh, R. P. *Indian J. Chem. B* **1978**, *16B*, 892-894.
18. Edin, M.; Grivas, S. *Arkivoc*, **2000**, 1-5.
19. Riesgo, E. C.; Jin, X.; Thummel, R. P. *J. Org. Chem.* **1996**, *61*, 3017-3022.
20. Senskey, M. D.; Bradshaw, J. D.; Tessier, C. A.; Youngs, W. J. *Tet. Lett.* **1995**, *36*, 6217-6220.
21. Rizzacasa, M. A.; Sargent, M. V. *Aust. J. Chem.* **1998**, *41*, 1087-1097.

CHAPTER 5: GENERAL CONCLUSIONS AND FUTURE DIRECTIONS

Through the research in the VanVeller lab, we have greatly expanded the knowledge of benzo(heteroatom)diazoles. In our initial work altering the EWG of NBD derivatives, we were able to demonstrate the cyano group functions as an acceptable electron acceptor for this class of molecules. The CBD derivatives maintained the solvatochromic properties that make NBD so useful: highly emissive in nonpolar solvents while almost nonemissive in polar solvents. Additionally CBD displayed some of the largest solvatochromic emission range seen in this class of molecules (Figure 5.1).

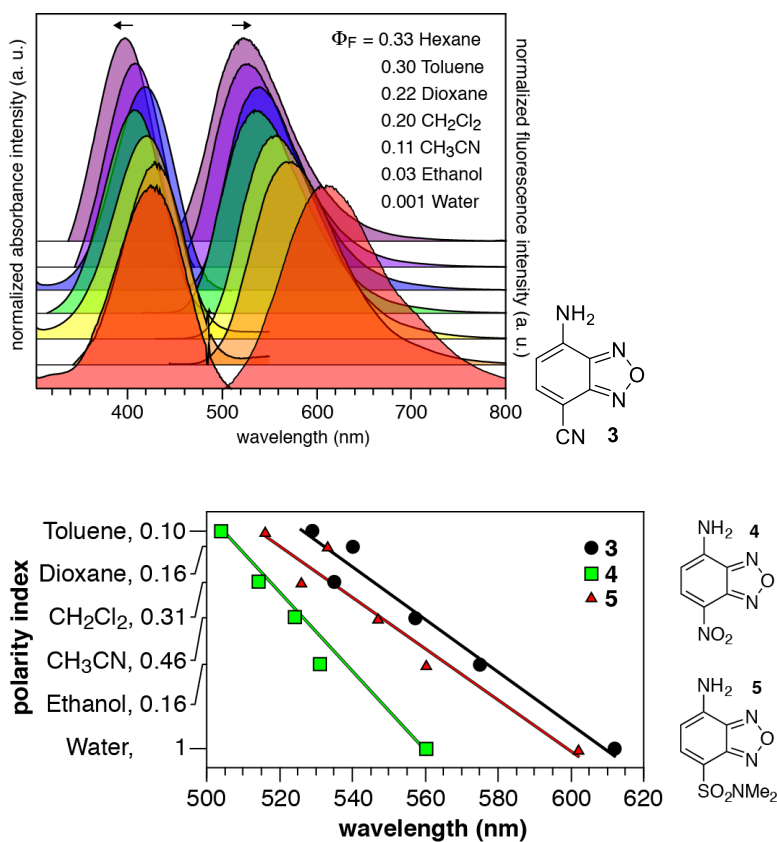


Figure 5.1 Solvatochromism emission of CBD (**3**) and comparison of CBD to other common benzoxadiazoles.

Ongoing research for this project involves exploration of elements within the ring system. Work is currently being done to explore what role the nitrogens in the five-

membered ring play in the photophysical properties (denoted by Z in Figure 5.2).

Additionally in the future we hope to explore if addition of a nitrogen in the 6-membered ring would enhance or hinder the photophysical properties (denoted by Q in Figure 5.2). We hope that our work in altering the structures will help expand the knowledgebase not only in the field of benzo(heteroatom)diazoles, but will also help in designing other push-pull fluorophores to best meet the need of individual research projects.

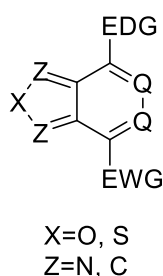


Figure 5.2 NBD derivatives under investigation.

We have investigated the use of benzothiadiazoles as photocleavable protecting groups. Our first investigation looked into the possibility of using an ortho-nitrobenzyl PPG based on the structure of the fluorophore NBD (Figure 5.3). Work is still ongoing to confirm if the photocleavage was successful or not as the preliminary NMR indicated possible formation of a photocleavage intermediate (Figure 5.4).

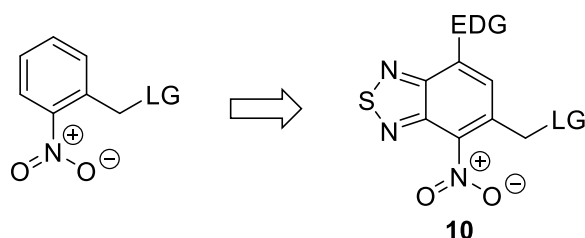


Figure 5.3 Proposed ortho-nitrobenzyl PPG using benzothiadiazole as a scaffold.

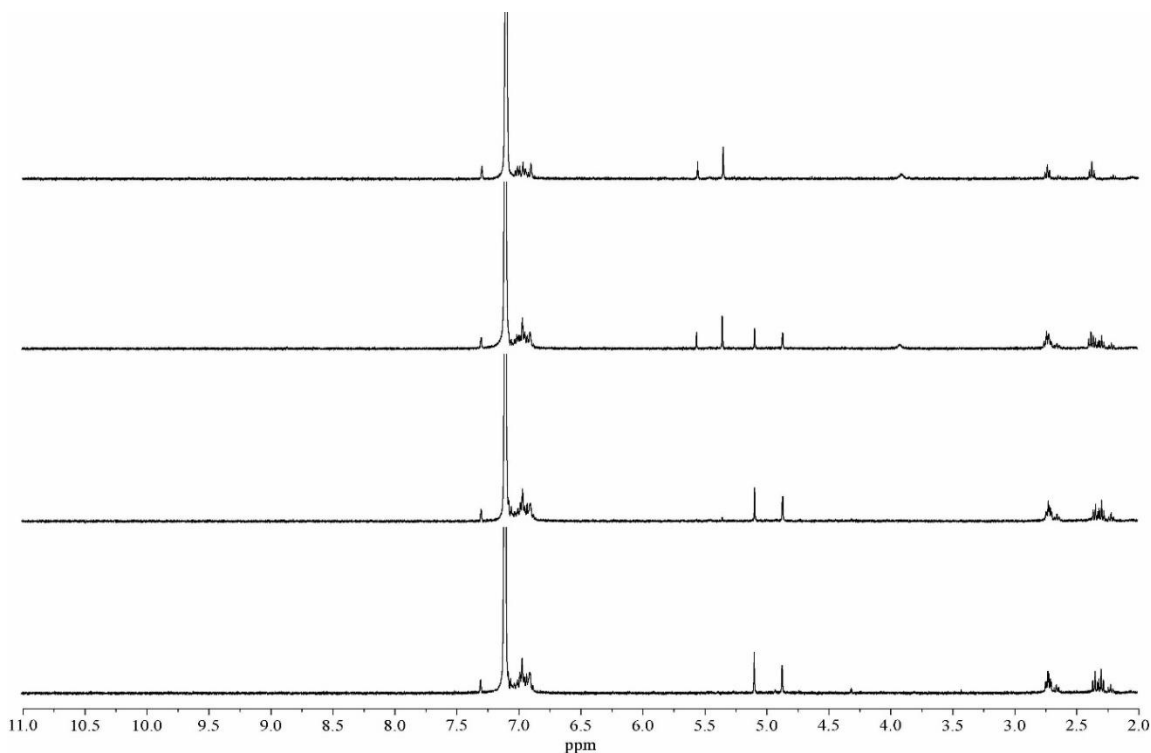


Figure 5.4 Irradiation at 455 nm in benzene exposed to air.

Finally we were successfully able to photocleave our acetate leaving group in a nonpolar solvent (CDCl_3) while no photocleavage was seen in a polar solvent (D_2O) (Figure 5.5). Investigations are currently underway in our group to demonstrate selective photocleavage of our new PPG when multiple PPGs are used in the same system (Figure 5.6).

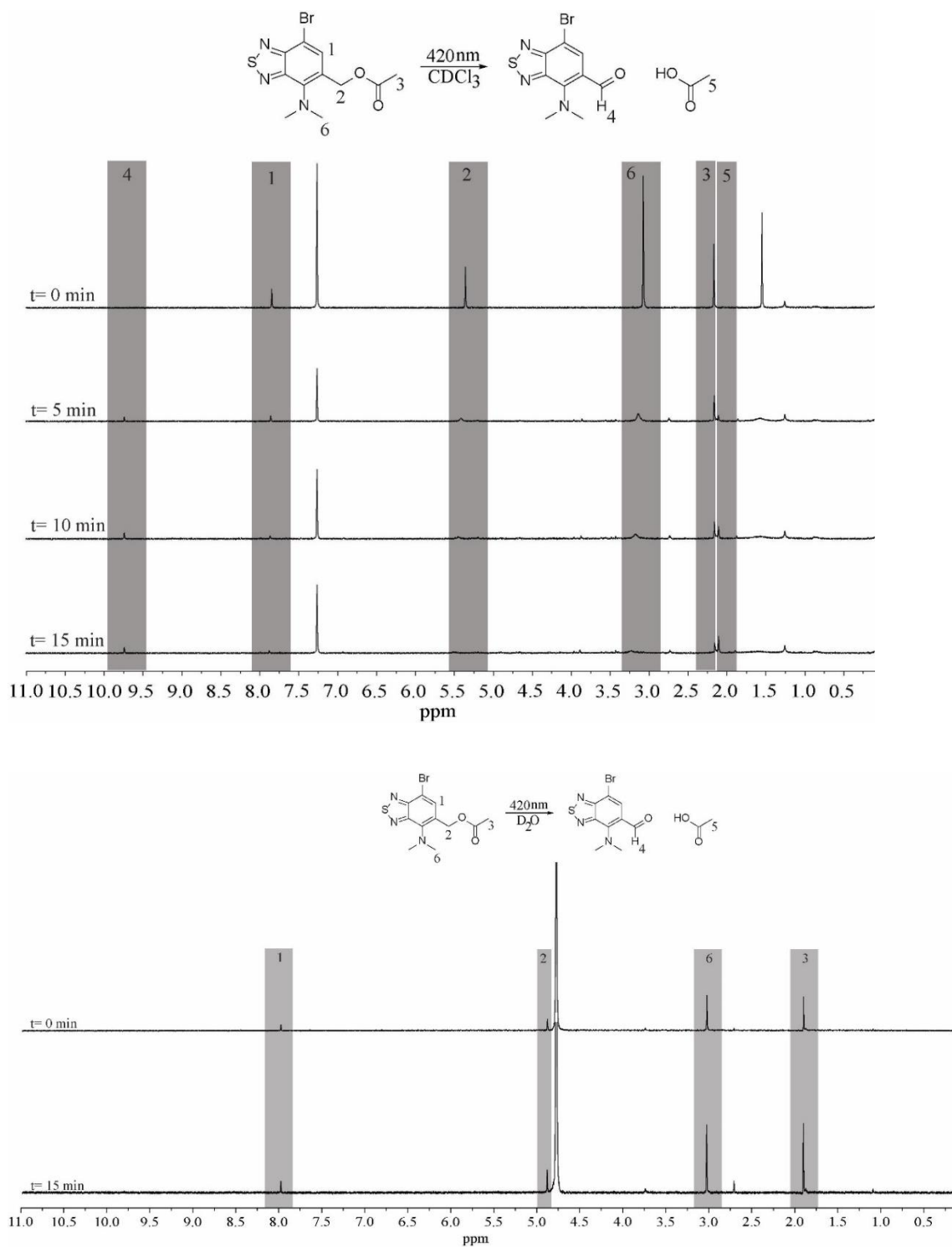


Figure 5.5 Irradiation of PPG in CDCl_3 (top) and D_2O at 420 nm for 15 min.

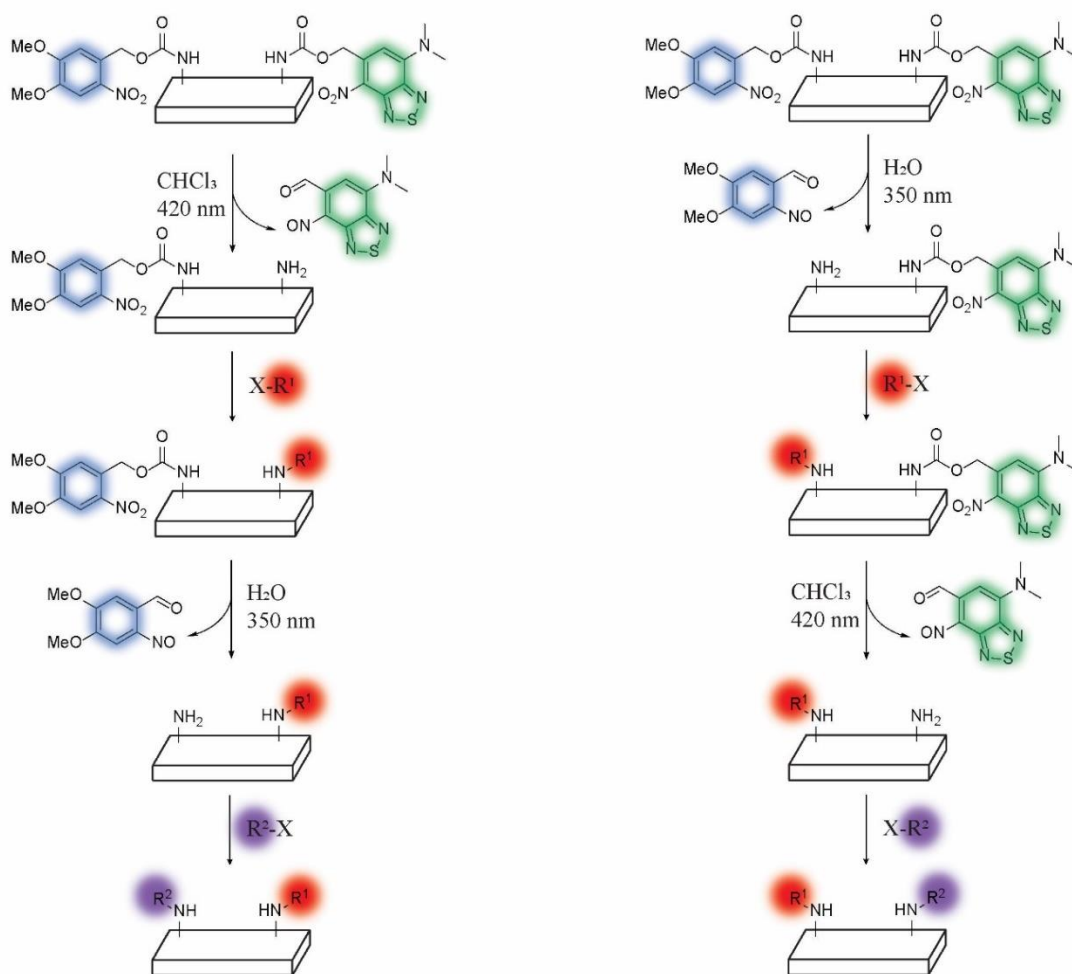


Figure 5.6 Differential deprotection of PPGs in the same system by altering solvent environment.